องค์ประกอบทางเคมีของเพรียงหัวหอมสกุล *Ecteinascidia* ชนิดหนึ่งของไทย

นางสาวกรวิกา จารุพันธ์

วิทยานิพนธ์นี้เป็นส่วนหนึ่งของการศึกษาตามหลักสูตรปริญญาเภสัชศาสตรมหาบัณฑิต
สาขาวิชาเภสัชเวท ภาควิชาเภสัชเวท
คณะเภสัชศาสตร์ จุฬาลงกรณ์มหาวิทยาลัย
ปีการศึกษา 2543

ISBN 974-13-0819-1

CHEMICAL CONSTITUENTS OF A THAI *ECTEINASCIDIA* TUNICATE

Miss Kornvika Charupant

A Thesis Submitted in Partial Fulfillment of the Requirements

for the Degree of Master of Science in Pharmacy

Department of Pharmacognosy

Faculty of Pharmaceutical Sciences

Chulalongkorn University

Academic Year 2000

ISBN 974-13-0819-1

Thesis Title	CHEMICAL CONSTITUENTS OF A THAI *ECTEINASCIDIA* TUNICATE
By	Miss Kornvika Charupant
Field of Study	Pharmacognosy
Thesis Advisor	Associate Professor Surattana Amnuoypol
Thesis Co-advisor	Mr. Khanit Suwanborirux, Ph.D.

Accepted by the Faculty of Pharmaceutical Sciences, Chulalongkorn University in Partial Fulfillment of the Requirements for the Master's Degree.

……Dean of the Faculty of Pharmaceutical Sciences

(Associate Professor Sunibhond Pummangura, Ph.D.)

THESIS COMMITTEE

……Chairman

(Associate Professor Kittisak Likhitwitayawuid, Ph.D.)

……Thesis Advisor

(Associate Professor Surattana Amnuoypol, M.Sc. in Pharm.)

……Thesis Co-advisor

(Mr. Khanit Suwanborirux, Ph.D.)

……Member

(Assistant Professor Rutt Suttisri, Ph.D.)

กรวิกา จารุพันธ์ : องค์ประกอบทางเคมีของเพรียงหัวหอมสกุล *Ecteinascidia* ชนิดหนึ่งของไทย (CHEMICAL CONSTITUENTS OF A THAI *ECTEINASCIDIA* TUNICATE) อ. ที่ปรึกษา : รศ.สุรัตนา อำนวยผล อ. ที่ปรึกษาร่วม : อ. ดร. คณิต สุวรรณบริรักษ์ 142 หน้า ISBN 974-13-0819-1

ในการศึกษาการสกัดสารเคมีจากเพรียงหัวหอมในสกุล *Ecteinascidia* ชนิดหนึ่งที่เก็บจากทะเลบริเวณจังหวัดภูเก็ต โดยการเติมสารโปแตสเซียมไซยาไนด์ก่อนทำการสกัด ทำให้สามารถแยกสารกลุ่มทริสเตตราไฮโดรไอโซควิโนลินในรูปของอนุพันธ์ไซยาโนได้ 2 สาร คือ สาร ecteinascidin 770 (ET 770) และสารชนิดใหม่ ecteinascidin 786 (ET 786) รวมทั้งสามารถแยกสารกลุ่มไพริมิดินนิวคลีโอไซด์ ได้ 1 สาร คือ สาร thymidine การศึกษาในครั้งนี้ได้กำหนดค่า chemical shifts ของคาร์บอนในตำแหน่งต่างๆ ของสาร ET 770 ได้อย่างสมบูรณ์ นอกจากนี้ยังได้ทำการเปลี่ยนสาร ET 770 ไปเป็นสาร ET 743 ซึ่งเป็นอนุพันธ์ไฮดรอกไซด์ที่พบในธรรมชาติโดยการทำปฏิกิริยากับ $AgNO_3$ การพิสูจน์เอกลักษณ์ โครงสร้างทางเคมี และ relative stereochemistry ของสารทั้งหมดนี้ ทำได้โดยการวิเคราะห์ข้อมูลทางสเปคโตรสโคปี โดยใช้ MS UV IR และ NMR spectroscopy รวมทั้งการเปรียบเทียบกับข้อมูลที่มีรายงานมาก่อน สาร ET 770 และ ET 786 แสดงฤทธิ์ความเป็นพิษอย่างสูงต่อ human epidermoid carcinoma cells ของ nasopharynx และ breast cancer cells

ภาควิชา เภสัชเวท	ลายมือชื่อนิสิต……
สาขาวิชา เภสัชเวท	ลายมือชื่ออาจารย์ที่ปรึกษา……
ปีการศึกษา 2543	ลายมือชื่ออาจารย์ที่ปรึกษาร่วม……

4276551333 : MAJOR PHARMACOGNOSY
KEY WORD : TUNICATE/ *ECTEINASCIDIA*/ ECTEINASCIDINS/ TRIS-TETRAHYDROISOQUINOLINE/ PYRIMIDINE NUCLEOSIDE/ CYTOTOXIC ACTIVITY.
KORNVIKA CHARUPANT: CHEMICAL CONSTITUENTS OF A THAI *ECTEINASCIDIA* TUNICATE. THESIS ADVISOR: ASSOCIATE PROFESSOR SURATTANA AMNUOYPOL, THESIS CO-ADVISOR: MR. KHANIT SUWANBORIRUX, PH.D. 142 pp. ISBN 974-13-0819-1

A Thai *Ecteinascidia* tunicate, collected from Phuket, was investigated for its chemical constituents. By treatment the tunicate sample with potassium cyanide, two cyano-derivatives of tris-tetrahydroisoquinolines, ecteinascidin 770 (ET 770) and the new compound ecteinascidin 786 (ET 786), were isolated together with a pyrimidine nucleoside, thymidine. The complete carbon-NMR assignments of ET 770 were reported herein. The cyano-derivative ET 770 was converted into the natural-occurring hydroxide derivative ET 743 by treatment with $AgNO_3$. The chemical structures and relative stereochemistry of these compounds were elucidated through extensive analyses of their MS, UV, IR, and NMR spectroscopy, as well as comparison with the previously reported data. The compounds ET 770 and ET 786 showed strong cytotoxicity against human epidermoid carcinoma cells of the nasopharynx and breast cancer cells.

Department Pharmacognosy Student's signature……
Field of study Pharmacognosy Advisor's signature……
Academic year 2000 Co-advisor's signature……

ACKNOWLEDGEMENT

I wish to express my grateful appreciation to my thesis advisor, Associate Professor Surattana Amnuoypol, Department of Pharmacognosy, Faculty of Pharmaceutical Sciences, Chulalongkorn University, for her advice, suggestion, encouragement, and kindness throughout this research studies.

I would also like to acknowledge my deepest appreciation to my thesis co-advisor, Dr. Khanit Suwanborirux, Department of Pharmacognosy, Faculty of Pharmaceutical Sciences, Chulalongkorn University, for his valuable guidance, suggestion, encouragement, and kindness throughout this research studies.

I am very thankful to my thesis committee, Associate Professor Dr. Kittisak Likhitwitayawuid, the Head of the Department of Pharmacognosy and Assistant Professor Dr. Rutt Suttisri of the Department of Pharmaceutical Botany, Faculty of Pharmaceutical Sciences, Chulalongkorn University, for their valuable suggestion and correctitude.

I am very grateful to Professor Akinori Kubo and Dr. Naoki Saito, Meiji Pharmaceutical University for their assistance in providing 500 MHz NMR data, optical rotation, melting point, and IR experiments and to Dr. Prasat Kittakoop for his assistance in performing MS experiment.

I would like to thank the Pharmaceutical Research Equipment Center for providing research facilities and the Phuket Marine Biological Center for providing sample collection facilities.

I also thank all researchers of the Bioassay Research Facility of the National Center for Genetic Engineering and Biotechnology (BIOTEC) for testing of the cytotoxic activity.

Finally, I wish to express my infinite gratitude to my family, teachers, and friends for their love, understanding and encouragement.

CONTENTS

Page

LIST OF TABLES

Table **Page**

LIST OF FIGURES

Figure **Page**

LIST OF SCHEMES

Scheme **Page**

LIST OF ABBREVIATIONS

$[\alpha]^{25}_{D}$	=	specific rotation at 25°C and sodium D line (589 nm)
$AgNO_3$	=	silver nitrate
BC	=	breast cancer cells
br d	=	broad doublet
br s	=	broad singlet
°C	=	degree Celsius
^{13}C NMR	=	carbon-13 nuclear magnetic resonance
$CDCl_3$	=	deuterated chloroform
$CHCl_3$	=	chloroform
cm	=	centimeter
COSY	=	^{1}H-^{1}H correlation spectroscopy
c	=	concentration
δ	=	chemical shift
2D	=	two dimensional
DEPT	=	distortionless enhancement by polarization transfer
d	=	doublet
dd	=	doublet of doublets
ddd	=	doublet of doublets of doublets
DMSO-d_6	=	deuterated dimethylsulphoxide
ED_{50}	=	50% effective dose
ET	=	ecteinascidin
EtOAc	=	ethyl acetate
ε	=	molar absorptivity
ESI-TOF MS	=	Electrospray Ionization Time of Flight Mass Spectroscopy

g	=	gram
HMBC	=	^{1}H-detected heteronuclear multiple bond correlation
HMQC	=	^{1}H-detected heteronuclear multiple quantum coherence
^{1}H NMR	=	proton nuclear magnetic resonance
Hz	=	hertz
IC_{50}	=	50% inhibition concentration
IR	=	infrared
J	=	coupling constant
KB	=	human epidermoid carcinoma cells of the nasopharynx
kg	=	kilogram
μM	=	micromolar
λ_{max}	=	wavelength at maximum absorption
$[M+H]^{+}$	=	protonated molecular ion
m	=	multiplet
MeOH	=	methanol
μg	=	microgram
MHz	=	megahertz
MIC	=	minimum inhibitory concentration
mM	=	milimolar
ml	=	milliliter
mm	=	millimeter
mp	=	melting point
ν_{max}	=	wave number at maximum absorption
NOESY	=	nuclear overhauser effect correlation spectroscopy
nM	=	nanomolar

nm	=	nanometer
NMR	=	nuclear magnetic resonance
pM	=	picromolar
ppm	=	part per million
s	=	singlet
sp.	=	species
t	=	triplet
TLC	=	thin layer chromatography
TOCSY	=	total correlation spectroscopy
UV	=	ultraviolet

CHAPTER I

INTRODUCTION

Natural products are organic compounds produced by microbes, plants, and marine organisms. Some of these natural products exhibit biological activities in human being such as anticancer, antibacterial, antifungal, anti-inflammatory, and antiviral activities (Rinehart *et al.*, 1990b).

Natural products from marine plants and animals are interesting. There are several well-known marine natural products that have been in use, for example, cod liver oil, protamine sulfate, and marine macroalgae. Seaweeds, as they are more generally known, have been used as crude drugs in the treatment of iodine deficiency states, such as hypothyroidism and goitre (Evans, 1996). Natural products, especially those produced by organisms in the marine environment, have received increasing attention from chemists because numerous novel compounds have been isolated from marine organisms and many of these substances have been demonstrated to possess interesting biological activities. In the decade from 1977 to 1987, approximately 2500 new metabolites were reported from a wide variety of marine organisms ranging from prokaryotic microbes and soft-bodied invertebrates to vertebrate fish. An analysis of the phyletic distribution of these compounds covering the years 1977-1985 shows that the majority are confined to four groups; macroalga, coelenterates, echinoderms, and sponges. The modest compounds are from microbes, bryozoans, and tunicates. Sponges are prominent source of marine organisms because they have a wider range of biosynthetic capabilities than any other groups of marine invertebrates. Although the contribution from tunicates remains modest, there is increasing interest in this group. Interest in the former reflects recognition that in spite of their small size and general difficulty in collecting, tunicates produce an array of very potent bioactivities (Ireland *et al.*, 1993) and some compounds have reached clinical trial. The first example, didemnin B, a cyclic depsipeptide, was isolated from the tunicate *Tridemnum* sp. (family Didemnidae) that is most often found as a gray-green, flat, pancake-like coating on rocks or corals at the depth of upto 120 feet. The compound exhibited antitumor activity, antiviral activity (Rinehart *et al*., 1981;

Canonico *et al.*,1982) and immunosuppressive activity (Montgomery and Zukoski, 1985). Didemnin B is the most prominent member of this group; it showed the best antitumor activity and was evaluated in phase I and phase II clinical trials by National Cancer Institute (Sakai *et al*., 1996b). The second example, ecteinascidin 743, a tris-tetrahydroisoquinoline alkaloid isolated from the Caribbean tunicate, *Ecteinascidia turbinata*, possesses cytotoxic (Sakai *et al.*, 1996a) and anticancer activity against breast, non-small cell lung, melanoma, colon, and ovarian cancer (Hendriks *et al.*, 1999).

In the course of our investigation for bioactive marine natural products, the author has found a species of tunicate *Ecteinascidia* sp. growing around Phuket Island. Based on our knowledge, the *Ecteinascidia* tunicate from Thai marine environment had never been chemically studied, therefore the tunicate had been chosen to be investigated for its chemical constituents.

The main objectives of this study are to

1. isolate ecteinascidin compounds and other chemicals from the tunicate *Ecteinascidia* sp.
2. elucidate the structures of the isolated compounds.
3. evaluate cytotoxic activity of the isolated compounds.

CHAPTER II

LITERATURE REVIEW

In addition to the 48,000 more familiar species contained in the subphylum Vertebrata, the phylum Chordata also includes some 1,400 invertebrate species in the subphyla Urochordata and Cephalochordata. The nonvertebrate chordates are all marine. About 90% of the invertebrate chordate species are contained within the subphylum Urochordata. The Urochordata is one of the few major taxonomic groups to contain no parasitic species; all urochordates feed by straining small particles (especially phytoplankton) from the surrounding water. The method of generating the water current from which these food particles are obtained differs dramatically among different urochordate classes. Members of this subphylum are commonly referred to as "tunicates" and are distributed among three classes: Ascidiacea, Thaliacea, and Appendicularia (Scheme 1). None of these animals have left a fossil record (Pechenik, 1996).

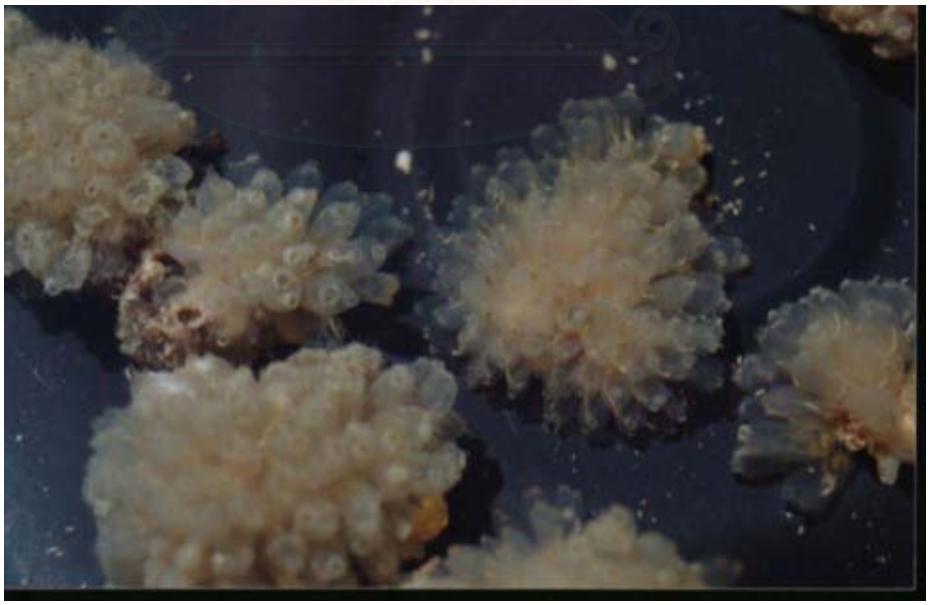

Figure 1 A Thai *Ecteinascidia* tunicate.

Scheme 1 Tunicate phylogenetic chart (Sterrer, 1986).

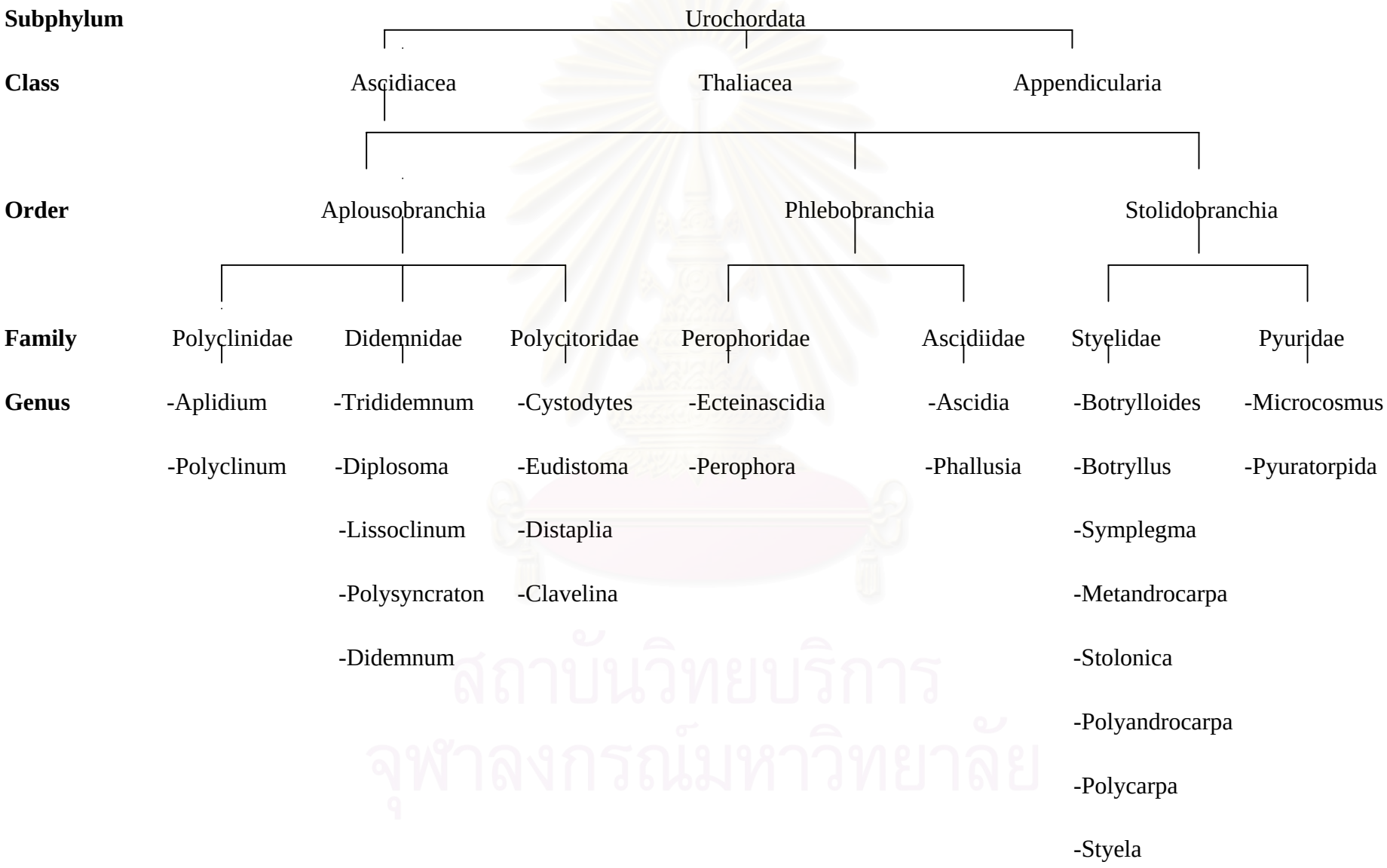

1. General characteristics of tunicates

Most of the approximate 1,500 species of urochordates are tunicates or ascidians or sea squirts. Tunicates have notochord and nerve cord in free-swimming larva only. They are sessile as adults and are either solitary or colonial. Sessile tunicates attach their saclike bodies to rocks, shell, pilings, ship bottoms, wrecks, alga, sea grasses, and mangrove roots, and are particularly common in shaded areas (on overhangs, in caves and on the underside of stones). In a colonial tunicate, there are several to many members, call zooids. Each zooid of a colonial tunicate contains two siphons that permit seawater to circulate through the body. One siphon is the oral siphon which is the inlet for water circulating through the body and is usually directly opposite the attached end of the tunicate. It also serves as the mouth opening. The second siphon is the atrial siphon which is the opening for excurrent water (Miller and Harley, 1999). The body is bag-like and covered by a secretion of the epidermal. This secreted, protective cover, also called the tunic, is composed largely of protein and a polysaccharide (tunicin) that closely resembles cellulose (Pechenik, 1996). The tunicate heart lies at the base of the pharynx. One vessel from the heart runs anteriorly under the endostyle, and another runs posteriorly to the digestive organs and gonads. Blood flow through the heart is not unidirectional. Peristaltic contractions of the heart may propel blood in one direction for a few beats; then the direction is reversed. Tunicate blood plasma is colorless and contains various kinds of amoeboid cells. Gonads are located near the loop of the intestine, and genital ducts open near the atrial siphon. Gametes may be shed through the atrial siphon for external fertilization, or eggs may be retained in the atrium for fertilization and early development. Although self-fertilization occurs in some species, cross-fertilization is the rule. The majority of these tunicates are found in shallow subtidal zone (Hickman, Roberts, and Larson, 1997).

2. Taxa and description of tunicate in the genus *Ecteinascidia*

(Sterrer, 1986)

Kingdom : Animal

Phylum : Chordata

Subphylum : Urochordata

Class : Ascidiacea

Order : Phlebobranchia

Family : Perophoridae

Genus : Ecteinascidia

Colonial tunicates of the genus *Ecteinascidia* have oblong or clavate zooids, which are connected by thin, vine-like stolons with 15-30 rows of stigmata.

3. Characteristics of each species of the genus *Ecteinascidia*

(Sterrer, 1986)

Species	Characteristics
E. turbinata	Orange-colored, forming dense grape-like clusters 15 cm or more in diameter. Zooids to 5 cm long with very transparent tunic and up to 30 rows of stigmata; intestine forming a wide loop on left side of the body around the rosette-shaped gonads. The oviduct, in which the large transparent larvae are brooded, opens to the right side of the body. Rather ubiquitous from intertidal to the outer reefs: on exposed surfaces, often on gorgonians; very common.
E. conklini	Zooids to 10 mm long, lemon-yellow to greenish, both siphons usually with a bright red border. With up to 15 rows of stigmata. Forms small colonies on the underside of stones; rare.
E. minuta	Zooids about 8 mm, whitish; branchial siphon long, ending in a prominent white crown. With up to 13 rows of stigmata. Forms dense carpets on the underside of stones, or muffs around mangrove roots; common.

4. Tunicate metabolites

During the last three decade, marine natural product chemists have enjoyed unrivaled success in the discovery of unique, new compounds (Bradley, 1993). Marine organisms, especially invertebrates such as sponges, soft corals, mollusks and tunicates, produce many secondary metabolites which have biological activities (antibacterial, antifungal, anticancer, antiviral, immunomodulatory and anti-inflammatory). More recently, tunicates have become the target of natural product research. The metabolite of these tunicates can be divided based on the presence or absence of nitrogen in the molecule.

1. Nitrogenous metabolites

1.1 Peptide metabolites

Peptides have continued to be one of the major structural classes isolated from tunicates, for example, didemnin B [1] was isolated from tunicate *Tridemnum solidum* (Rinehart *et al*., 1981; Sakai *et al.*, 1996b), lissoclinamide 5 [2] from tunicate *Lissoclinum pattella* (Schmitz *et al*., 1989; Hawkins *et al*., 1990), and mollamide [3] from tunicate *Didemnum molle* (Carroll *et al*., 1994).

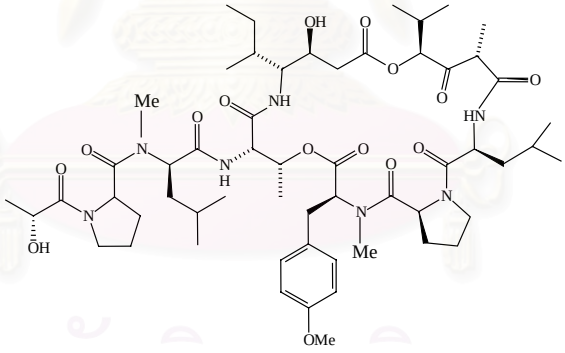

[1]

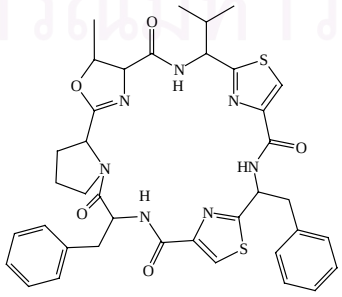

[2]

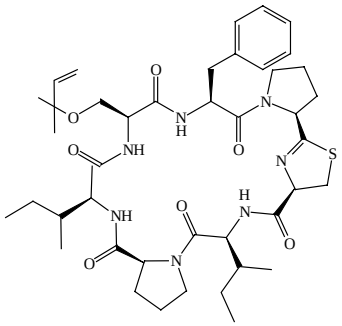

[3]

1.2 Polycyclic aromatic alkaloids

The polycyclic aromatic alkaloids based on the pyrido[*k,l*] acridine skeleton have been reported over the last decade. This group of alkaloids is currently of great interest due to their significant biological activities (Molinski, 1993). Most pyridoacridines have been reported as having significant cytotoxicity. Other activities, such as the regulation of cellular growth and differentiation, effect on cAMP-mediated processes, inhibition of topoisomerase II, and anti-HIV activity, have also been reported from the alkaloids such as ascididemnin [4] was isolated from tunicate *Didemnum* sp. (Kobayashi *et al*., 1988), cystodytin J [5] from tunicate *Cystodytes dellechiajei* (Kobayashi *et al*., 1991), diplamine [6] from tunicate *Diplosoma* sp. (Ciufolini and Shen, 1995), and meridine [7] from tunicate *Amphicarpa meridiana* (Kitahara *et al*., 1997).

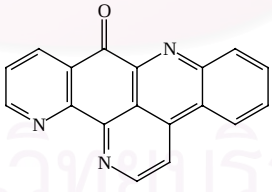

[4]

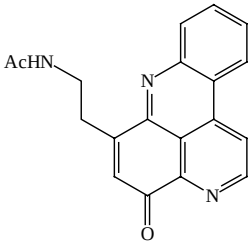

[5]

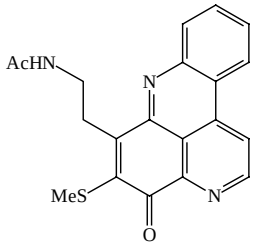

[6]

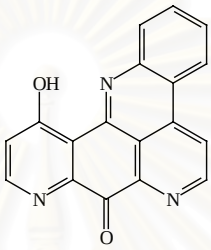

[7]

1.3 Tryptophan-derived metabolites

Tryptophan-derived metabolites are based on a β-carboline ring system, for example, eudistomin U [8] was isolated from tunicate *Lissoclinum fragile* (Badre *et al.*, 1994).

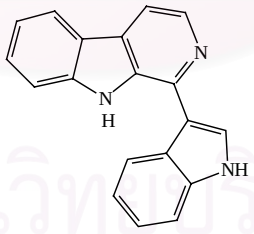

[8]

1.4 Lysine-derived metabolites

Lysine is a homologue of ornithine, and it also functions as an alkaloid precursor (Dewick, 1997) to compounds such as piclavine A_2 [9] which was isolated from tunicate *Clavelina picta* (McAlonan *et al*., 2000).

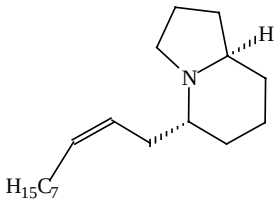

[9]

1.5 Tyrosine- and phenylalanine-derived metabolites

In one of the early reports on tumor-inhibiting effects of the extracts from marine invertebrates, it was noted that the extract of the Caribbean tunicate *Ecteinascidia turbinata* caused dramatic increase in the lifetime of mice inoculated with P388 cells (Schmitz *et al*., 1993). The active compounds isolated were tyrosine-derived compounds called the ecteinascidins, for example, ecteinascidin 743 [10] (Wright *et al*., 1990; Rinehart *et al*., 1990a).

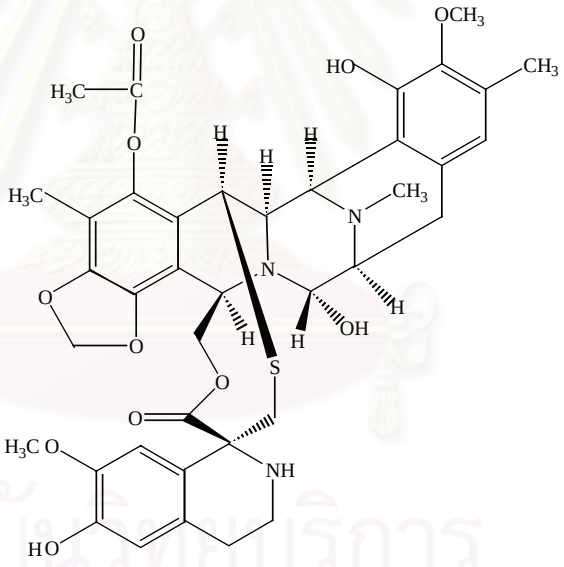

[10]

1.6 Nucleosides

The nucleoside is composed of a purine or a pyrimidine base attached to a sugar, for example, 2′-deoxyuridine [11] and 2′-deoxycytidine [12] were isolated from tunicate *Trididemnum cereum* (Dematte *et al*., 1985).

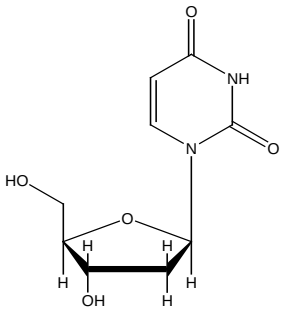

[11]

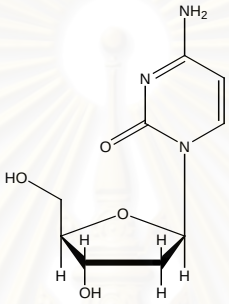

[12]

1.7 Miscellaneous nitrogenous metabolites

Petellazole A [13] is a cytotoxic thiazole-containing macrolide, which was isolated from the tunicate *Lissoclinum patella* (Zabriskie, Mayne, and Ireland, 1988).

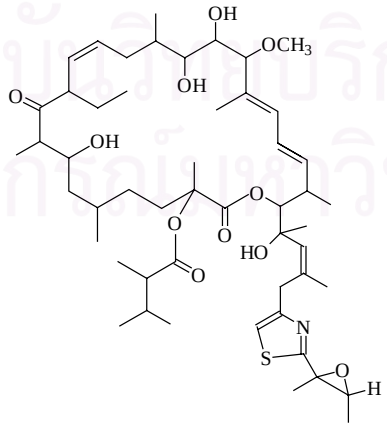

[13]

2. Non-nitrogenous metabolites

The non-nitrogenous metabolites examples are enterocin [14] which was isolated from tunicate *Didemnum* sp. (Kang, Jensen, and Fenical, 1996) and didemnilactone, [15], a ten-membered lactone, was isolated from tunicate *Didemnum moseleyi* (Niwa, Inagaki and Yamada, 1991).

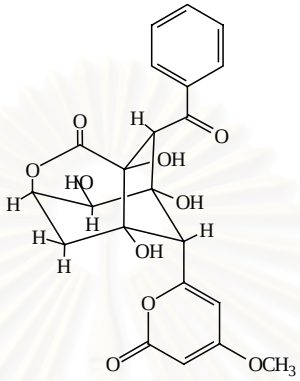

[14]

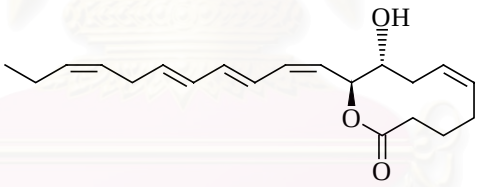

[15]

5. Chemistry and biological activities of the compounds from tunicates of the genus *Ecteinascidia*

The tunicates of the genus *Ecteinascidia*, especially *Ecteinascidia turbinata*, have been of long-standing interest due to reports as far back as 1969 of antitumor activity (Rinehart *et al*., 1990b). *Ecteinascidia turbinata* produced secondary metabolites of the ecteinascidin group. Ecteinascidins are isoquinoline alkaloids which composed of either the bis- or tris-tetrahydroisoquinolines units (Wright *et al*., 1990; Sakai *et al*., 1996a) and can be divided into three groups based on their C ring as follows.

1. Ecteinascidins with three tetrahydroisoquinoline subunits (A-C)

These ecteinascidins are composed of three tetrahydroisoquinolines (units A-C), which have the amino acid tyrosine as the biosynthetic precursor. The members of this group are ET 729, ET 743, ET 745, and ET 770 (the number indicates the molecular weight of each compound) (Rinehart *et al*., 1990a).

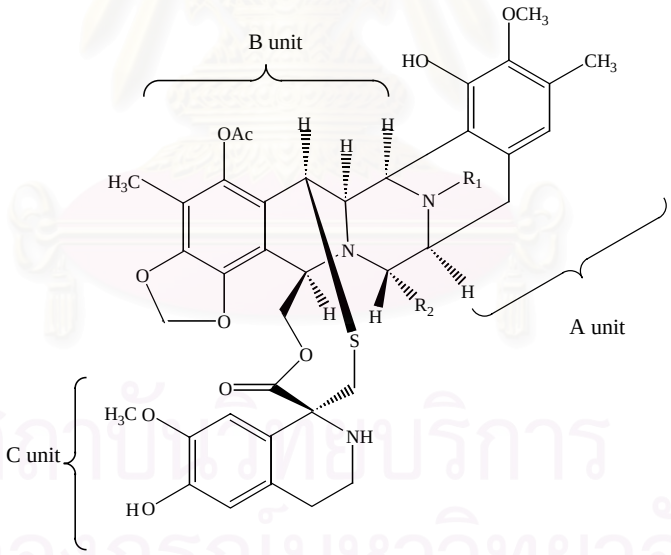

	R_1	R_2
ET 729 (746)*	H	OH
ET 743 (761)*	CH_3	OH
ET 745	CH_3	H
ET 770	CH_3	CN

*( ) = molecular weight

2. Ecteinascidins with two tetrahydroisoquinoline units (A, B) plus one tetrahydro-β-carboline unit (C)

These ecteinascidins having two tetrahydroisoquinoline units (A, B) plus one tetrahydro-β-carboline unit (C) exemplify the formation of a six-membered heterocyclic ring using the ethylamine side-chain of tryptamine. The members of this group are ET 722 and ET 736.

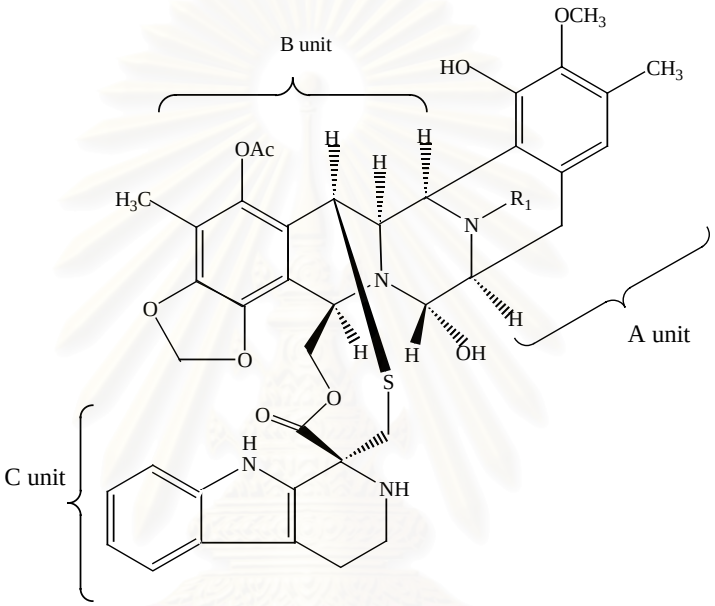

ET 722: R_1= H

ET 736: R_1= CH_3

3. Ecteinascidins with two tetrahydroisoquinoline units (A, B) plus a chain of carbon (unit C)

These ecteinascidins are composed of two tetrahydroisoquinoline units (A, B) plus a chain of carbon (unit C). Compounds ET 583, ET 594, ET 596 and ET 597 are the members of this group.

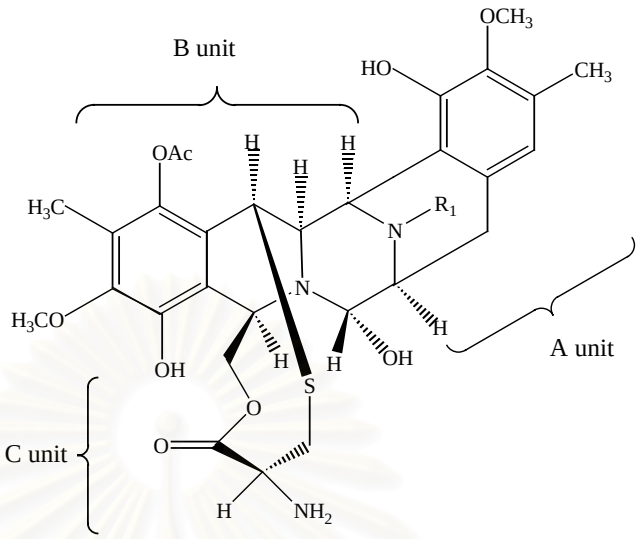

ET 583: R_1 = H

ET 597: R_1 = CH_3

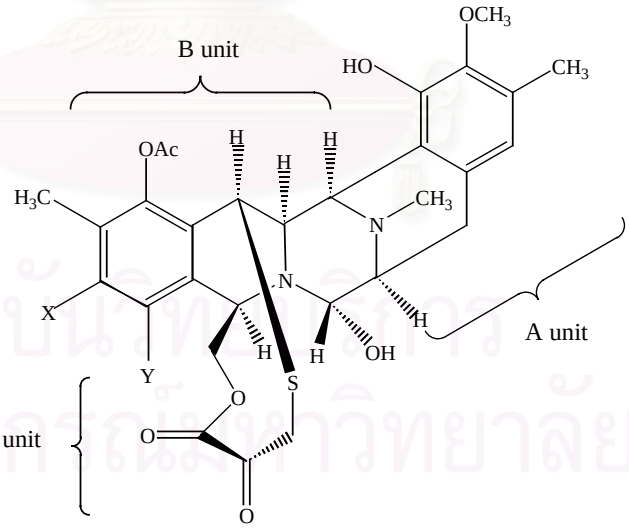

ET 594: X,Y = -O- CH_2-O

ET 596: X = OCH_3, Y = OH

The attachment of the third tetrahydroisoquinoline or the tetrahydro-*β*-carboline (unit C) to unit B by a 10-membered sulfide-containing lactone ring is quite a distinctive feature of ecteinascidin molecules. Unequivocal assignments of the relative configuration of all the chiral centers in these molecules have been performed. Ecteinascidins have absolute configuration at C1, C3, C4, C11, C13, and C21 as *R*, *R*, *R*, *R*, *S*, and *S*, respectively (Guan *et al*., 1993).

5.1 Biogenesis of ecteinascidin 743

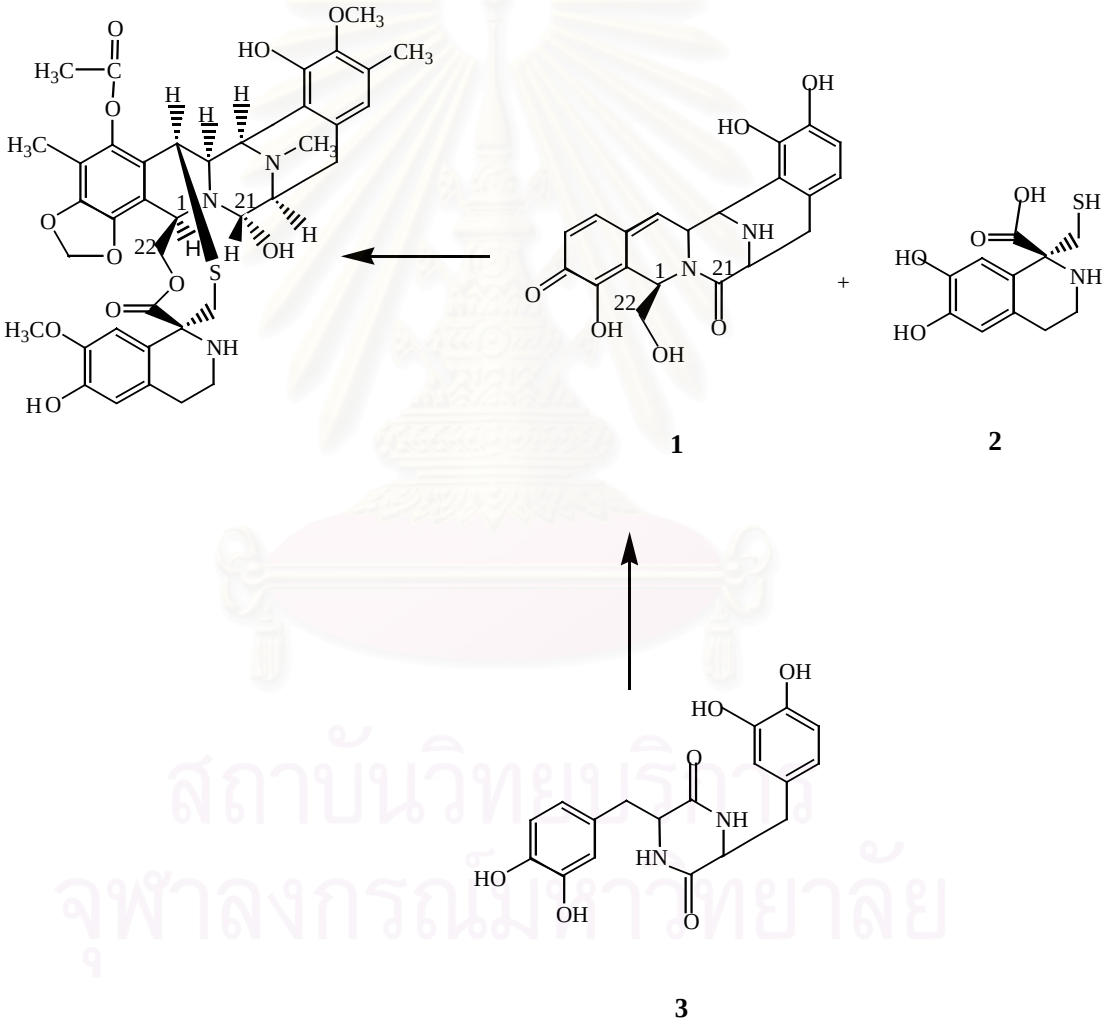

Figure 2 Biogenesis of ecteinascidin 743.

The ecteinascidin skeleton is composed of a functionalized diketopiperazine **1** and fragment **2**. Compound **1** is likely derived from the diketopiperazine **3,** which is either a condensation product of two molecules of DOPA or is the result of hydroxylation of the diketopiperazine from tyrosine. The two-carbon unit (C-1, C-22), is presumably derived from glyoxylate (or a glycoaldehyde). The glyoxylate could, in turn, be produced from either serine or glycine. Fragment **2** appears to be derived from the condensation of β-mercaptopyruvic acid with dopamine. It is also conceivable that **1** could condense with β-mercaptopyruvic acid and this subsequently combines with dopamine. Thus, while it seems reasonable to suggest which building blocks are involved in ecteinascidin production, the order in which they assemble is not yet clear (Kerr and Miranda, 1995).

5.2 Biological activites of ecteinascidins (ETs)

ETs 729, 743, 583, 594, and 597 exhibited several biological activities; including cytotoxicity against P388 (murine lymphoma), A549 (human lung carcinoma), HT29 (human colon carcinoma), MEL28 (human melanoma), and CV-1 (monkey kidney); antimetabolic activities; and enzyme inhibitions. ET 583, 594 and 597 which lacked the aromatic C unit, showed cytotoxic activity 5-25 times less active than ETs 729 and 743 against the MEL28 and CV-1. ETs 729, 743, 583, 594, and 597 showed potent inhibition of DNA and RNA syntheses. For enzyme inhibition, they inhibited DNA and RNA polymerase activity. Ets 583, 594 and 597 showed some inhibition of protein synthesis, while ETs 729 and 743 were less active (Sakai *et al*., 1996a). ET 729 showed potent antitumor activities against P388 and B16 melanoma (Sakai *et al*., 1992). Of the several ETs isolated, ET 743 was selected for clinical trials to use for anticancer therapy because of its greater abundance (1×10^{-4} % yield wet weight of the tunicates) and its potent cytotoxic activity. ET 743 is presently being evaluated in clinical trials phase II (Zewail-Foote and Huley, 1999).

5.3 Biological activities of ecteinascidin 743

Ecteinascidin 743 is currently under investigated in clinical trials phase II. It showed cytotoxicity (*in vitro*) against a variety of tumor cell lines for examples P388, L1210 (mouse leukemia), A549 , HT29 , and MEL28 at IC_{50}

3.4×10^{-4}, 6.6×10^{-4}, 2.6×10^{-4}, 4.6×10^{-4}, and 5.0×10^{-4} μM, respectively. This compound is tested at dose of 60 μg/kg for advanced stage MX-1 mammary tumor xenografts (9 of 10 mice were tumor free on day 23) and early stage MX-1 mammary tumor xenografts (10 of 10 mice tumor free on day 23) (Rinehart, 2000). These cell studies were followed by *in vitro* studies against freshly explanted human tumors such as breast, colon, renal, non-small cell lung carcinoma (NSCLC), melanoma, and ovarian, which showed a wide range of activities at very low concentrations (generally 0.01 μM to less than 1 pM). *In vitro* studies were followed by *in vivo*, showing tumor growth reduction of breast, melanoma nonsmall cell lung cancer, and ovarian cancer (Rinehart, 2000). Additional *in vivo* studies, ET 743 showed complete regressions in xenografts of ovarian carcinoma HOC22, non-small cell lung carcinoma LXFL 529, and melanoma MEXF 989 at maximum tolerated dose 200 μ g/kg (Valoti *et al*., 1998; Hendriks *et al*., 1999). The optimum dose regimen in clinical trials phase I, appeared to be 24 hr. infusion on day 1, repeated on day 22 (Rinehart, 2000).

5.4 Mechanism of action of ecteinascidin 743

1. Effect on DNA: Ecteinascidin 743 binds in the minor groove of DNA forming adducts at N2 position of guanine (Pommier *et al*., 1996; Erba *et al*., 1998) with DNA sequence preference for 5´-AGC, 5´-GGC and 5´-GGC (Zewail-Foote and Hurley, 1999). The mechanism of covalent adduct formation involves the reaction of ET 743 with DNA via an iminium intermediate caused by the carbinolamine functional group suitable for nucleophilic attack by the amino group of an adjacent guanine base. Furthermore, an NMR-based model of ET 743 with duplex DNA indicates that the A- and B-subunits are responsible for DNA recognition and bonding, while the C-subunit is projected out of the minor groove and makes limited contacts with the DNA (Moore *et al*., 1998; Seaman and Hurley, 1998; Zewail-Foote and Hurley, 1999). ET 743 also induces topoisomerase I -mediated protein-linked DNA breaks and that topoisomerase I is a target for ET 743 both *in vitro* and *in vivo* (Takebayashi *et al*., 1999).

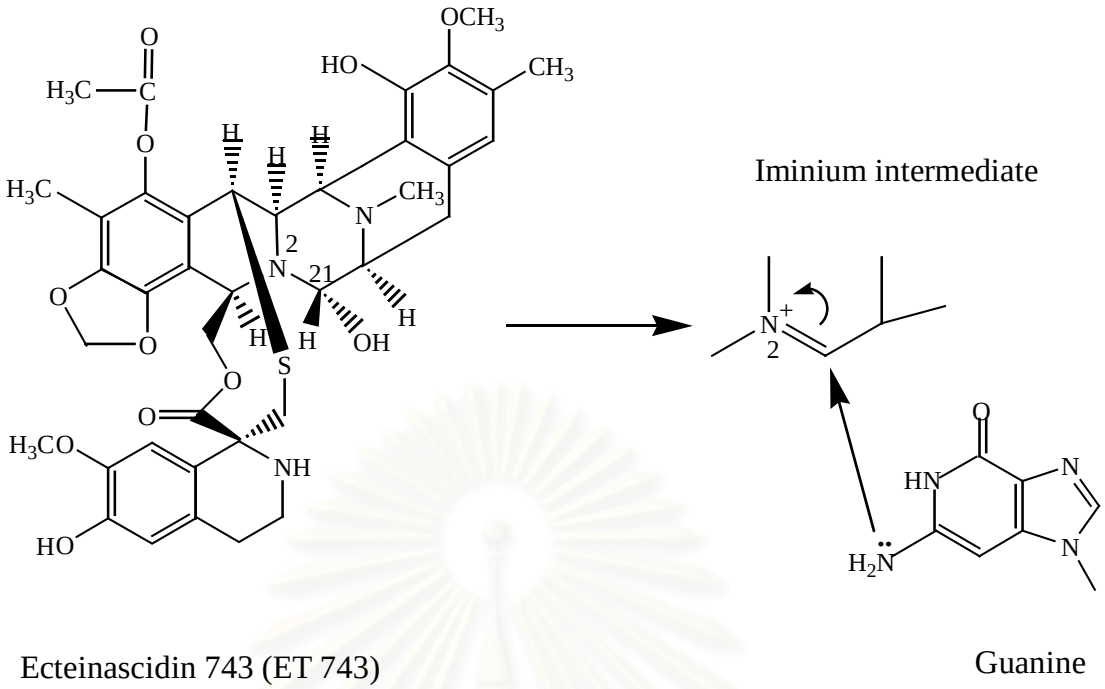

Figure 3 Chemical structure of ecteinascidin 743 and proposed reaction of its reactive iminium intermediate with the guanine 2-amino group.

2. Inhibition of transcription mechanism: Recently, Jin *et al*., 1999 reported some preliminary data on the inhibition of the transcription of multidrug resistance gene type 1 (mdr-1 gene) by ET 743. The effect appeared to be due to the ability of ET 743 to inhibit the binding of the nuclear transcription factor Y (NFY) to a CCAAT BOX present in the mdr-1 gene promoter. These data confirm previous *in vitro* finding on the ability of ET 743 to prevent the formation of the NFY complex with its consensus DNA sequence (Mantonvani *et al*., 1998; Bonfanti *et al*., 1999).

3. Effect on microtubules: ET 743 disorganises the microtubule network but it does not seem to interact directly with tubulin (Garcia-Rocha, Garcia-Gravolos, and Avila, 1996). It promotes as a first step decrease in the proportion of microtubules located close to the cell membrane and afterwards it results in the appearance of collapsed microtubules surrounding the cell nucleus. It thus appears to change the microtubule distribution to that of curved microtubules forming a circle around the cell nucleus, whereas in control cells microtubules are arranged in a line

from the centrosome to the cell membrane (Schiff, Fanat, and Horwitz, 1979). It seems that, with ET 743, microtubules are not anchored at the centrosome. Several analyses have been done to test the possible mechanisms of ET 743 on microtubule protein and the results have indicated that the compound does not interfere with colchicine or GTP binding to tubulin. Also, as indicated above, it appears that it does not produce a decrease in the *in vitro* polymerisation of tubulin.

4. Cell cycle perturbations: In the human tumor cell lines examined, ET 743 was found to decrease the rate of progression of cell in late S phase towards G_2 phase and caused a prolonged blockade in G_2-M phase (Ghielmini *et al*., 1998; Erba *et al*., 2001) as assessed by biparametric Brd Urd/DNA flow cytometry.

5.5 Synthesis of ecteinascidin 743

Ecteinascidin 743 (ET 743) is an exceedingly potent and rare marine-derived antitumor agent which is now being studied in various clinics with human patients. Because this compound is not sufficiently available from the natural source, the tunicate *Ecteinascidia turbinata*, it is being produced industrially by the total synthetic route described in 1996. (Corey, Gin and Kania, 1996; Martinez and Corey, 2000). More recently, phthalascidin a structural analogue of ET 743, was synthesized. It is an antitumor agent very similar to ET 743 with regard to *in vitro* potency and mode of action across a variety of cell types. The antiproliferative activity of phthalascidin (IC_{50} = 0.1-1 nM) is greater than taxol, camptothecin, adriamycin, mitomycin C, cisplatin, bleomycin, and etoposide by 1-3 orders of magnitude, and its mechanism of action is clearly different from these currently used drugs. Phthalascidin induces DNA-protein cross-linking, although it seems to interact with topoisomerase I but not topoisomerase II and is more stable than ET 743 (Martinez *et al*., 1999). ET 743 and phthalascidin (PT-650) can also be synthesized from cyanosafracin B (Cuevas *et al*., 2000).

CHAPTER III

EXPERIMENTAL

1. Source and sample collection

Transparent colonies of a Thai tunicate, *Ecteinascidia* sp., were collected from Phuket by SCUBA diving at the depth of 1-5 meters in March and May, 2000 and were stored frozen at -20°C prior to extraction.

2. General techniques

2.1 Chromatography

2.1.1 Analytical thin-layer chromatography (TLC)

Technique : One way, ascending

Adsorbent : Silica gel 60 GF-254 precoated plate (E. Merck)

Layer thickness : 250 μm

Distance : 5 cm

Temperature : Room temperature 25-30^{0}C

Detection : 1) Visual detection under daylight

2) Ultraviolet light at the wavelengths of 254 and 365 nm

3) Spraying with anisaldehyde-sulfuric acid reagent and heating until colors developed

2.1.2 Column chromatography

2.1.2.1 Gel filtration chromatography

Adsorbent : Sephadex LH-20 (Pharmacia Biotech AB)

Packing : The adsorbent was suspended in the eluant and left standing to swell for 24 hours before using, then poured into the column and allowed to settle tightly.

Sample loading : The sample was dissolved in a small volume of the eluant and loaded onto the top of the column.

Detection : Fractions were examined by TLC under ultraviolet light at wavelengths of 254 and 365 nm and sprayed with anisaldehyde-sulfuric reagent, respectively.

2.1.2.2 Flash column chromatography

Adsorbent : Silica gel 60 (No. 7734), particle size 0.063-0.200 nm (70-230 mesh ASTM) (E.Merck)

Packing : The adsorbent was suspended in the eluant. The slurry of adsorbent was poured into the column, tapped and pressed down under an air pump, and then allowed to settle overnight.

Sample loading : The sample was dissolved in a small volume of the eluant and loaded onto the top of the column.

Detection : Fractions were examined in the same manner as described above.

2.2 Spectroscopy

2.2.1 Ultraviolet (UV) Absorption Spectra

Ultraviolet-visible (UV) absorption spectra were obtained on a Milton Roy spectronic 3000 Diode Array spectrometer (Pharmaceutical Research Instrument Center, Faculty of Pharmaceutical Sciences, Chulalongkorn University).

2.2.2 Infrared (IR) Absorption Spectra

Infrared spectra (KBr disc and NaCl cell) were obtained on a Perkin Elmer FT-IR 1760X spectrometer (the Scientific and Technological Research Equipment Center (STREC), Chulalongkorn University) or a Hitachi 260 spectrophotometer (Meiji Pharmaceutical University).

2.2.3 Mass Spectra (MS)

Mass spectra were obtained by an Electron spray Ionization-Time of Flight (ESI-TOF) made on a Micromass LCT mass spectrometer. Acetonitrile:H_2O (1:1) containing 0.02% formic acid was used as the solvent (the National Center for Genetic Engineering and Biotechnology, BIOTEC).

2.2.4 Proton and Carbon Nuclear Magnetic Resonance (^{1}H and ^{13}C-NMR) Spectra

^{1}H and ^{13}C-NMR, DEPT 90 and 135, COSY, TOCSY, HMQC, NOESY, and HMBC Spectra were recorded on a Bruker AVANCE DPX-300 FT-NMR Spectrometer operating at 300 MHz for protons and 75 MHz for carbons, and chemical shifts (ppm) of the residual undeuterated solvent were used as references. Proton detected heteronuclear correlations were measured using HMQC (optimized for $^nJ_{HC}$ = 145 Hz) and HMBC (optimized for $^nJ_{HC}$ = 3, 4, and 8 Hz) pulse sequences (Faculty of Pharmaceutical Sciences, Chulalongkorn University).

Some ^{1}H and ^{13}C NMR spectra were measured at 500 and 125 MHz, respectively, with a JEOL JNM-LA 500 spectrometer (Meiji Pharmaceutical University).

Deuterated solvents: dimethyl sulfoxide-d_6 (CD_3SOCD_3) and chloroform ($CDCl_3$) were used in NMR experiments. Reference signals were the signals of residual undeuterated solvents at δ 2.49 (^{1}H) and 39.7 (^{13}C) ppm for CD_3SOCD_3, 7.24 (^{1}H) and 77.0 (^{13}C) ppm for $CDCl_3$.

2.3 Physical properties

2.3.1 Optical rotations

Optical rotations were measured on a Perkin-Elmer 341 polarimeter using a sodium lamp operating at 589 nm, 25°C (Pharmaceutical Research Instrument Center, Faculty of Pharmaceutical Sciences, Chulalongkorn University), or a Horiba-SEPA-200 automatic digital polarimeter at 23°C (Meiji Pharmaceutical University).

2.3.2 Melting point

Melting temperatures were determined on YANACO micro melting point apparatus (Meiji Pharmaceutical University).

3. Solvents

All of the organic solvents used in this work excluding the deuterated solvents for NMR spectra were commercial grade, which were redistilled prior to use.

4. Extraction of a Thai *Ecteinascidia* tunicate

The homogenized tunicate (38 kg wet wt.) was adjusted by adding a phosphate buffer solution to pH 7, added with a solution of 10% KCN for 5 hours, adjusted to pH 7 again and macerated with methanol for 1 night (x3 times). The supernatant was further concentrated by rotary evaporator at temperature not exceeding 50°C and partitioned with ethyl acetate. The ethyl acetate layer was evaporated under reduced pressure at temperature not exceeding 50°C to give the ethyl acetate extract (dark-brown oil, 19.7 g), which was dissolved in methanol (15 ml) and re-extracted with hexane (3 x 30 ml). Both extracts were evaporated under reduced pressure to yield 12.2 g of the methanol extract and 8.4 g of the hexane extract (0.032% and 0.022% of wet wt., respectively) as shown in Scheme 2.

The methanol extract and the hexane extract were examined using proton NMR measurement. The methanol extract showed intense characteristic signals of the ecteinascidins, and was further isolated.

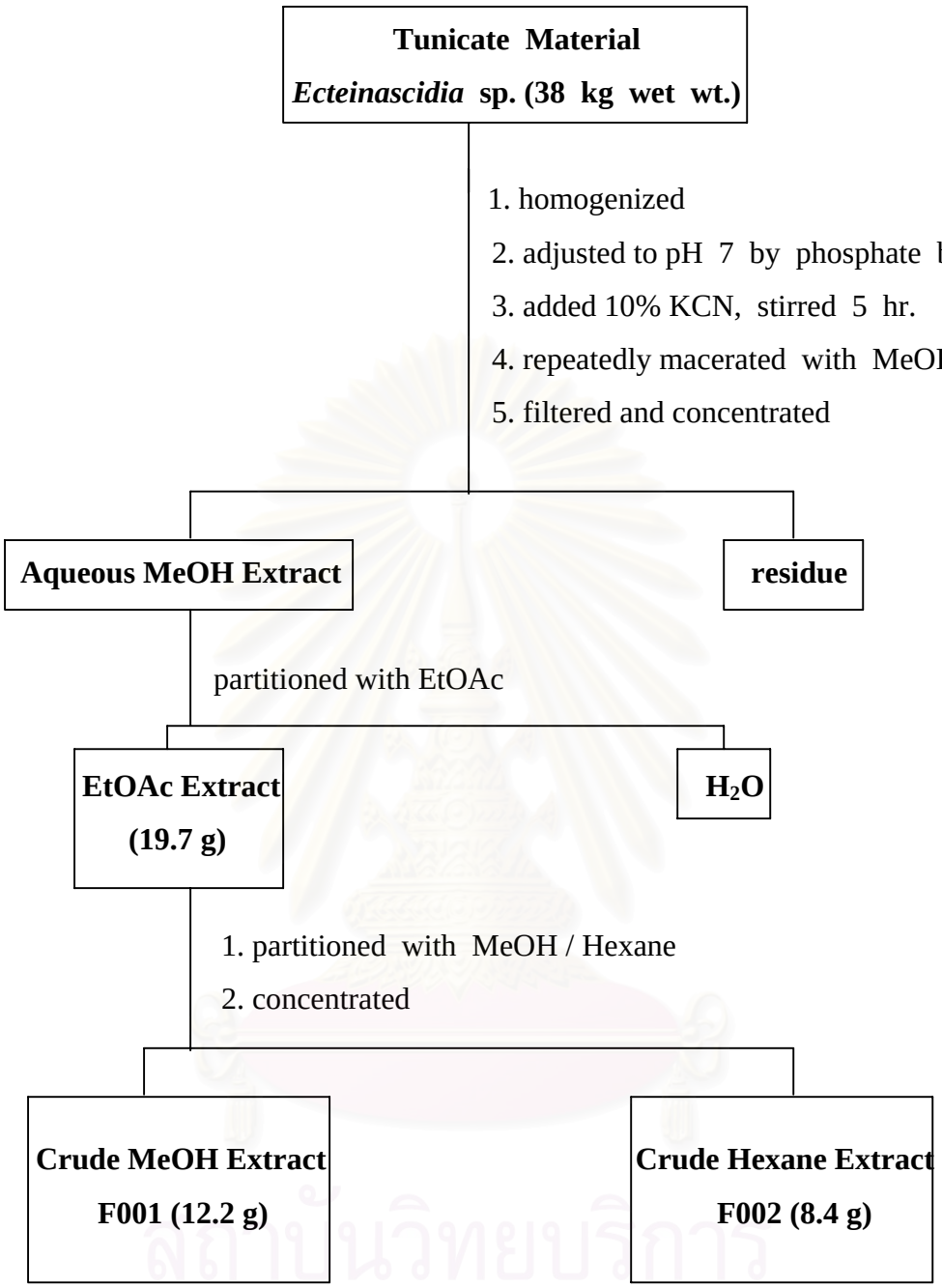

Scheme 2. Extraction of a Thai *Ecteinascidia* tunicate.

5. Isolation of chemical constituents from a Thai *Ecteinascidia* tunicate

The methanol extract F001 (12.2 g) was fractionated by gel filtration chromatography. It was dissolved in a small amount of a mixture of chloroform-methanol (1:1) and added on the top of a Sephadex LH-20 column (column 2.5 x 70 cm) using a mixture of chloroform-methanol (1:1) as the eluting solvent. Fractions of 25 ml each were collected and combined according to TLC patterns (by using 20% methanol in chloroform as the developing solvent) and evaporated to dryness to give 6 fractions, F003-F008, as shown in Table 1.

Table 1 Combined fractions from F001.

Fraction	Number of eluate	Total weight (g)
F003	1-2	2.5
F004	3-4	5.2
F005	5	1.7
F006	6	0.9
F007	7-8	0.5
F008	9-20	1.1

Each fraction was examined by proton NMR measurement. Fraction F004 (5.2 g) showed intense characteristic signals of the ecteinascidins, therefore it was further isolated by gel filtration chromatography. The column was eluted with EtOAc. Fractions (25 ml each) were collected and combined according to TLC patterns by using 10% methanol in chloroform as the developing solvent to give 5 fractions, F009-F013, as shown in Table 2.

Table 2 Combined fractions from fraction F004.

Fraction	**Number of eluate**	**Total weight (g)**
F009	1-2	0.4
F010	3-6	3.0
F011	7-12	0.5
F012	13-17	0.2
F013	18-22	0.9

5.1 Isolation of ecteinascidin 770 (ET1K) from fractions F010, F025, and F032

A white powder precipitated from the fraction F010 was recrystallized in a mixture of chloroform and ethyl acetate to give fine needle crystals (131 mg, 0.67 % by weight of the ethyl acetate extract) and assigned as ET1K (see Scheme 3). Compound ET1K gave a quenching spot on TLC when detected with UV at 254 nm (Si gel, 10% methanol in chloroform, R_f = 0.56) and was later identified as ecteinascidin 770 (Section 2.1, Chapter IV).

Fraction F010 (2.0 g) was further separated by Sephadex LH-20 column (column 2.5 x 60 cm) using a mixture of ethyl acetate-hexane (9:1) as the eluting solvent. Fractions of 25 ml each were collected and combined according to TLC patterns by using 10% methanol in chloroform as the developing solvent to give 4 fractions, F023-F026, as shown in Table 3.

Table 3 Combined fractions from fraction F010.

Fraction	Number of eluate	Total weight (mg)
F023	1-3	130
F024	4	540
F025	5-8	800
F026	9-15	170

A white powder precipitated from the fraction F025 was recrystallized in a mixture of $CHCl_3$-EtOAc to give fine needle crystals (66 mg, 0.33 % by weight of the ethyl acetate extract). This compound gave the same R_f value in the same solvent system as ET1K as shown in Scheme 3.

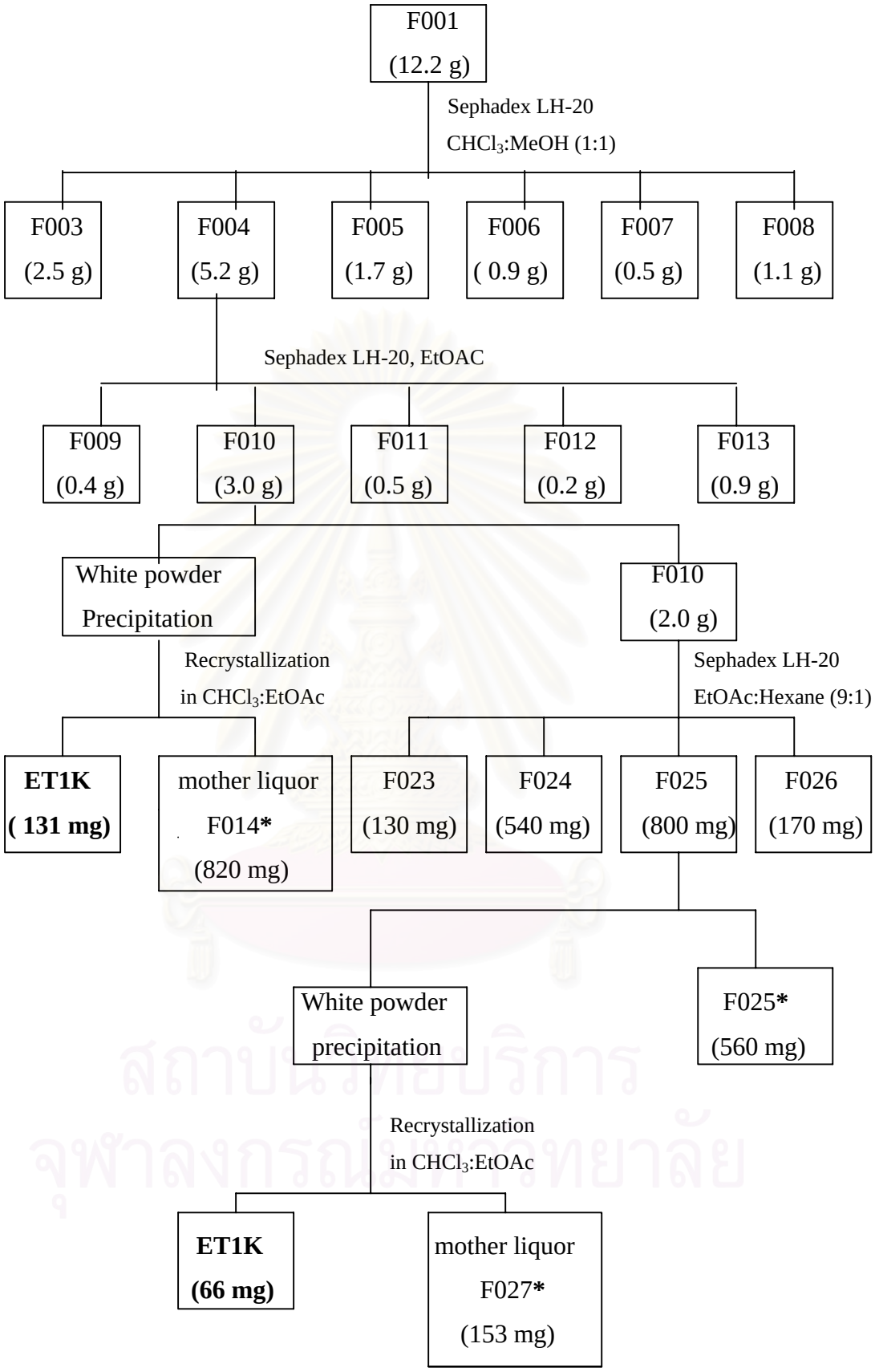

Scheme 3 Isolation of the methanol extract (F001).

***** was further separated.

Fraction F025 (560 mg) was further separated by silica gel column (column 2.5 x 20 cm) using a mixture of ethyl acetate-hexane (4:1) as the eluting solvent. Sixteen fractions (each 25 ml) were collected. The eluates were pooled according to TLC patterns (Si gel, 10% methanol in chloroform as the developing solvent) to give 4 fractions, F031-F034, as shown in Table 4.

Table 4 Combined fractions from fraction F025.

Fraction	Number of eluate	Total weight (mg)
F031	1-4	230
F032	5-7	80
F033	8-9	39
F034	10-16	70

White powder precipitated from the fraction F032 was recrystallized in a mixture of chloroform and ethyl acetate to give fine needle crystals (27 mg, 0.13 % by weight of ethyl acetate extract). This compound gave the same R_f value in the same solvent system as ET1K (Scheme 4).

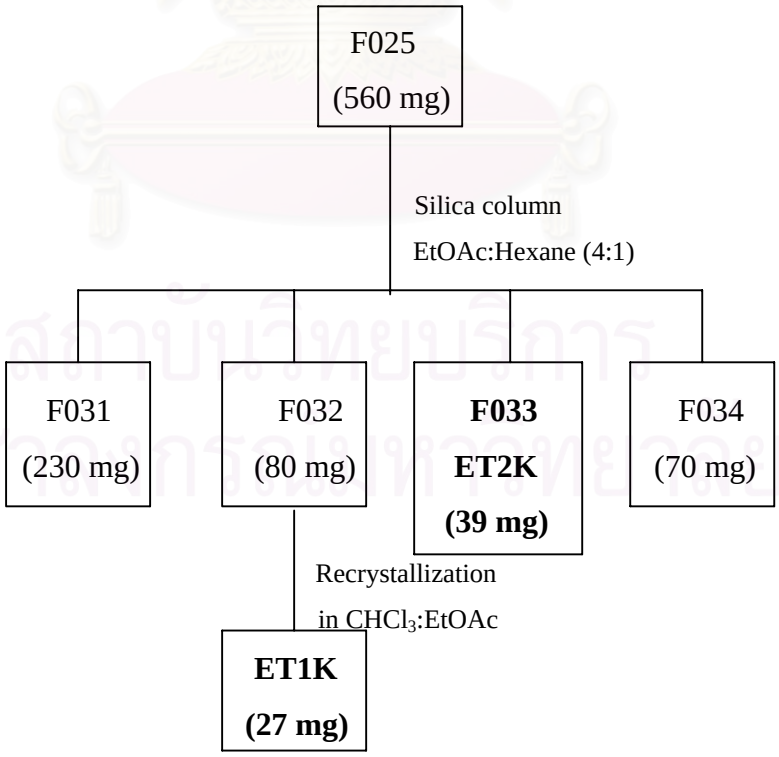

Scheme 4 Separation of fraction F025.

5.2 Isolation of ecteinascidin 786 (ET2K) from fractions F014 and F027

The mother liquor (F014, 820 mg) was fractionated on Sephadex LH-20 gel filtration column (column 2.5 x 70 cm) using a chloroform-methanol (2:1) as the eluting solvent. Fractions (25 ml) were collected and combined by using TLC technique (10% methanol in chloroform). Fractions with the same TLC patterns were concentrated to give 3 fractions, F015-F017, as shown in Table 5.

Table 5 Combined fractions from fraction F014.

Fraction	Number of eluate	Total weight (mg)
F015	1-3	10
F016	4-6	570
F017	7-12	20

The TLC chromatogram (Si gel, 20% hexane in ethyl acetate) of fraction F016 (570 mg) showed interesting spot at R_f = 0.44 and therefore the fraction was further separated by a silica gel column (column 2.5 x 20 cm, 38.5g of Si gel) using an isocratic elution of ethyl acetate-hexane (4:1) to give 5 fractions, F018-F022. The fractions (25 ml each) were combined according to their TLC patterns, developed with the solvent system of EtOAc:hexane (4:1) as shown in Table 6.

Table 6 Combined fractions from fraction F016.

Fraction	**Number of eluate**	**Total weight (mg)**
F018	1	167
F019	2-4	145
F020	5-6	97
F021	7-13	17
F022	14-30	84

Fraction F021 contained compound ET2K (17 mg, 0.09 % by weight of the ethyl acetate extract) which was later elucidated as ecteinascidin 786 (Section 2.2, Chapter IV) as shown in Scheme 5.

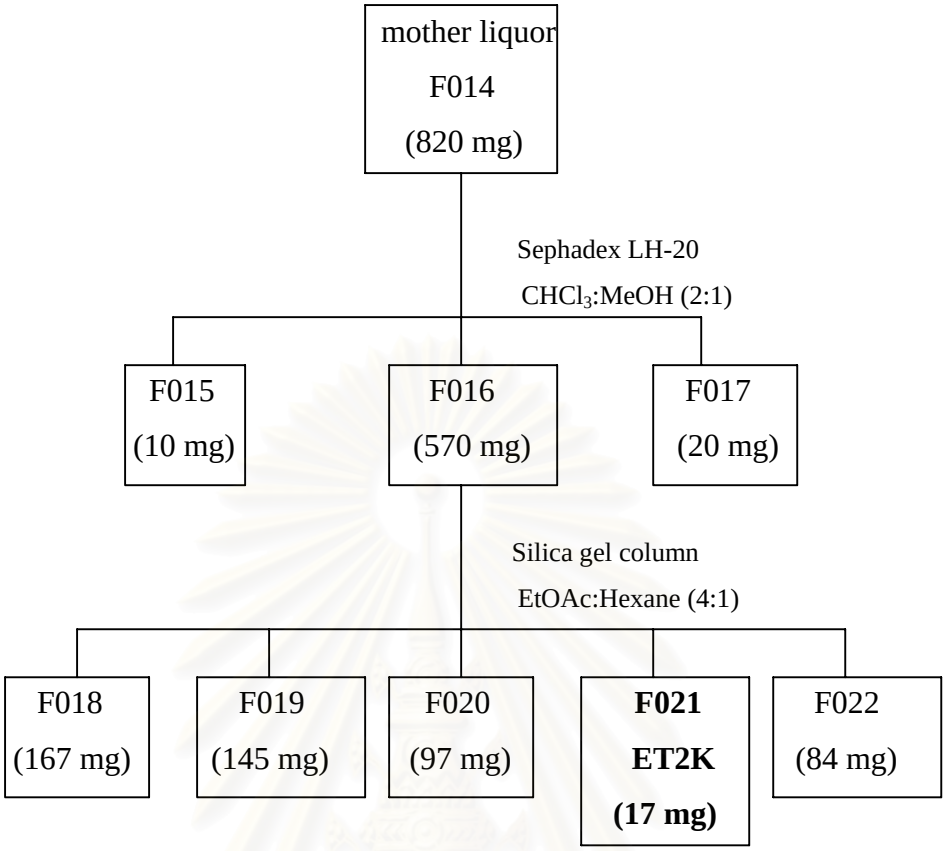

Scheme 5 Isolation of the mother liquor (F014).

The mother liquor (F027, 153 mg) was further separated by a silica gel column (column 2.5 x 20 cm, 38.5 g of Si gel) using an isocratic elution of ethyl acetate-hexane (4:1). Eleven fractions (25 ml) were collected and combined guided by TLC technique (20% hexane in ethyl-acetate the developing solvent). Fractions with the same TLC patterns were concentrated to give 3 fractions, F028-F030, as shown in Table 7.

Table 7 Combined fractions from fraction F027.

Fraction	Number of eluate	Total weight (mg)
F028	1-2	40
F029	4-6	8
F030	7-11	20

The TLC chromatogram (Si gel, 20% hexane in ethyl acetate) of fraction F029 (8 mg, 0.04 % by weight of the ethyl acetate extract) gave the same R_f value as ET2K (Scheme 6).

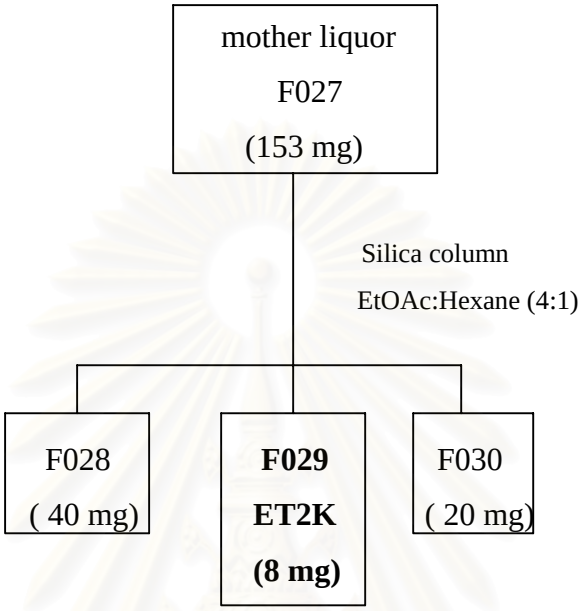

Scheme 6 Isolation of the mother liquor (F027).

Fraction F025 was separated into 4 fractions as previously mentioned (Table 4), and fraction F033 (39 mg, 0.20 % by weight of the ethyl acetate extract) gave the same R_f value as ET2K (see Scheme 4).

5.3 Isolation of thymidine (ET3K)

Fractions F006 and F007 were combined and renamed as fraction F035 (1.1 g). The TLC chromatogram (Si gel, 10% methanol in chloroform) of this fraction showed an interesting spot at R_f = 0.08, and, hence, it was further fractionated by using Sephadex LH-20 gel filtration column. The column (2.5×70 cm) was eluted with MeOH:$CHCl_3$:hexane (1:3:1) to give 5 fractions as shown in Table 8.

Table 8 Combined fractions from fraction F035.

Fraction	Number of eluate	Total weight (mg)
F036	1-2	20
F037	3-6	390
F038	7-8	300
F039	6-10	290
F040	11-20	50

Fraction F038 (300 mg) was further separated on a silica gel flash column (column 2.5 x 20 cm, 38.5 g of Si gel) using a gradient elution of $CHCl_3$ and MeOH from $CHCl_3$: MeOH (19:1) to 100% MeOH to yield 5 fractions, F041-F045, as shown in Table 9.

Table 9 Combined fractions from fraction F038.

Fraction	Number of eluate	Total weight (mg)
F041	1-3	120
F042	4-5	30
F043	6-10	6
F044	11-15	40
F045	17-34	30

Colorless rosette crystals were obtained from fraction F043 (6 mg, 0.03 % by weight of the ethyl acetate extract). This compound showed black color spot after spraying with anisaldehyde reagent and was assigned as ET3K (shown in Scheme 7). It was later identified as thymidine (Section 2.4, Chapter IV).

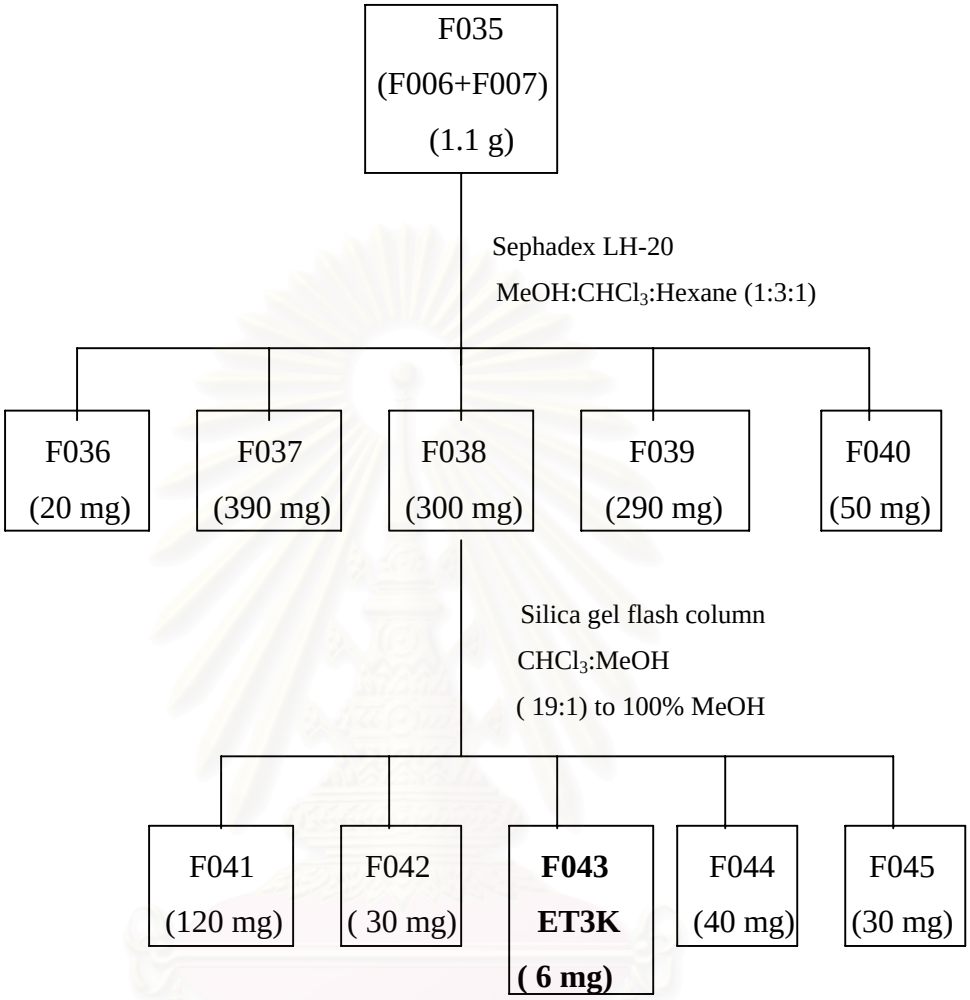

Scheme 7 Separation of fraction F035.

6. Conversion of ecteinascidin 770 to ecteinascidin 743

(Cuevas *et al.*, 2000)

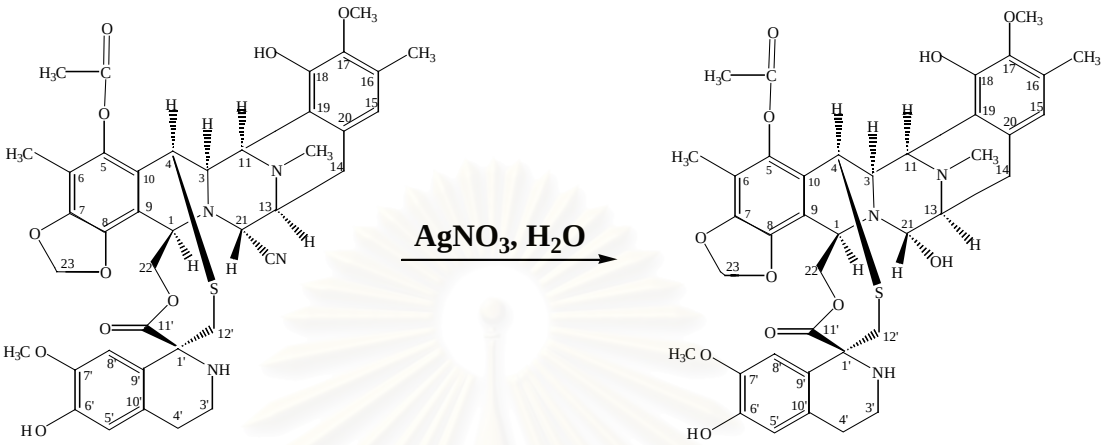

ecteinascidin 770 (ET1K) ecteinascidin 743 (ET4K)

Figure 4 Conversion of ecteinascidin 770 to ecteinascidin 743.

Ecteinascidin 770 (23 mg, 0.03 mM) was dissolved in a mixture of acetonitrile and water (3:2 (v/v), 7.5 ml), and solid silver nitrate (102 mg, 0.6 mM, 20 equiv.) was added. The suspension was stirred at room temperature for 26 hrs at which time a mixture of saturated aqueous sodium chloride solution and saturated aqueous sodium bicarbonate solution (1:1 (v/v), 18.75 ml) was added. The mixture was stirred vigorously for 10 min and partitioned between a mixture of saturated aqueous sodium chloride solution and saturated aqueous sodium bicarbonate solution (1:1 (v/v), 60 ml) and dichloromethane (3x60 ml). The combined organic layers were dried with sodium sulfate anhydrous and filtered through a pad of celite. The filtrate was concentrated to give ET4K (19 mg, 80 % yield), which was investigated by using NMR technique to determine the structure and later identified as ecteinascidin 743 (Section 2.3, Chapter IV).

7. Biolgical activity

7.1 Cytotoxic activity

Cytotoxic assay was performed according to the sulforhodamine B (SRB) colorimetric method (Skehan *et al.*, 1990) using breast cancer cells (BC), human epidermoid carcinoma cells of the nasopharynx (KB), and Vero cells. The results are expressed as ED_{50} (μM) and IC_{50} (μg/ml), respectively.

7.2 Antituberculosis activity

Antituberculosis activity was investigated by using the microplate alamar blue assay (MABA). The candidate compounds were tested against *Mycobacterium tuberculosis* $H37R_a$ strain. The minimum inhibition concentrations (MICs) of the candidate compounds were measured as μg/ml (Collins and Franzblau, 1997).

CHAPTER IV

RESULTS AND DISCUSSION

1. Comparative study of the extraction methods

A large amount of ET 743 is currently required for clinical trial phase II study. At this stage, ET 743 has been supplied from both natural source, the Caribbean tunicate *Ecteinascidia turbinata* and synthesis source. However, both approaches are unlikely suitable for the ecteinascidin demand because of their low total yields.

For the production of ET 743 from natural source, research for tunicate cultivation is still underway. Therefore, the efficient extraction and isolation method must be studied to improve the yield since ET 743 was isolated from the tunicate in the yield of $1x10^{-4}$% wet weight (Rinehart *et al*.,1990a).

The Thai *Ecteinascidia* tunicate sample from the Andaman sea was used to comparatively study the conventional extraction method **(A)** with the modified one **(B)** as shown in Scheme 8.

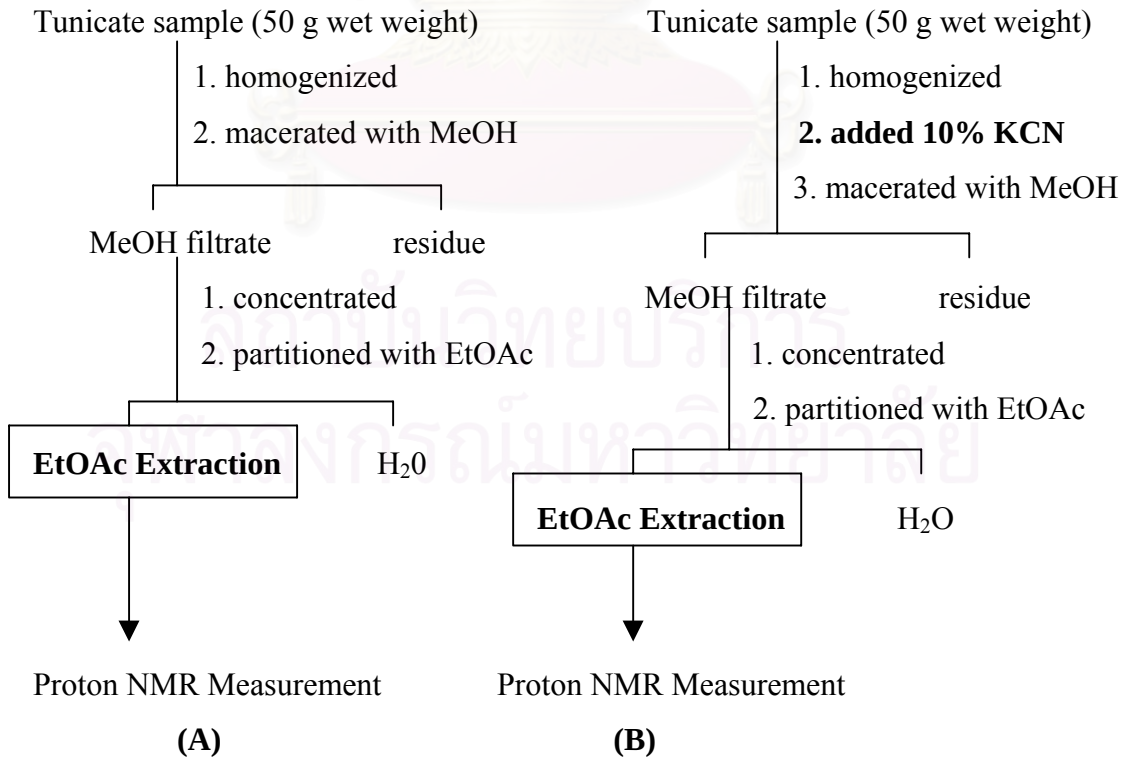

Scheme 8 Comparison of the conventional extraction method with the modified extraction method.

Both ethyl acetate extracts were measured for their proton NMR spectra (Figure 11). The proton NMR spectrum of the extract from **(B)** clearly showed more intense characteristic aromatic proton signals of the ecteinascidins (δ 5.5 to 6.5 ppm) than that of the extract from **(A)**.

2. Structure elucidation of the isolated compounds

The *Ecteinascidia* tunicate (38 kg wet weight) was homogenized and treated with KCN, and then macerated with methanol. The concentrated methanol extract was successively partitioned with ethyl acetate to yield 19.7 g of the ethyl acetate extract which was re-dissolved in methanol and partitioned with hexane. Both extracts were evaporated under reduced pressure to yield 12.2 g of the methanol extract and 8.4 g of the hexane extract ($3.2x10^{-2}$% and $2.2x10^{-2}$% of wet weight, respectively). Three compounds were isolated from the methanol extract. Compound ET1K (224 mg, $5.9x10^{-4}$% of wet weight) was obtained as fine needle crystals by recrystallization from the fractions F010, F025, and F032 using the mixture of $CHCl_3$ and EtOAc. Compound ET2K (64 mg) and ET3K (6 mg) were separated from the methanol extract by using several chromatographic techniques. The percentage yields of the compounds were $1.7x10^{-4}$% and $1.6x10^{-5}$% based on the sample wet weight, respectively. Compound ET4K, (19 mg) was obtained by treatment of compound ET1K with $AgNO_3$. The chemical structures of these compounds were characterized according to analyses of their spectroscopic data including MS, IR, UV, and NMR spectroscopy, together with literature data comparison.

2.1 Structure elucidation of ecteinascidin 770 (ET1K)

Compound ET1K was isolated as colorless prisms from MeOH, mp. 214-216°C (dec.); and fine needle crystals from EtOAc, mp. 223-226°C (dec.); $[\alpha]^{23}_D$ -58.51° (c = 1.0 g/dl, $CHCl_3$). This compound has the molecular formula $C_{40}H_{42}N_4O_{10}S$ as deduced by ESI-TOF MS (Figure 12) showing a protonated molecular ion peak of $[M+H]^+$ at m/z 771, which indicated twenty two degrees of unsaturation.

The UV spectrum (Figure 13) exhibited λ_{max} at 240 (ε 13860) and 286 nm (ε 6237). The IR spectrum (Figure 14) showed absorption bands for hydroxy at

3560 cm^{-1} , amine at 3450 cm^{-1}, cyanide (CN) at 2250 cm^{-1}, and ester carbonyls at 1740 and 1770 cm^{-1}.

The 300 MHz ^{1}H NMR spectrum (Figure 15) of ET1K showed the signals attributable to an *N*-methyl protons at δ 2.17 ppm (12-NCH_3), two aromatic methyl protons appearing as two singlets at δ 2.01 ppm (6-CH_3) and 2.29 ppm (16-CH_3). Two methoxy groups were presented as two singlets at δ 3.76 ppm (17-OCH_3) and δ 3.59 ppm (7′-OCH_3). The methyl protons of an acetoxyl group were at δ 2.24 ppm (5-OAc). The ^{1}H-NMR spectrum also showed two doublets with J = 1.2 Hz at δ 6.02 ppm (1H) and 5.95 ppm (1H) which were assigned as bisoxymethylene protons at C-23. Three singlets of aromatic protons at 6.58 ppm, 6.44 ppm, and 6.42 ppm were assigned to H-15, H-5′, and H-8′, respectively. The signals of two phenolic hydroxyl protons were at δ 5.77 ppm (18-OH) and 5.45 ppm (6′- OH).

The 75 MHz ^{13}C NMR spectral data in $CDCl_3$ (Figure 16) showed forty signals. The DEPT-90 (Figure 17), DEPT-135 (Figure 17), and HMQC (Figure 18) spectra of ET1K were used to classify the types of carbons and their connectivity with nearby protons. The 75 MHz ^{13}C NMR spectrum possessed the signals of two methyl carbons connecting to double bonds at δ 9.8 ppm (6-CH_3) and 15.9 ppm (16-CH_3); an *N*-methyl carbons at δ 41.7 ppm (12-NCH_3); an acetate methyl carbon at δ 20.5 ppm (5-OAc); two methoxy carbons at δ 60.3 ppm (17-OCH_3) and 55.2 ppm (7′-OCH_3). Three sp^2 methine carbons appeared at δ 120.6 ppm (C-15), 114.0 ppm (C-5′), and 109.7 ppm (C-8′); whereas six sp^3 methine carbons appeared at δ 61.2 ppm (C-1), 59.7 ppm (C-3), 41.9 ppm (C-4), 54.8 ppm (C-11), 54.7 (C-13), and 59.7 ppm (C-21) and six sp^3 methylene carbons at δ 24.3 ppm (C-14), 60.0 ppm (C-22), 39.7 ppm (C-3′), 28.9 ppm (C-4′), and 42.3 ppm (C-12′). The most downfield sp^3 methylene carbon signal at δ 101.8 ppm (C-23) was the methylenedioxy carbon. There were nineteen quaternary carbon signals in the ^{13}C NMR spectrum, of which the most upfield quaternary carbon was at δ 64.6 ppm (C-1′). The downfield quaternary carbon signals at δ 141.2 ppm (C-5), 145.1 ppm (C-7), 139.9 ppm (C-8), 142.9 ppm (C-17), 147.6 ppm (C-18), 144.4 ppm (C-6′), and 144.1 ppm (C-7′) were assignable to oxygenated sp^2 carbons. The carbon signals at δ 113.3 ppm (C-6), 114.0 ppm (C-9), 121.1 ppm (C-10), 129.1 ppm (C-16), 118.0 ppm (C-19), 130.6 ppm (C-

20), and 125.6 ppm (C-9′) were defined as un-oxygenated sp^2 quaternary carbons. One quaternary carbon signal at δ 118.0 ppm (21-CN) was that of a sp carbon connected to a nitrogen atom. The most downfield carbon signals at δ 167.9 (5-O<u>C</u>OCH$_3$) and 172.3 ppm (C-11′) were those of ester carbonyl carbons. The ^{1}H and ^{13}C NMR assignments of ET1K were achieved by interpretation of the data obtained from the ^{1}H -^{1}H COSY spectrum (Figure 19), TOCSY spectrum (Figure 20), and long-range ^{1}H-^{13}C connectivities which were determined through a series of the ^{1}H-detected 2D HMBC ($^nJ_{HC}$ = 8 Hz, Figures 21-24 and 4 Hz, Figure 25) experiments.

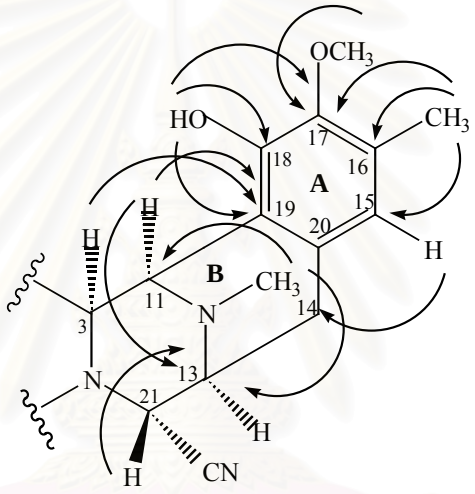

The aromatic substituents of ring A were assigned as follows: methyl group has been located at C-16 based upon ^{1}H-^{13}C long-range correlations (HMBC) of H-15 to the 16-CH$_3$ carbon and of the 16-CH$_3$ protons to both C-15 and C-16. The position of C-17 was assigned on the basis of ^{1}H-^{13}C long-range correlations of the H-15 and 16-CH$_3$ protons to C-17. The chemical shift of C-17 (δ 142.9 ppm) suggested an oxygen substitution. A methoxy group was attached to C-17 based upon long-range correlation of the 17-OCH$_3$ protons to C-17, whereas C-18 was confirmed by the HMBC correlation between H-11 and C-18. The position of C-19 (118.0 ppm) was assigned by the HMBC correlations of H-3, H-11, H-14, and H-15 to C-19. The HMBC correlations of H-11 and H-14 to the quaternary carbon signal at δ 130.6 ppm helped in the assignment of that carbon signal as that of C-20. And also, from the

HMBC spectral data, the 18-OH showed long-range correlations to C-17, C-18, and C-19, confirming the 18-OH as located on C-18.

Closure of B ring was achieved by insertion of a nitrogen between C-11 and C-13. The positions of C-11 and C-13 were determined by ^{1}H-^{13}C long-range correlations of H-11 and H-21 to C-13. The HMBC correlations were also observed between the 12-NCH_3 protons and both C-11 and C-13, which therefore placed the N-CH_3 group at position 12. C-14 was confirmed by ^{1}H-^{13}C long-range correlation observed between H-15 and C-14.

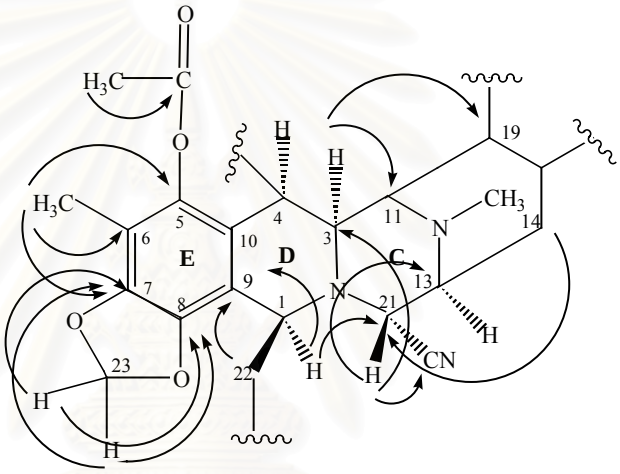

The C, D, and E rings were elucidated based on the following arguments: the C ring was formed by insertion of a nitrogen between C-1, C-3, and C-21, which was confirmed by the chemical shifts of C-3 and C-21 as well as the HMBC correlations between H-21 to C-3 and between H-1 and H-14 to C-21. The positions of C-1 and C-22 were confirmed by the ^{1}H-^{13}C long-range correlations between H-22 to C-9 and C-11′ and between H-1 to C-9. The 21-CN carbon was assigned as the carbon signal at δ 118.0 ppm which showed ^{1}H-^{13}C long-range correlation between H-21 and the 21-CN carbon. The ^{1}H -^{1}H COSY and TOCSY spectra suggested that C-4 and C-12′ were not vicinal but was separated by insertion of a sulfur atom. The sulfur attached to C-4 could be identified by NMR resonances of H-4 at δ 4.54 ppm and C-4 at δ 41.9 ppm, very similar to the other ecteinascidins (Wright, 1990). A methylene carbon at δ 42.3 ppm (C-12′) correlated to very broad proton signals at δ 2.11 ppm and 2.31 ppm (H-12′) was also assignable to a sulfide-

substituted methylene carbon. The substituents on the E ring were confirmed as follows: the downfield chemical shifts of C-7 (δ 145.1 ppm) and C-8 (δ 139.9 ppm) both suggested oxygen substitution. The HMBC correlations were observed between the bisoxymethylene protons, H_2-23, and C-8 and C-7. The 6-CH_3 protons have long-range correlations to C-5, C-6, and C-7 which helped in assigning the positions of these three carbons. A methyl group was located at C-6 based upon ^{1}H-^{13}C long-range correlation observed between the 6-CH_3 protons and C-6.

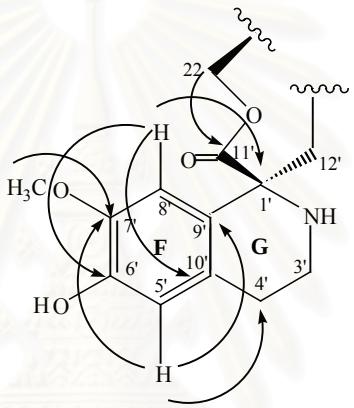

The isoquinoline ring (F and G) was assigned from the HMBC correlations of H-5′ to C-4′ and H-8′ to C-1′. The positions of C-7′ and C-9′ were both confirmed by the HMBC correlations between H-5′ and the 7′-OCH_3 protons to C-7′ which located the methoxy group at this position and H-5′ to C-9′. The H-8′ also displayed long-range correlations to C-6′ and C-10′ which suggested the positions of these two carbons. The position of the carbonyl C-11′ was assigned by the HMBC correlation between H-22 and C-11′.

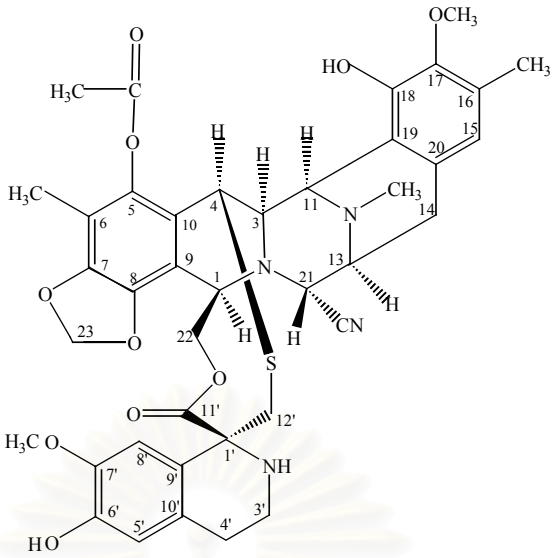

Figure 5 Structure of ecteinascidin 770 (ET1K).

The relative stereochemistries at C-1, C-3, C-4, C-11, and C-13 of ET1K were deduced from NOESY experiments (Figures 26-28). The clear ^{1}H-^{1}H NOE correlations of H-1/H-3/H-4/H-11/H-13 assured the α-orientation of these protons in the molecule. Substitution of the cyano group at the α-position of C-21 was confirmed by the following ^{1}H-^{1}H NOE correlations H-21 to H_2-14, H-1, and H-13 and no correlation between H-21 and H-3. These stereochemistries of ET1K was found to be the same as those of other reported ecteinascidins (Wright, 1990).

ET1K was identified as ecteinascidin 770 (ET 770), which was previously obtained from ET 743 of *Ecteinascidia turbinata* by treatment with KCN (Rinehart *et al*., 1991a). The assignments of protons and carbons for the structure of ET1K with ^{1}H-^{13}C long-range correlations are summarized in Table 10.

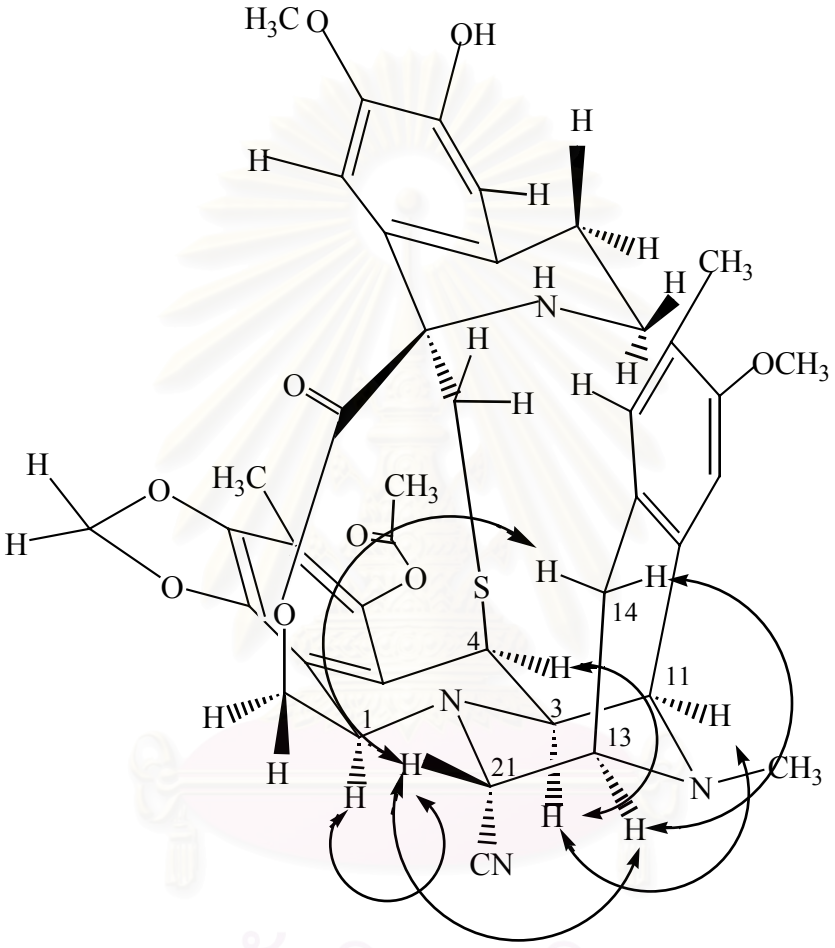

Figure 6 Correlations observed in the NOESY spectrum of ecteinascidin 770 (ET1K).

Table 10 ^{1}H and ^{13}C NMR spectral data and ^{1}H-^{13}C long-range correlations in the HMBC spectra of ET1K[a].

Position	δ_C(ppm)	δ_H(ppm), mult. (*J* in Hz)	HMBC ($^nJ_{HC}$ = 8Hz)	HMBC ($^nJ_{HC}$ = 4Hz)
1	61.2	4.32, br s	C-9, C-21	–
3	59.7	3.50, d (4.4)	C-11, C-19	C-21
4	41.9	4.54, br s	–	–
5	141.2	–	–	–
6	113.3	–	–	–
7	145.1	–	–	–
8	139.9	–	–	–
9	114.0	–	–	–
10	121.1	–	–	–
11	54.8	4.26, d (4.4)	C-3, C-4, C-13, C-18, C-19, C-20	C-3, C-18, C-19, C-20
13	54.7	3.40, m	C-11	–
14	24.3	2.92, 2H, m	C-13, C-15, C-19, C-20, C-21	–
15	120.6	6.58, s	16-CH_3, C-14, C-17, C-19	16-CH_3
16	129.1	–	–	–
17	142.9	–	–	–
18	147.6	–	–	–
19	118.0	–	–	–
20	130.6	–	–	–
21	59.7	4.16, d (2.3)	C-3 C-13, 21-CN	C-13
22	60.0	α 4.12, dd (11.4, 2.1) β 5.01, d (11.4)	C-9, C-11′	C-11′, C-9, C-1
23	101.8	6.02, s 5.95, s	C-7, C-8	C-7, C-8
1′	64.6	–	–	–
3′	39.7	α 3.07, ddd (10.9, 10.5, 4.3) β 2.76, m	–	–
4′	28.9	α 2.44, m β 2.59, m	– –	– –
5′	114.0	6.44, s	C-4′, C-6′, C-7′, C-9′	C-4′, C-6′, C-7′
6′	144.4	–	–	–
7′	144.1	–	–	–

Table 10 (continued)

Position	**δ_C(ppm)**	**δ_H(ppm), mult. (*J* in Hz)**	**HMBC (^nJ = 8Hz)**	**HMBC ($^nJ_{HC}$ = 4Hz)**
8′	109.7	6.42, s	C-1′, C-4′, C-6′, C-7′, C-10′,	C-1′, C-4′, C-6′, C-7′, C-9′
9′	125.6	–	–	–
10′	129.0	–	–	–
11′	172.3	–	–	–
12′	42.3	2.31, d 2.11, d	–	–
5-O<u>C</u>OCH$_3$	167.9	–	–	–
5-OCO<u>C</u>H$_3$	20.5	2.24, s	5-O<u>C</u>OCH$_3$	5-O<u>C</u>OCH$_3$
6-CH$_3$	9.8	2.01, s	C-5, C-6, C-7	C-5, C-6, C-7, C-8
16-CH$_3$	15.9	2.29, s	C-15, C-16, C-17	C-15, C-16, C-17, C-19
17-OCH$_3$	60.3	3.76, s	C-17, C-18	C-11, C-17, C-18
7′-OCH$_3$	55.2	3.59, s	C-6′, C-7′	C-7′
12-NCH$_3$	41.7	2.17, s	C-11, C-13	C-11, C-13
21-CN	118.0	–	–	–
18-OH	–	5.77, s	C-17, C-18, C-19	C-17, C-18, C-19
6′-OH	–	5.45, br s	–	–

[a]recorded in $CDCl_3$.

Table 11 Comparison of ^{1}H NMR spectral data of ET1K[a] with ET 770[a,b].

Position	δ_H(ppm), mult, (*J* in Hz)	
	ET1K[a]	**ET 770[a,b]**
1	4.32, br s	4.32, br s
3	3.50, d (4.4)	3.50, d (5)
4	4.54, br s	4.57, br s
11	4.26, d (4.4)	4.28, d (5.3)
13	3.40, m	3.42, m
14	2.92, 2H, m	2.94, m
15	6.58, s	6.60, s
21	4.16, d (2.3)	4.18, d (2.5)
22	α 4.12, dd (11.4, 2.1) β 5.01, d (11.4)	4.12, dd (11.5, 2.1) 5.02, d (11)
23	6.02, s 5.95, s	6.05, s 5.98, s
3′	α 3.07, ddd (10.9, 10.5, 4.3) β 2.76, m	3.10, ddd (11, 10, 4) 2.79, m
4′	α 2.44, m β 2.59, m	2.47, m 2.61, m
5′	6.44, s	6.47, s
8′	6.42, s	6.45, s
12′	2.31, d 2.11, d	2.34, d 2.09, d
5-OCO$\underline{C}H_3$	2.24, s	2.27, s
6-CH_3	2.01, s	2.04, s
16-CH_3	2.29, s	2.32, s
17-OCH_3	3.76, s	3.78, s
7′-OCH_3	3.59, s	3.62, s
12-NCH_3	2.17, s	2.20, s
18-OH	5.77, s	–
6′-OH	5.45, br s	–

[a]recorded in $CDCl_3$

[b]Rinehart *et al*., 1990a

2.2 Structure elucidation of ecteinascidin 786 (ET2K)

The ESI-TOF mass spectrum of ET2K (Figure 29) showed a protonated molecular ion $[M+H]^+$ at m/z 787 implying a molecular formula $C_{40}H_{42}N_4O_{11}S$, which had one more oxygen atom than ET1K. The compound had melting point of 197-199°C (dec.) and $[\alpha]^{23}_D$ -156.9 ^{o} (c = 0.6, $CHCl_3$). The UV spectrum of ET2K (Figure 30) displayed maximum absorption at 243 nm (ϵ 15720) and 289 nm (ϵ 8332). The IR spectrum (Figure 31) revealed the absorption bands at ν_{max} 3430 cm^{-1} (hydroxyl OH), 3300 cm^{-1} (amine NH), 2250 cm^{-1} (cyanide CN), 1730 cm^{-1} and 1760 cm^{-1} (ester carbonyl).

The 500 MHz ^{1}H NMR spectrum of ET2K in $CDCl_3$ (Figure 32) exhibited two methoxy protons at δ 3.85 ppm (3H, s; 17-OCH_3) and δ 3.63 ppm (3H, s; 7'-OCH_3), six methylene protons at δ 3.01 ppm (1H, dd, *J* = 17.2, 9.2 Hz; H-14α); 2.69 ppm. (1H, d, *J* = 17.7 Hz; H-14β); 4.31 ppm (1H, dd; *J* = 11.6, 2.1 Hz ; H-22α); 4.59 ppm (1H, d, *J* = 11.6 Hz; H-22β); 2.99 ppm (1H, ddd, *J* = 12.2, 8.2, 4.0 Hz ; H-3'α); 2.86 ppm (1H, ddd, *J* = 12.2, 5.2, 4.9 Hz; H-3'β); 2.46 ppm (1H, ddd, *J* = 15.9, 5.2, 4.0 Hz ; H-4' α); 2.61 ppm (1H, ddd, *J* = 15.9, 8.2, 4.9 Hz; H-4'β); 2.18 ppm (1H, d, *J* = 14.3 Hz; H-12'α); 3.66 ppm (1H, d, *J* = 14.3 Hz; H-12' β); and bisoxymethylene δ 6.06 ppm (1H, d, *J* = 1.2 Hz) and δ 6.01 ppm (1H, d, *J* = 1.2 Hz). Four methyl proton signals at δ 2.27, 2.06, 2.31, and 2.24 ppm were assigned to 5-OAc, 6-CH_3, 16-CH_3, and 12-NCH_3, respectively.

The 125 MHz ^{13}C NMR spectrum of ET2K in $CDCl_3$ (Figure 33) displayed forty carbon signals. Classification of these carbon signals by DEPT-135 and DEPT-90 (Figure 34) experiments indicated two methoxy carbons at δ 60.4 ppm and δ 55.2 ppm, nine methine carbons (δ 54.6, 54.9, 60.0, 60.6, 60.7, 71.0, 109.4 114.5, and 122.6 ppm), and nineteen quaternary carbons. According to the HMQC spectrum (Figures 35-36), three downfield methine carbon signals at δ 122.6 ppm (C-15), δ 114.5 ppm (C-5'), and δ 109.4 ppm (C-8') were aromatic carbons. The downfield quaternary carbon signals at δ 142.2 ppm (C-5), 146.1 ppm (C-7), 140.7 ppm (C-8), 147.0 ppm (C-17), 148.0 ppm (C-18), 145 ppm (C-6'), and 144.7 ppm (C-7') appeared to be those of oxygenated carbons. The most downfield carbon signals at δ 168.9 ppm(5-O<u>C</u>OCH_3) and δ 171.8 ppm (C-11') were ester carbonyl carbons. One

quaternary carbon signal at δ117.6 ppm (21-CN) was that of a carbon connected to a nitrogen atom.

The ^{1}H-^{1}H COSY spectrum of ET2K (Figure 37) exhibited the correlations of the coupled protons as follows: H-3'α (δ 2.99 ppm) was coupled with H-3'β (2.86 ppm) with *J* = 12.2 Hz of geminal coupling and was vicinal coupled with H-4'α (δ 2.46) and H-4'β (δ 2.61); H-4'α was coupled with H-4'β with *J* = 15.9 Hz of geminal coupling; H-14β (δ 2.69 ppm) was geminal coupled with H-14α (δ 3.01 ppm) with *J* = 17.7 Hz and was coupled with H-13 (δ 3.43 ppm) with *J* = 9.2 Hz; H-13 was coupled with H-21 (δ 4.07 ppm) and H-11 (δ 4.67 ppm) with *J* = 2.8 and 1.2 Hz, respectively; H-11 was vicinal coupled with H-3 (δ 3.74 ppm) with *J* = 4.3 Hz; H-22 α (δ 4.31 ppm) was coupled with H-22 β (δ 4.59 ppm) with *J* = 11.6 Hz of geminal coupling and H-1 (δ 4.31 ppm) in vicinal coupling; and H-12' α (δ 2.18 ppm) was coupled with H-12' β (δ 3.66 ppm) with *J* = 14.3 Hz of geminal coupling.

Structure determination of ET2K was finally accomplished by the HMBC spectrum ($^{n}J_{HC}$ = 8 Hz) (Figures 38-40). The assignments of protons and carbons and long-range correlations of ET2K are summarized in Table 12.

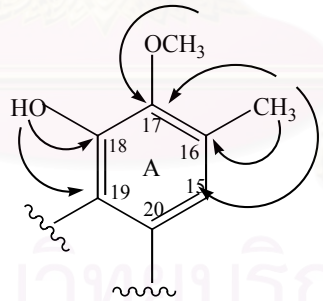

The aromatic substituents of the ring A were assigned as follows: the signal at δ 122.6 ppm was assigned to C-15 based on ^{1}H-^{13}C long-range correlations observed between C-15 and the H-14 and 16-CH_3 protons. A methyl group (δ 16.0 ppm) was located on C-16 (δ 130.6 ppm) based on ^{1}H-^{13}C long-range correlation between the 16-CH_3 protons and C-16. A methoxyl group at δ 60.4 ppm (17-OCH_3) was attached to C-17 (δ 147.0 ppm) based on ^{1}H-^{13}C long-range correlation between the 17-OCH_3 protons and C-17. The 18-OH showed ^{1}H-^{13}C long-range correlations to C-18 and C-19, suggesting that the 18-OH was located on C-18 (δ 148.0 ppm).

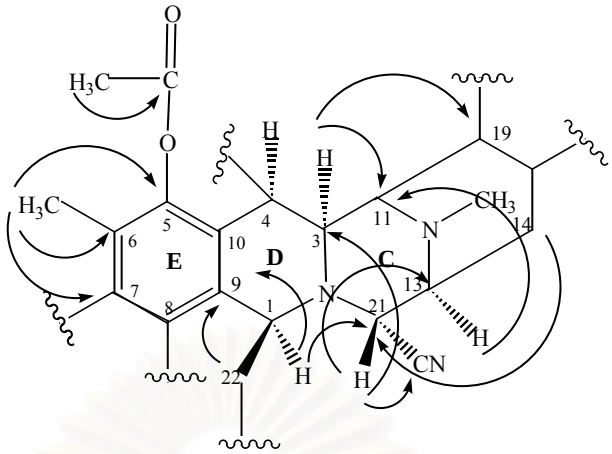

The B, C, D, and E rings were determined as follows: the position C-11 (δ 54.9 ppm) and C-13 (δ 54.6 ppm) were assigned by long-range ^{1}H-^{13}C correlations of H-3 and H-13 to C-11 and H-11, H-14α, H-21 to C-13. The N-CH_3 group was located at position 12, which was confirmed by long-range ^{1}H-^{13}C correlations observed between the 12-NCH_3 protons and C-11 and C-13. The chemical shift of C-21 (δ 60.6 ppm) was confirmed by HMBC correlations of H-1 and H-14α to C-21. The cyano group at position 21, which was assigned to the carbon signal at δ 117.6 ppm by a long-range ^{1}H-^{13}C correlation between H-21 to 21-CN carbon. The downfield chemical shifts of both C-7 (δ 146.1 ppm) and C-8 (δ 140 ppm) suggested oxygen substitution at these positions. The ^{1}H-^{13}C long-range correlations were also observed between the bisoxymethylene protons to C-7 and C-8. The positions C-5 (δ 142.2 ppm), C-6 (δ 114.1 ppm), and C-7 (δ 146.1 ppm) were assigned according to HMBC correlations observed between the 6-CH_3 protons and these three carbons. Comparison of the ^{13}C signals of C-4 and C-12′ of ET2K with those of ET 770 revealed the downfield shifts of C-4 (δ 71.0 ppm in ET2K and δ 41.9 ppm in ET 770) and C-12′ (δ 67.7 ppm in ET2K and δ 42.3 ppm in ET 770). The data suggested the replacement of the sulfide bridge by the sulfoxide functional group between the two carbons.

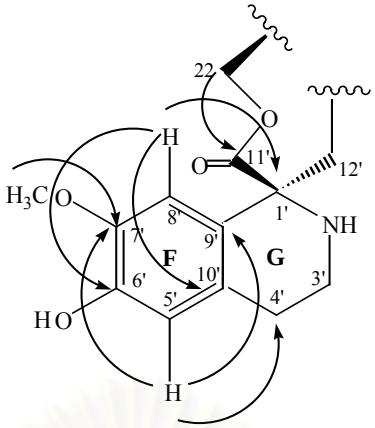

On the G ring, C-4' (δ 29.1 ppm) and C-7′ (δ 144.7 ppm) were assigned by the long-range ^{1}H-^{13}C correlations observed between H-5' and these two carbon signals. The proton H-8' displayed ^{1}H-^{13}C long-range correlations to C-1' (δ 61.6 ppm), C-6' (δ 145.0 ppm), and C-10' (δ 129.5 ppm), therefore confirmed the positions of the three carbons.

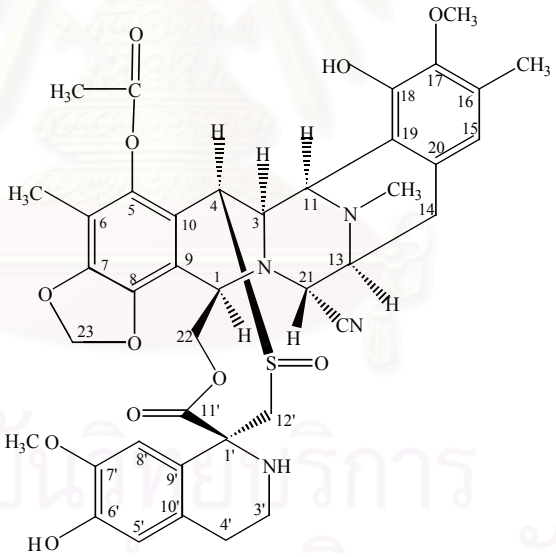

Figure 7 Structure of ecteinascidin 786 (ET2K).

Relative stereochemistries of ET2K at C-1, C-3, C-4, C-11, and C-13 were found to be the same as those of ET 770 by the correlations observed from NOESY experiments (Figures 41-42). The cross-peak between H-21 and H-14β

confirmed that 21-CN was in the same α-position as in ET 770. ET2K was identified as a new ecteinascidin derivative, ecteinascidin 786 (ET 786).

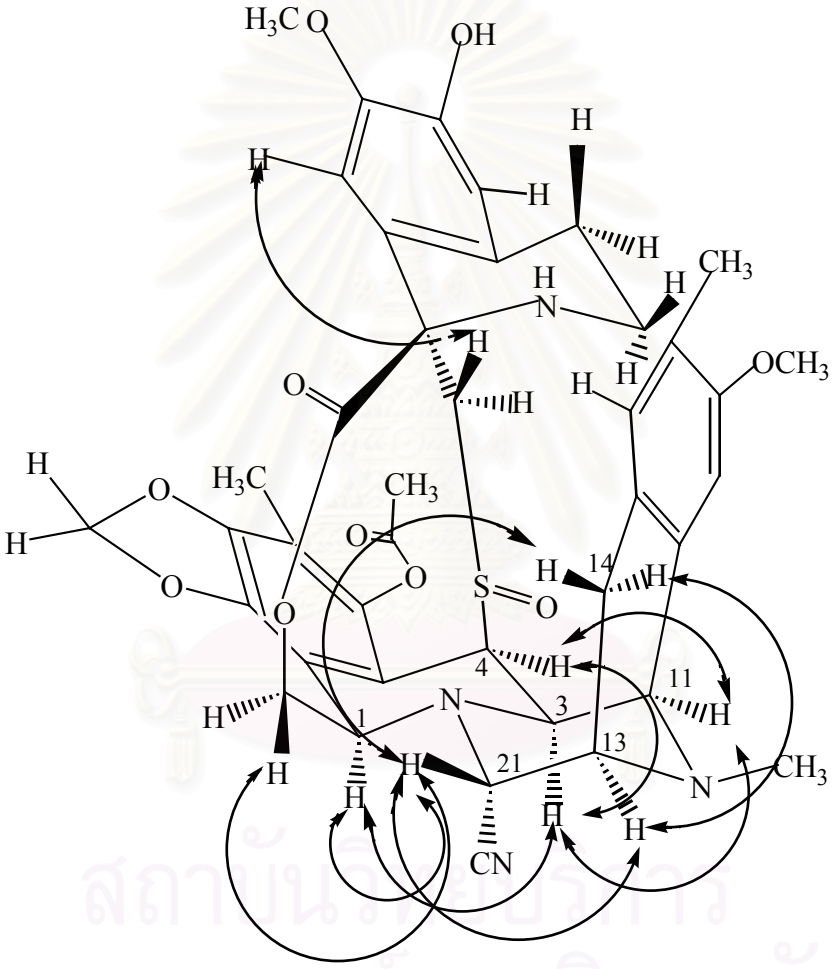

Figure 8 Correlations observed in the NOESY spectrum of ecteinascidin 786 (ET2K).

Table 12 ^{1}H and ^{13}C NMR spectral data and ^{1}H-^{13}C long-range correlations in the HMBC spectrum of ET2K[a].

Position	δ_C(ppm)	δ_H(ppm), mult. (*J* in Hz)	HMBC ($^nJ_{HC}$ = 8Hz)
1	60.7	4.31, d (2.1)	C-8, C-9, C-10, C-21
3	60.0	3.74, dd (4.3, 2.8)	C-11, C-19,
4	71.0	4.19, br s	–
5	142.2	–	–
6	114.1	–	–
7	146.1	–	–
8	140.7	–	–
9	111.6	–	–
10	120.3	–	–
11	54.9	4.67, dd (4.3, 1.2)	C-13, C-18, C-19, C-20
13	54.6	3.43, ddd (9.2, 2.8, 1.2)	C-11, C-20
14	24.9	α 3.01, dd (17.7, 9.2) β 2.69, d (17. 7)	C-13, C-15, C-19, C-20, C-21
15	122.6	6.65, s	16-CH_3, C-14, C-17, C-19
16	130.6	–	–
17	147.0	–	–
18	148.0	–	–
19	120.2	–	–
20	129.4	–	–
21	60.6	4.07, d (2.8)	C-3, C-13, 21-CN
22	61.8	α 4.31, dd (11.6, 2.1) β 4.59, d (11.6)	C-1, C-9, C-11′
23	102.3	6.06, d (1.2) 6.01, d (1.2)	C-7, C-8
1′	61.6	–	–
3′	39.9	α2.99, ddd (12.2, 8.2, 4.0) β 2.86, ddd (12.2, 5.2, 4.9)	–
4′	29.1	α 2.46, ddd (15.9, 5.2, 4.0) β 2.61, ddd (15.9, 8.2, 4.9)	–
5′	114.5	6.49, s	C-4′, C-7′, C-9′
6′	145.0	–	–
7′	144.7	–	–
8′	109.4	6.19, s	C-1′, C-6′, C-9′, C-10′
9′	124.5	–	–

Table 12 (continued)

Position	δ_C(ppm)	δ_H(ppm), mult. (*J* in Hz)	HMBC ($^nJ_{HC}$ = 8Hz)
10′	129.5	–	–
11′	171.8	–	–
12′	67.7	α 2.18, d (14.3) β 3.66, d (14.3)	–
5-O<u>C</u>OCH$_3$	168.9	–	–
5-OCO<u>C</u>H$_3$	20.8	2.27, s	5-O<u>C</u>OCH$_3$
6-CH$_3$	10.1	2.06, s	C-5, C-6, C-7
16-CH$_3$	16.0	2.31, s	C-15, C-16, C-17
17-OCH$_3$	60.4	3.85, s	C-17
7′-OCH$_3$	55.2	3.63, s	C-7′
12-NCH$_3$	41.8	2.24, s	C-11, C-13
21-CN	117.6	–	–
18-OH	–	6.37, s	C-18, C-19
6′-OH	–	5.49, br s	–

[a]recorded in $CDCl_3$

2.3 Structure elucidation of ecteinascidin 743 (ET4K)

Compound ET4K was a product from the reaction of ET 770 (ET1K) with $AgNO_3$ in water. The ESI-TOF MS of ET4K (Figure 43) showed a protonated molecular ion $[M+H]^+$ peak at m/z 762 corresponding to the tentative molecular formula $C_{39}H_{43}N_3O_{11}S$ and also presented $[MH^+-H_2O]$ peak at m/z 744. The 9 mass unit different from ET 770 suggested the replacement of the cyano group in ET 770 by hydroxyl group in ET4K. The UV spectrum (Figure 44) showed absorption maxima at λ_{max} 245 nm (ε 15220) and 286 nm (ε 8219). The IR spectrum (Figure 45) suggested the presence of hydroxy OH at ν_{max} 3423 cm^{-1}, ester carbonyl (C=O) at 1741 cm^{-1}. Optical rotation $[\alpha]^{25}_D$ was -54.52°C (c = 0.16, $CDCl_3$).

The 300 MHz ^1H NMR spectrum in $CDCl_3$ of ET4K (Figure 46) showed a number of recognizable groups of signals including those of three aromatic protons at δ 6.58 ppm (H-15), 6.41 ppm (H-5') and 6.44 ppm (H-8'); two aromatic methyl groups at δ 2.01 ppm (6-CH_3) and 2.29 ppm (16-CH_3); two aromatic methoxyls at δ 3.78 ppm (17-OCH_3) and 3.58 ppm (7'-OCH_3); an *N*-methyl at δ 2.15 ppm (12-NCH_3); an aromatic methylenedioxy unit at δ 5.91 and 5.99 ppm (H_2-23) and one methyl group of an acetate group at δ 2.24 ppm (5-OAc).

Analyses of the 75 MHz ^{13}C NMR (Figure 47), DEPT-135, and DEPT-90 (Figure 48) NMR spectra revealed that compound ET4K contained six methyl carbons which appeared as signals at δ 20.4 ppm (5-OAc), 9.7 ppm (6-CH_3), 15.8 ppm (16-CH_3), 41.4 ppm (12-NCH_3), 60.3 ppm (17-OCH_3), and 55.1 ppm (7'-OCH_3). Six methylene carbon signals appeared at δ 24.0 ppm (C-14), 61.4 ppm (C-22), 101.6 ppm (C-23), 39.7 ppm (C-3'), 28.8 ppm (C-4'), and 42.1 ppm (C-12'), whereas nine methine carbons at δ 55.9 ppm (C-1), 57.7 ppm (C-3), 42.1 ppm (C-4), 54.9 ppm (C-11), 57.8 ppm (C-13), 120.9 (C-15), 82.1 ppm (C-21), 114.0 ppm (C-5'), and 109.8 ppm (C-8'). A missing quaternary carbon signal (at δ 168.3 ppm) of the 5-OAc ester carbonyl was identified through its correlation in the HMBC spectrum with the methyl proton signal of that acetyl group at δ 2.24 ppm. The absence of the cyano carbon signal at δ 118.0 ppm and the presence of the carbon signal of C-21 at δ 82.1 ppm clearly demonstrated that the hydroxy group must be located at C-21. This was also confirmed by the absence of CN absorption in the IR spectrum. The NOESY

spectrum (Figures 52-53) showed correlation between H-21 and H-14, therefore establishing 21-OH as in the alpha position.

From the ^{1}H-^{1}H COSY (Figure 50) and HMQC (Figure 49) spectra all protonated carbons could be assigned. The HMBC experiment (Figure 51) showed long-range correlations between ^{1}H and ^{13}C signals, which helped in assigning carbon positions. The 300 MHz ^{1}H NMR and 75 MHz ^{13}C NMR data of compound ET4K were compared with those of ecteinascidin 743 isolated from *Ecteinascidia turbinata* (Table 13), and conclusively confirmed that ET4K is identical to ecteinascidin 743. These ^{1}H and^{13}C NMR data of compound ET4K including long-range HMBC correlations are summarized in Table 13.

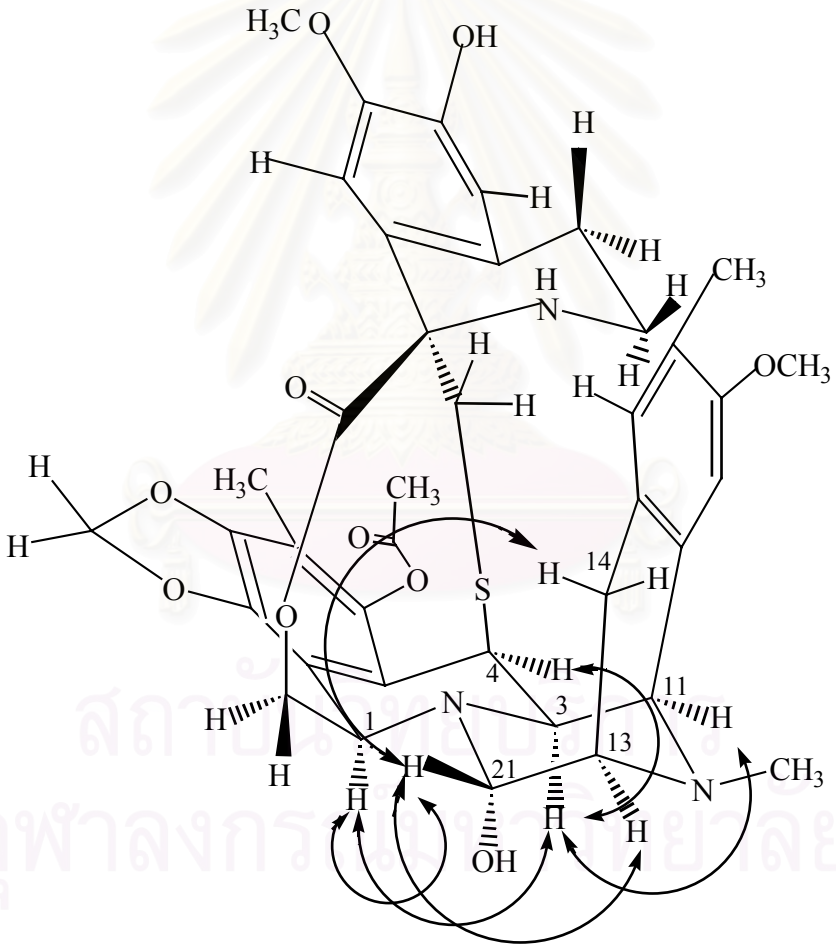

Figure 9 Correlations observed in the NOESY spectrum of ecteinascidin 743 (ET4K).

Table 13 Comparison of ^{1}H and ^{13}C NMR spectral data of ET4K and ecteinascidin 743 and ^{1}H-^{13}C long-range correlations in the HMBC spectrum of ET4K[a].

Position	ET4K[a]			ET743[a,b]	
	δ_C (ppm)	δ_H(ppm), mult. (*J* in Hz)	HMBC ($^nJ_{HC}$ = 8Hz)	δ_C (ppm)	δ_H(ppm), mult. (*J* in Hz)
1	55.9	4.79, br s	C-8, C-9, C-21	56.0	4.83, br s
3	57.7	3.54, d (4.8)	C-19	57.7	3.59, d (4.4)
4	42.1	4.45, d (3.0)	–	42.1	4.50 br s
5	141.3	–	–	141.3	–
6	114.1	–	–	112.5	–
7	145.1	–	–	145.1	–
8	140.5	–	–	140.4	–
9	115.9	–	–	115.9	–
10	121.8	–	–	121.8	–
11	54.9	4.15, d (4.9)	C-19, C-20	54.9	4.18, dd (4.2, 1.6)
13	57.8	3.18, br d (6.2)	–	57.8	3.23, m
14	24.0	2.85, 2H, m	C-21	24.1	2.91, d (18.0) 2.88, dd (18.0, 9.2)
15	120.9	6.58, s	16-CH_3, C-17, C-19	120.9	6.62, s
16	129.2	–	–	129.1	–
17	142.9	–	–	142.9	–
18	147.7	–	–	147.5	–
19	117.9	–	–	117.9	–
20	131.5	–	–	131.5	–
21	82.1	4.45, d (3.0)	–	82.1	4.50, d (3.3)
22	61.4	α 4.00, dd (11.2, 2.1) β 5.08, d (11.2)	C-9, C-11′	61.3	4.06, dd (11.3, 2.5) 5.14, dd (11.3, 0.9)
23	101.6	5.99, s 5.91, s	C-7, C-8	101.6	5.95, d (1.2) 6.03, d (1.2)
1′	64.6	–	–	64.7	–
3′	39.7	α 3.09, ddd (15.4, 10.6, 3.8) β 2.79, m	–	39.7	3.14, ddd (11.8, 9.8, 4.2) 2.82 (11.8, 5.4, 3.8)
4′	28.8	α 2.45, d (15.9) β 2.59, m	–	28.9	2.49, ddd (15.7, 4.2, 3.8) 2.62, ddd (15.7, 9.8, 5.4)
5′	114.0	6.41, s	C-4′, C-6′, C-7′, C-9′	114.9	6.48, s
6′	144.4	–	–	144.4	–

Table 13 (continued)

Position	ET4K[a]			ET743[a,b]	
	δ_C (ppm)	δ_H(ppm), mult. (*J* in Hz)	HMBC ($^nJ_{HC}$ = 8Hz)	δ_C (ppm)	δ_H(ppm), mult. (*J* in Hz)
7′	144.2	–	–	144.2	–
8′	109.8	6.44, s	C-6′, C-7′, C-9′, C-10′	109.8	6.46, s
9′	126.0	–	–	126.0	–
10′	129.1	–	–	129.0	–
11′	172.5	–	–	172.5	–
12′	42.1	2.15 2.34	–	42.2	2.18, d (13.9) 2.37, d (13.9)
5-O<u>C</u>OCH$_3$	168.3	–	–	168.3	–
5-OCO<u>C</u>H$_3$	20.4	2.24, s	5-O<u>C</u>OCH3	20.4	2.28, s
6-CH$_3$	9.7	2.01, s	C-5, C-6, C-7	9.7	2.04, s
16-CH$_3$	15.8	2.29, s	C-15, C-16, C-17	15.8	2.33, s
17-OCH$_3$	60.3	3.78, s	C-17	60.3	3.81, s
7′-OCH$_3$	55.1	3.58, s	C-6′, C-7′	55.1	3.63, s
12-NCH$_3$	41.4	2.15, s	C-11, C-13, C-21	41.4	2.19, s

[a]recorded in $CDCl_3$

[b]Rinehart *et al*., 1990a

2.4 Structure elucidation of thymidine (ET3K)

Compound ET3K was obtained as colorless rosette crystals, and its TLC spot (silica gel) showed black color after spraying with anisaldehyde reagent. The ESI-TOF MS (Figure 54) of ET3K showed a molecular ion peak $[M+H]^+$ at *m/z* 243 corresponding to the molecular formular $C_{10}H_{14}O_5N_2$. The mass spectra have a fragment ion at *m/z* 127 due to the loss of one molecule of deoxy sugar and also showed a fragment ion at 117 m/z due to loss of pyrimidine base. The UV spectrum (Figure 55) showed absorption maxima at λ_{max} at 215 nm (ε 3973). and 266 nm (ε 6998). The IR spectrum (Figure 56) indicated the presence of hydroxyl group at ν_{max} 3396 cm^{-1} , an amide group at 3250 cm^{-1} , an amide carbonyl group at 1694 cm^{-1}.

The 300 MHz ^1H NMR spectrum (Figure 57) of this compound, recorded in DMSO-d_6, showed 13 proton signals including those of four methine protons (δ 3.73, 4.22, 6.15, and 7.61 ppm), two methylene protons (δ 2.08 and 3.52 ppm), two hydroxyl groups (δ 5.01 and 5.22 ppm), one methyl protons (δ 1.75 ppm) and one amide proton (δ 11.27 ppm). Analyses of the 75 MHz ^{13}C (Figure 58), DEPT-135 and DEPT-90 (Figure 59) NMR spectra revealed the presence of ten signals of carbons which could be classified into those of one methyl carbon at δ 12.4 ppm (CH_3-5); two methylene carbons at δ 39.6 (C-2′) and 61.5 ppm (C-5′); four methine carbons at δ 136.3 (C-6), 83.9 (C-1′), 70.6 (C-3′), and 87.4 ppm (C-4′); and three quaternary carbon at δ 150.6 (C-2), 163.9 (C-4), and 109.5 ppm (C-5), which two out of these three quaternary carbons were amide carbonyls (C-2 and C-4).

The 2′-deoxy sugar part was analyzed through the ^1H-^1H COSY spectrum (Figure 61), which demonstrated the coupling of H-1′ triplet at δ 6.15 ppm to H-2′ multiplet at δ 2.08 ppm with the coupling constant of 6.8 Hz. The H-2′ multiple showed further coupling with the broad singlet of H-3′ at δ 4.22 ppm, which, in turn, showed coupling with H-4′ doublet at δ 3.73 ppm (J = 2.9 Hz). In addition, the 3′-OH doublet at δ 5.22 ppm was coupled with H-3′ (J = 3.9 Hz), while the H-4′ alternately coupled with H-5′ multiplet at δ 3.52 ppm. Finally, the 5′-OH triplet at δ 5.01 ppm also showed coupling with H-5′ with the coupling constant of 4.9 Hz.

These spectral evidences suggested the linkage of C-1′/C-2′/C-3′/C-4′/C-5′/C-3′/3′-OH and C-5′/5′-OH.

The complete carbon and proton assignments of compound ET3K were achieved by the analysis of HMQC (Figure 60) and HMBC (Figure 62) spectra.

The quaternary carbon assignments were determined by the long-range coupling observed in the HMBC spectra (Figure 62). The signal at δ 150.6 ppm was assigned as C-2 by the long range coupling with H-6 (δ 7.61 ppm). The signal at δ 163.9 ppm was assigned as C-4 by the long range coupling with 5-CH_3 (δ 1.75 ppm) and H-6 (δ 7.61 ppm). Analyses of the spectral data indicated that compound ET3K was thymidine or thymine-2′-deoxyriboside. The ^{1}H and ^{13}C NMR data of compound ET3K with long-range correlations are summarized in Table 14.

Thymidine is a nucleoside composed of a pyrimidine base and a deoxysugar (deoxyribose). The pyrimidine base is thymine which can be found in DNA. There have been reports showing that some tunicates such as a *Didemnum voeltzkowi* (Mitchell *et al*., 1996) also produced thymidine.

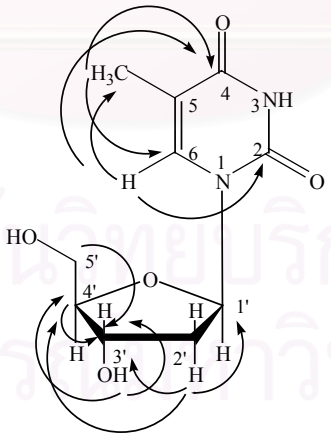

Figure 10 The long-range heteronuclear correlations observed in the HMBC spectrum of thymidine (ET3K).

Table 14 ^{1}H and ^{13}C NMR spectral data and ^{1}H-^{13}C long-range correlations in the HMBC spectrum of ET3K[a].

Position	δ_C(ppm)	δ_H(ppm), mult. (*J* in Hz)	HMBC (^nJ = 8 Hz
2	150.6	–	–
4	163.9	–	–
5	109.5	–	–
6	136.3	7.61, br s	5-CH_3, C-2, C-4
5-CH_3	12.4	1.75	C-4, C-6
1′	83.9	6.15, t (6.83)	–
2′	39.6	2.08, m	C-1′, C-3′, C-4′
3′	70.6	4.22, br s	–
4′	87.4	3.73, d (2.9)	C-3′
5′	61.5	3.52, m	C-3′
3′-OH	–	5.22, d (3.9)	C-3′, C-4′
5′-OH	–	5.01, t (4.9)	–
3-NH	–	11.27, s	–

[a]recorded in DMSO-d_6.

3. Biological activity of the isolated compounds

3.1 Cytotoxic activity

The isolated compounds were tested for cytotoxic activity against KB cells, BC cells and Vero cells . The results are shown in Table 15.

Table 15 Cytotoxic activity of the ecteinascidins.

Compound	**KB cells** ED_{50} **(μM)**	**BC cells** ED_{50} **(μM)**	**Vero cells** IC_{50} **(μM)**
ET 770	3.4×10^{-2}	3.2×10^{-3}	-
ET 786	1.5×10^{-1}	4.3	-
ET 743	-	-	$2.7x10^{-2}$

Compounds ET 770 and ET 786 were strongly cytotoxic to KB and BC cells. ET 743 showed cytotoxic activity against Vero cells.

3.2 Antituberculosis activity

The isolated compounds were tested for antituberculosis activity against *Mycobacterium tuberculosis* $H37R_a$ by microplate alamar blue assay (MABA). The results are shown in Table 16.

Table 16 Antituberculosis activity of the ecteinascidins.

Compound	***Mycobacterium tuberculosis*** **MIC (μg/ml)**
ET 770	0.1
ET 786	1.56

Compounds ET 770 and ET 786 showed antituberculosis activity against *Mycobacterium tuberculosis* $H37R_a$ at MIC of 0.1 and 1.56 μg/ml, respectively.

Compound ET 786, which contains the sulfoxide group, is less active than compound ET 770, which has the sulfide group, in both cytotoxicity and antituberculosis activity.

CHAPTER V

CONCLUSION

A specimen of a Thai tunicate, *Ecteinascidia* sp., was collected from Phuket. We reported the isolation method for more stable ecteinascidins by treatment of the tunicate with KCN before the extraction. The first isolated compound was identified as ecteinascidin 770, which showed potent cytotoxicity against human epidermoid carcinoma cells of the nasopharynx and breast cancer cells with ED_{50} of $3.4x10^{-2}$ and $3.2x10^{-3}$ μM, respectively. The antituberculosis activity of ecteinascidin 770 against *Mycobacterium tuberculosis* was at MIC of 0.1 μg/ml. This is the first report of the antituberculosis activity of this compound, which might be due to its cytotoxic activity. The second isolate was elucidated as a new ecteinascidin derivative, ecteinascidin 786, which also exhibited potent cytotoxicity against human epidermoid carcinoma cells of the nasopharynx and breast cancer cells with ED_{50} of $1.5x10^{-1}$ and 4.3 μM, respectively. The antituberculosis activity of ecteinascidin 786 against *Mycobacterium tuberculosis* was at MIC of 1.56 μg/ml. The third compound was ecteinascidin 743, which was produced by treatment of ecteinascidin 770 with $AgNO_3$, in 80% yield and showed cytotoxic activity against Vero cells at IC_{50} 2.7×10^{-2} μM. Ecteinascidin 743 is a promising anticancer agent which is currently being studied in clinical trials phase II. The last compound was determined as thymidine, which has been reported from a *Didemnum voeltzkowi*.

In order to obtain higher yield of ecteinascidin 743 from natural sources, addition of KCN into the tunicate suspension might be applied for the extraction method. Ecteinascidin 743 is converted to the more stable cyano-derivative ET 770 before the extraction. After the isolation, the cyano-derivative is able to be reconverted to the hydroxy derivative ET 743.

The information gained in this study is valuable for further research on the chemical constituents of the genus *Ecteinascidia*.

REFERENCES

Badre, A., Boulanger, A., Mansour, A. E., Banaigs, B., Combaut, G., and Francisco, C. 1994. Eudistomin U and isoeudistomin U, new alkaloids from the Caribbean ascidian *Lissoclinum fragile*. J. Nat. Prod. 57 (4): 528-533.

Bonfanti, M., Caretti, G., La Valle, E., Sousa Faro, J. M. F., Faircloth, G., Mantonvani, R., and D' Incalci, M. 1999. Effect of ecteinascidin-743 (ET-743) on the interaction between DNA binding proteins and DNA. Anti-Cancer Drug Res. 14: 179-186.

Bradley, S. D. 1993. Ascidians: Producers of amino acid derived metabolites. Chem. Rev. 93: 1771-1791.

Canonico, P. G., Pannier, W. L., Huggins, J. W., and Rinehart, K. L., 1982. In hibition of RNA viruses *in vitro* and in rift Valley fever-infected mice by didemnins A and B. Antimicrob. Agents Chemother. 22: 696-697.

Carroll, A. R., Bowden, B. F., Coll, I. C., Hockless, D. C. R., Skelton, B. W., and White, A. H. 1994. Studies of Australian ascidians. IV Mollamide, a cytotoxic cyclic heptapeptide from the compound ascidian *Didemnum molle*. Aust. J. Chem. 47: 61-69.

Ciufolini, A. M., and Shen, Y.– C. 1995. Total synthesis of cystodytin J, diplamine and shermilamine B. Tetrahedron Lett. 36 (27): 4709-4712.

Collins, L. A., and Franzblau, S. G. 1997. Microplate alama blue assay versus BACTEC 460 system for high-throughput screening of compounds against *Mycobacterium avium*. Antimicrob. Agents Chemother. 41 (5): 1004-1009.

Corey, E. J., Gin, D. V., and Kania, R. S. 1996. Enantioselective total synthesis of ecteinascidin 743. J. Am. Chem. Soc. 118: 9202-9203.

Cuevas, C., Perex, M., Martin, M. J., Chicharro, J. L., Fernandez-Rivas, C., Flores, M., Francesch, A., Gallego, P., Zarzeelo, M., Calle, F., Garcia, J., Polanco, C., Rodriguz, I., and Manzanares, I. 2000. Synthesis of the ecteinascidin ET-743 and phthalascidin pt-650 from cyanosafracin B. Org. Lett. 2 (16): 2515-2548.

Dematte, N., *et al*. 1985. A screening of some colonial ascidiacea of Banyuls-sur-Mer of antibacterial and antifungal activities and, preliminarily for natural products: 2′-Deoxyribonucleosides from *Trididemnum cereum* (Giard, 1872). Com. Biochem. Physiol. 81B (2): 479-484.

Dewick, P. M. 1997. Alkaloids. Medicinal Natural Products: a Biosynthetic Approach, pp. 285. New york: John Wiley & Sons, Inc.

Erba, E., Bergamaschi, D., Bassano, L., Damia, G., Ronzoni, S., Faircloth, G. T., and D'Incalci, M. 2001. Ecteinascidin-743 (Et-743), a natural marine compound with a unique mechanism of action. Eur. J. Cancer 37 (1): 97-105.

Erba, E., Bergamaschi, D., Ronzoni, S., Faretta, M., Bassano, L., Cappella, P., Valoti, G., Riavazzi, R., Jimeno, J., Faircloth, G., D' Incalci, M., and Nergri, M. 1998. Mode of action of ecteinascidin 743, a natural marine compound with antitumoral activity. Ann. Oncol. 9 Suppl. 2: 139.

Evans, W. C. 1996. Biologically active compounds from marine organisms. Trease and Evans′ Pharmacognosy. (14th ed.), pp. 18-27. London: WB saunders company.

Garcia-Rocha, M., Garcia-Gravalos, MD., and Avila, J. 1996. Characterisation of antimitotic products from marine organisms that disorganise the microtubule net work: ecteinascidin 743, isohomohalichondrin-B and LL-15. Brit. J. Cancer 73: 875-883.

Ghielmini, M., Colli, E., Erba. E., Bergamaschi, D., Pampallona, S., Jimeno, J., Faircloth, G., and Sessa, C.1998. *In vitro* schedule-dependency of myelotoxicity and cytotoxicity of ecteinascidin 743 (Et-743). Ann. Oncol. 9: 989-993.

Guan, Y., Skai, R., Rinebart, K. L., and Wang, A. H.–J. 1993. Molecular and crystal structures of ecteinascidins: potent antitumor compounds from the Caribbean tunicate *Ecteinascidia turbinata*. J. Biomol. Struct. Dyn. 10 (5): 793-818.

Hawkins, C. J., Lavin, M. F., Marshall, K. A., van den Brenk, A. L., and Watters, D. J. 1990. Structure-activity relationships of lissoclinamides: Cytotoxic cyclic peptides from the ascidian *Lissoclinum pattella*. J. Med. Chem. 33: 1634-1638.

Hendriks, H. R., Fiebig, H. H., Giavazzi, R., Langdon, S. P., Jimeno, J. M., and Faircloth, G. T. 1999. High antitumor activity of ET743 against human tumor xenografts from melanoma, non-small-cell lung and ovarian cancer. Ann. Oncol. 10: 1233-1240.

Hickman, C. P., Roberts, L. S., and Larson, A. 1997. Intergrated Principles of Zoology, pp. 480-497. Boston: Times Mirror Higher Education Group, Inc.

Ireland, C. M., Copp, B. R., Foster, M. P., McDonald, L. A., Radisky, D. C., and Swersey, J. C. 1993. Biomedical potential of marine natural products. In D. H. Attaway and O. R. Zabarsky (eds.) Marine Biotechnology, Volume1: Pharmaceutical and Bioactive Natural Products, pp. 1-43. New York: Plenum Press.

Jin, S., Lin, Y., Magro, P. G., and Scotto, K. W. 1999. Regression of MDR1 gene transcription by ecteinascidin 743. Proc. Am. Assoc. Cancer Res. 40: 314.

Kang, H., Jensen, R. P., and Fenical, W. 1996. Isolation of microbial antibiotics from a marine ascidian of the genus *Didemnum*. J. Org. Chem. 61: 1543-1546.

Kerr, R. G., and Miranda, N. F. 1995. Biosynthetic studies of ecteinascidins in the marine tunicate *Ecteinascidia turbinata*. J. Nat. Prod. 58 (10): 1618-1621.

Kitahara, Y., Nakahara, S., Yonezawa, T., Nagatsu, M., Shibano, Y., and Kubo, A. 1997. Synthetic studies on pentacyclic aromatic alkaloids, kuanoniamine A, 11-hydroxyascididemin, and neocalliactine acetate. Tetrahedron 53 (50): 17029-17038.

Kobayashi, J., Cheng, J., Nakamura, H., Ohizumi, Y., Hirata, Y., Sasaki, T., Ohta, T., and Nozoe, S. 1988. Ascididemin, a novel pentacyclic aromatic alkaloid with potent antileukemic activity from the Okinawan tunicate *Didemnum* sp. Tetrahedron Lett. 29 (10): 1177-1180.

Kobayashi, J., Tsuda, M., Tanabe, A., Ishibashi, M., Cheng, J., Yamamura, S., and Sasaki, T. 1991. Cystodytins D-I, new cytotoxic tetracyclic aromatic alkaloids from the Okinawan marine tunicate *Cystodytes dellechiajei*. J. Nat. Prod. 54: 1634-1638.

Mantonvani, R., La Valle, E., Sousa Faro, J. M. F., Faircloth, G., and D'Incalci, M. 1998. Effect of ecteinascidin-743 (Et-743) on the interaction between transcription factors and DNA. Ann. Oncol. 9 Suppl. 2: 133-139.

Martinez, E. J., and Corey, E. J., 2000. A new, more efficient, and effective process for the synthesis of a key pentacyclic intermediate for production of ecteinascidin and phthalascidin antitumor agent. Org. Lett. 2 (7): 993-996.

Martinez, E. J., Owa, T., Schreiber, S. L., and Corey, E. J. 1999. Phthalascidin, a synthetic antitumor agent with potency and mode of action comparable to ecteinascidin 743. Proc. Natl. Acad. Sci. 96: 3496-3501.

McAlonan, H., Potts, D., Stevenson, J. P., and Thompson, N. 2000. Synthesis of (+)-piclavines A_1 and A_2. Tetrahedron Lett. 41: 5411-5414.

Miller, S. A. and Harley, J. B. 1999. Zoology. (4^{th} ed.), pp. 423-434. Boston: McGraw-Hill.

Mitchell, S. S., Pomerantz, S. C., Concepcion, G. P., and Ireland, C. M. 1996. Tubercidin analogs from the ascidian *Didemnum voeltzkowi*. J. Nat. Prod. 59: 1000-1001.

Molinski, T. F. 1993. Marine pyridoacridine alkaloids: Structure, synthesis, and biological chemistry. Chem. Rev. 93: 1825-1838.

Montgomery, D. W. and Zukoski, C. F. 1985. Didemnin B: A new immunosuppressive cyclic peptide with potent activity *in vitro* and *in vivo*. Transplantation 40: 49-56.

Moore, B. M., Seaman, F. C., Wheelhouse, R. T., and Hurley, L. H. 1998. Mechanism for the catalytic activation of ecteinascidin 743 and its subsequent alkylation of guanine N2. Ann. Oncol. 9 Suppl. 2: 139.

Niwa, H., Inagaki, H., and Yamada, K. 1991. Didemnilactone and neodidemnilactone, two new fatty acid metabolites possessing a ten-membered lactone from the tunicate *Didemnum moseleyi* (Herdman). Tetrahedron Lett. 32 (38): 5127-5128.

Pechenik, J. A. 1996. Biology of Invertebrates. (3^{rd} ed.), pp. 490-502. Dubuque: Wm. C. Brown.

Pommier, Y., Kohlhagen, G., Bailly, C., Waring, M., Mazumder, A., and Kohn, K. W. 1996. DNA sequence and structure-selective alkylation of guanine N2 in the DNA minor groove by ecteinascidin 743, a potent antitumor compound from the Caribbean tunicate *Ecteinascidia turbinata*. Biochemistry 35 (41): 13303-13309.

Rinehart, K. L. 2000. Antitumor Compounds from tunicates. Med. Res. 1: 1-27.

Rinehart., K. L., Gloer, J. B., Hughes, R. G., Renis, H. E., McGovren, J. P., Swynenberg, E. B., Stringfellow, D. A., Kuentzel, S. L., and Li, L. H. 1981. Didemnins: Antiviral and antitumor depsipeptides from a Caribbean tunicate. Science 212: 933-935.

Rinehart, K. L., Holt, T. G., Fregeau, N. L., Stroh, J. G., Keifer, P. A., Sun, F., Li, L. H., and Martin, D. G. 1990a. Ecteinascidins 729, 743, 745, 759A, 759B, and 770: Potent antitumor agents from the Caribbean tunicate *Ecteinascidia turbinata*. J. Org. Chem. 55: 4512-4515.

Rinehart, K. L., Holt, T. G., Fregeau, N. L., Keifer, P. A., Wilson, G. R., Perun Jr., T. J., Sakai, R., Thompson, A. G., Stroh, J. G., Shield, L. S., Seigler, D. S., Li, L. H., Martin, D. G., Grimmelikhuijzen, J. P. G., and Gade, G. 1990b. Bioactive compounds from aquatic and terrestrial sources. J. Nat. Prod. 53 (4): 771-792.

Sakai, R., Jares-Erijman, E. A., Manzanares, I., Silva Elipe, M. V., and Rinehart, K. L., 1996a. Ectienascidins: Putative biosynthetic precursors and absolute stereochemistry. J. Am. Chem. Soc. 118: 9017-9023.

Sakai, R., Rinehart, K. L., Guan, Y., and Wang, A. H.-J. 1992. Additional antitumor ecteinascidins from a Caribbean tunicate: Crystal structures and activities *in vivo*. Proc. Natl. Acad. Sci. 89: 11456-11460.

Sakai, R., Rinehart, K. L., Kishore, V., Kundu, B., Faircloth, G., Gleer, J. B., Carney, J. R., Namikoshi, M., Sung, F., Hughes, R. G., Gravalos, D. G., Garcia de Quesada, T., Wilson, G. R., and Heid, R. M. 1996b. Structure-activity relationships of the didemnins. J. Med. Chem. 39: 2819-2834.

Schiff, PH., Fanat, J., and Horwitz, SB. 1979. Promotion of tubulin assembly *in vitro* and by taxol. Nature 227: 665-667.

Schmitz, F. J., Ksebati, M. B., Chang, J. S., Wang, J. L., Hossain, M. B., and Van der Helm, D. 1989. Cycle peptides from the ascidian *Lissoclinum patella*: Conformation analysis of patellamide D by x-ray analysis and molecular modeling. J. Org. Chem. 54: 3463-3472.

Schmitz, J. F., Bowden, F. B. and Toth, I. S. 1993. Antitumor and cytotoxic compounds from marine organism. In D. H. Attaway, and O. R. Zaborsky (eds.), Marine Biotechnology, Volume 1: Pharmaceutical and Bioactive Natural Products, pp. 263-265. New York: Plenum Press.

Seaman, F. C., and Hurley, L. H. 1998. Molecular basis for the DNA sequence selectivity of ecteinascidin 736 and 743: Evidence for the dominant role of direct readout via hydrogen bonding. J. Am. Chem. Soc. 120: 13028-13041.

Skehan, P., Storeng, R., Scudiero, D., Monks, A., McMahon, J., Vistica, D., Warren, J., Bokesch, H., Kenny, S., and Boyd, M. R. 1990. New colorimetric cytotoxic assay for anticancer-drug screening. J. Natl. Cancer Insti. 82 (13): 1107-1112.

Sterrer, W. 1986. Marine fauna and flora of Bermuda: A systematic guide to the identification of marine organism, pp. 45-561. New York: A Wiley-Interscience.

Takebayashi, Y., Pourquier, P., Yoshida, A., Kohlhagen, G., and Pommier, Y. 1999. Poisoning of human DNA topoisomerase I by ecteinascidin 743 and anticancer drug that selectively alkylates DNA in the minor groove. Proc. Natl. Acad. Sci. 96: 7102-7196.

Valoti, G., Nicoletti, M.I., Pellegrino, A., Jimeno, A., Jimeno, J., Hendriks, H., D'Incalci, M., Faircloth, G., and Giavazzi, R. 1998. Ecteinascidin-743, a new marine natural product with potent antitumor activity on human ovarian carcinoma xenografts. Clin. Cancer Res. 4: 1977-1983.

Wright, A. E., Forleo, A. D., Gunawardana, P. G., Gunasekera, P. S., Koehn, E. F., and McConnell, J. O. 1990. Antitumor tetrahydroisoquinoline alkaloids from the colonial ascidian *Ecteinascidia turbinata*. J. Org. Chem. 55: 4508-4512.

Zabriskie, T. M., Mayne, C. L., and Ireland, C. M. 1988. Patellazole C: A novel cytotoxic macrolide from *Lissoclinum patella*. J. Am. Chem. Soc. 110: 7919-7920.

Zewail-Foote, M., and Hurley, L. H. 1999. Ecteinascidin 743: A minor groove alkylator that bends DNA toward the major groove. J. Med. Chem. 42 (14): 2493-2497.

APPENDIX

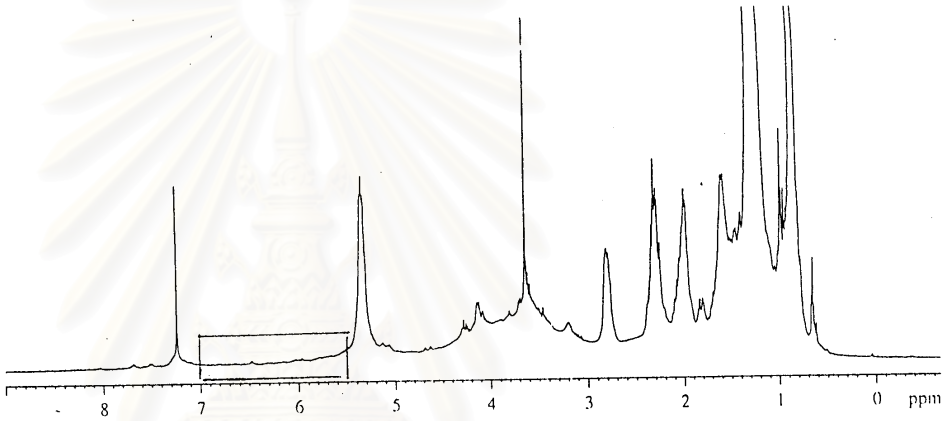

(A) Crude EtOAc extract from conventional extraction method.

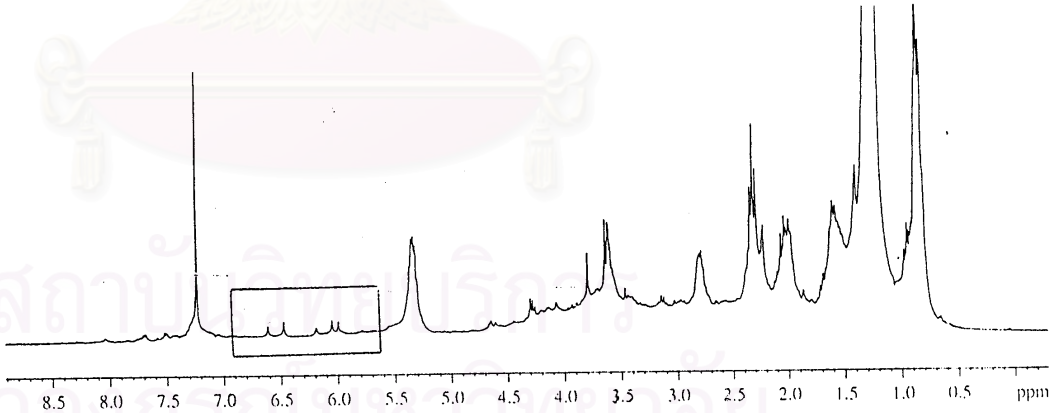

(B) Crude EtOAc extract from modified extraction method.

Figure 11 The 300 MHz ^{1}H NMR spectra of the crude extracts from conventional and modified extraction methods.

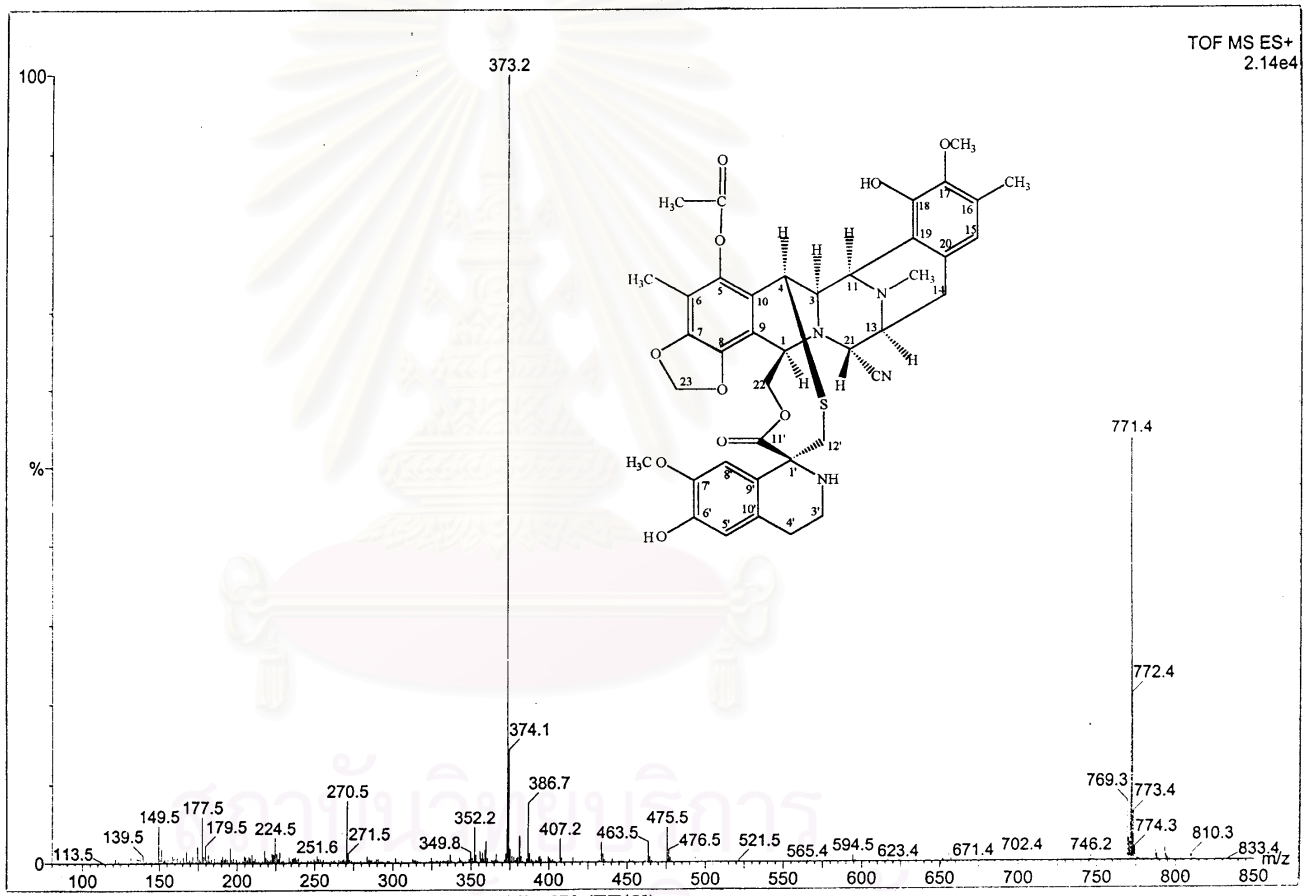

Figure 12 The ESI-TOF MS spectrum of ecteinascidin 770 (ET1K).

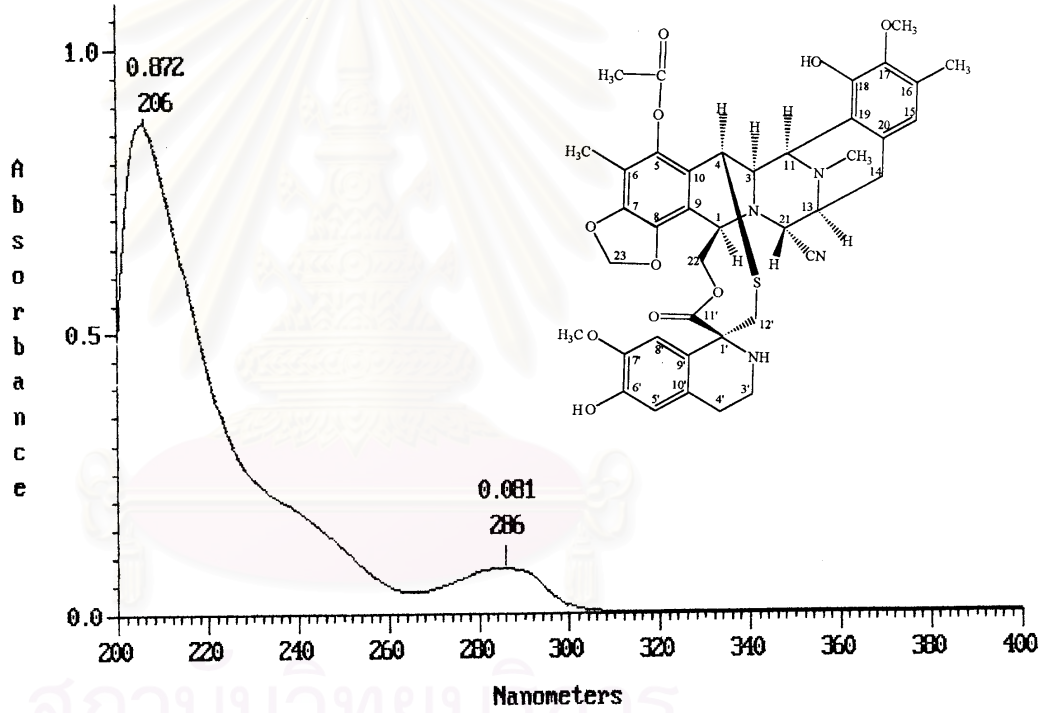

Figure 13 The UV spectrum (in MeOH) of ecteinascidin 770 (ET1K).

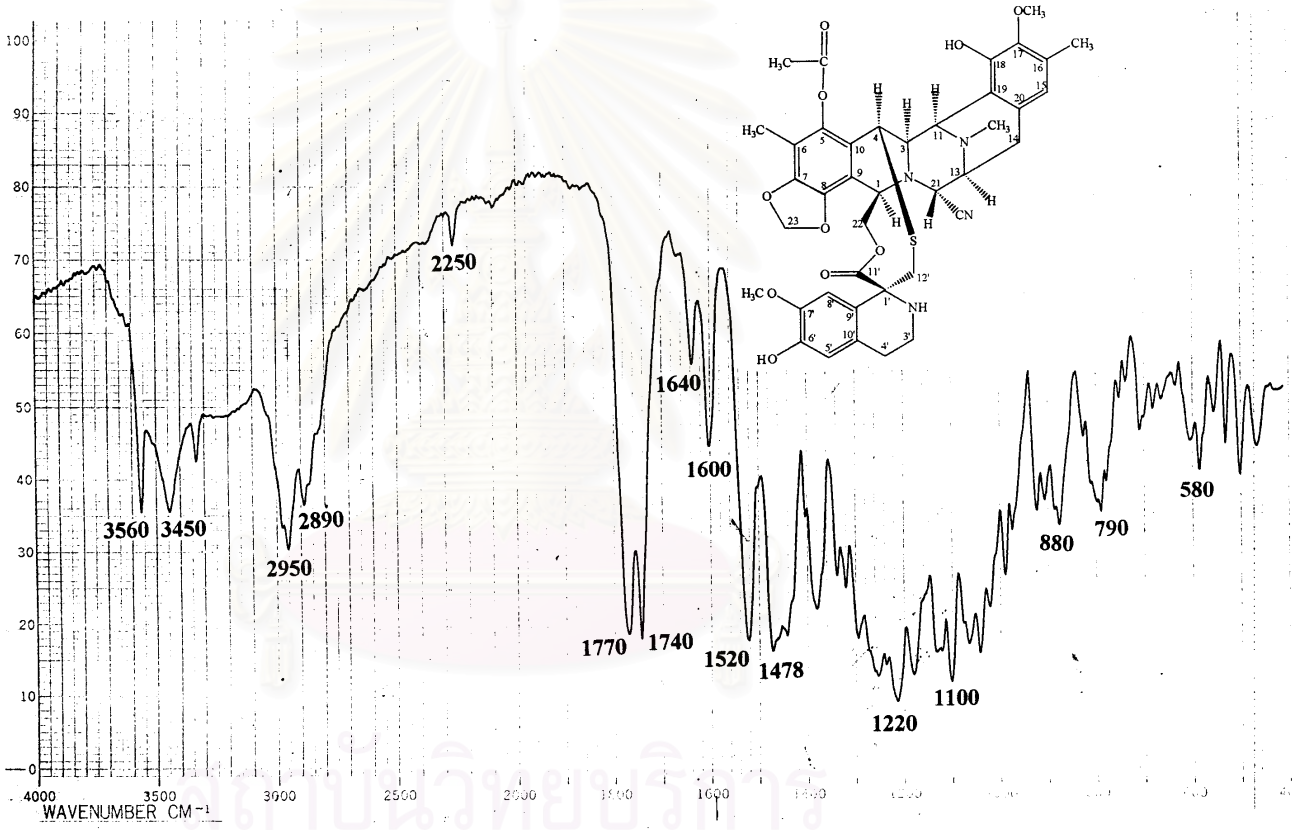

Figure 14 The IR spectrum (KBr disc) of ecteinascidin 770 (ET1K).

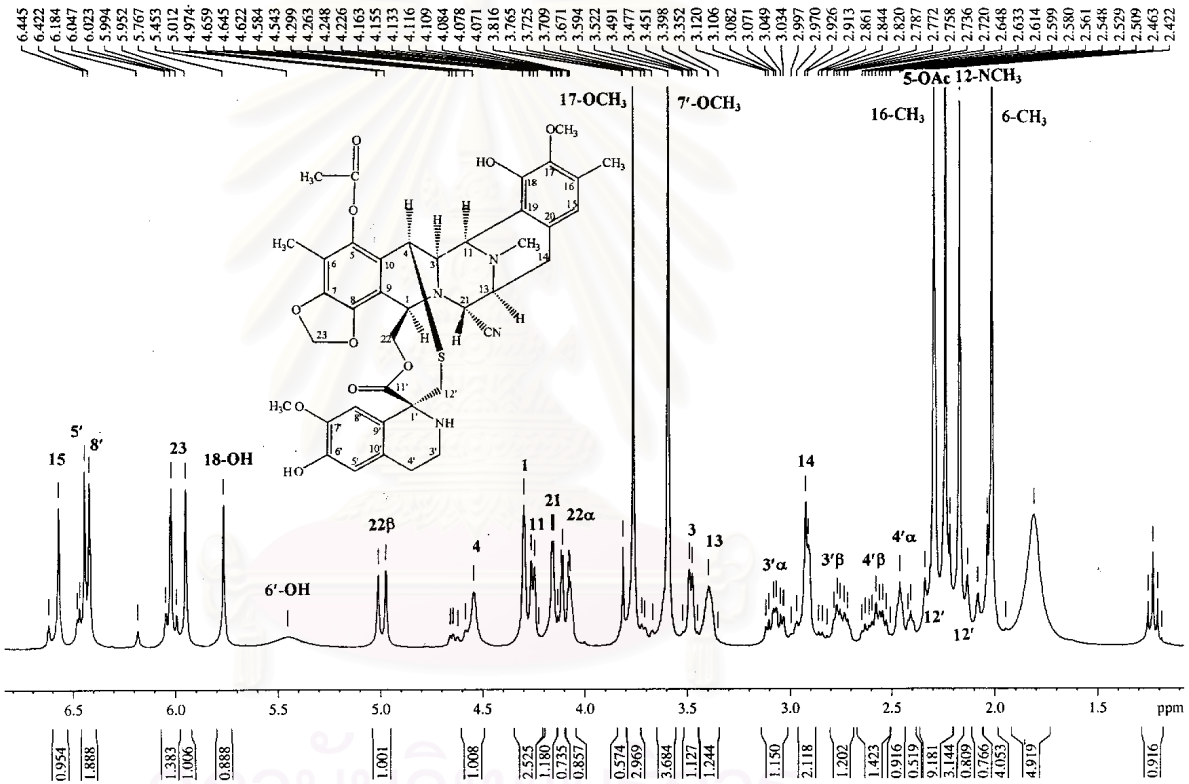

Figure 15 The 300 MHz ^{1}H NMR spectrum (in $CDCl_3$) of ecteinascidin 770 (ET1K).

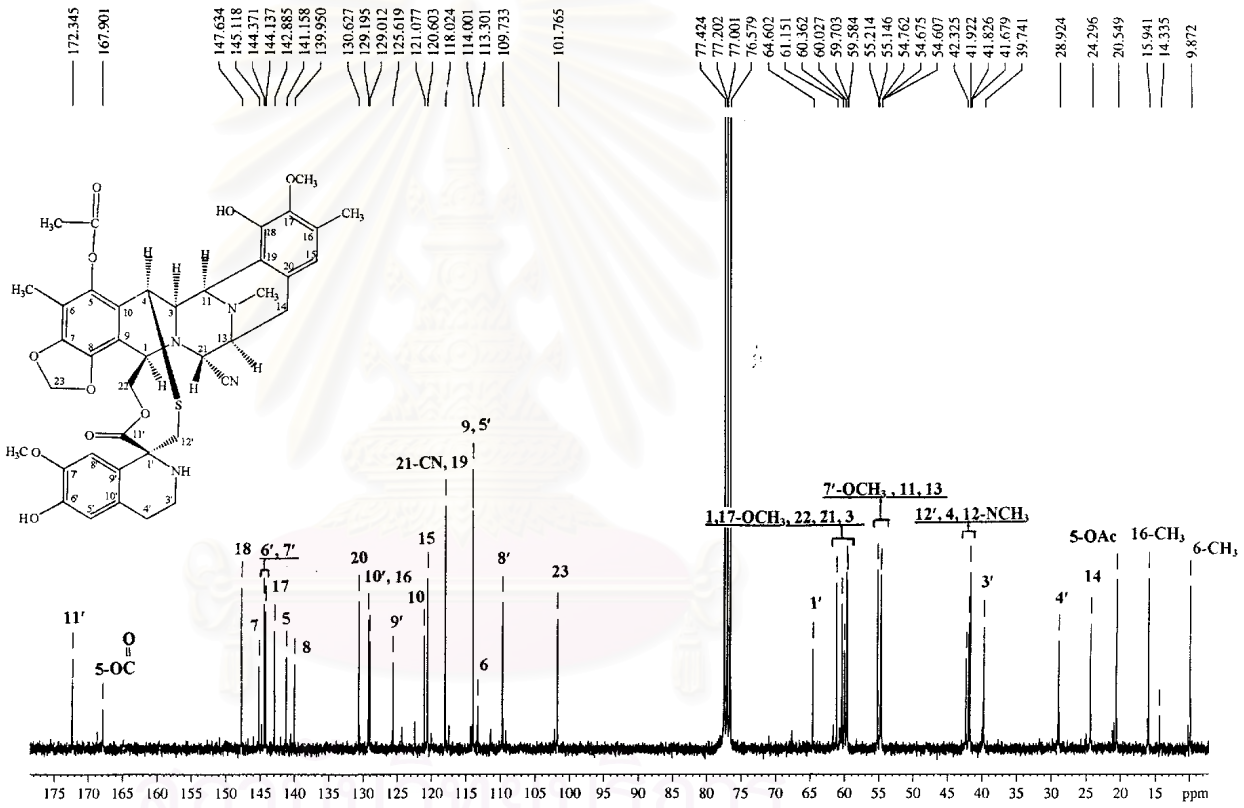

Figure 16 The 75 MHz ^{13}C NMR spectrum (in $CDCl_3$) of ecteinascidin 770 (ET1K).

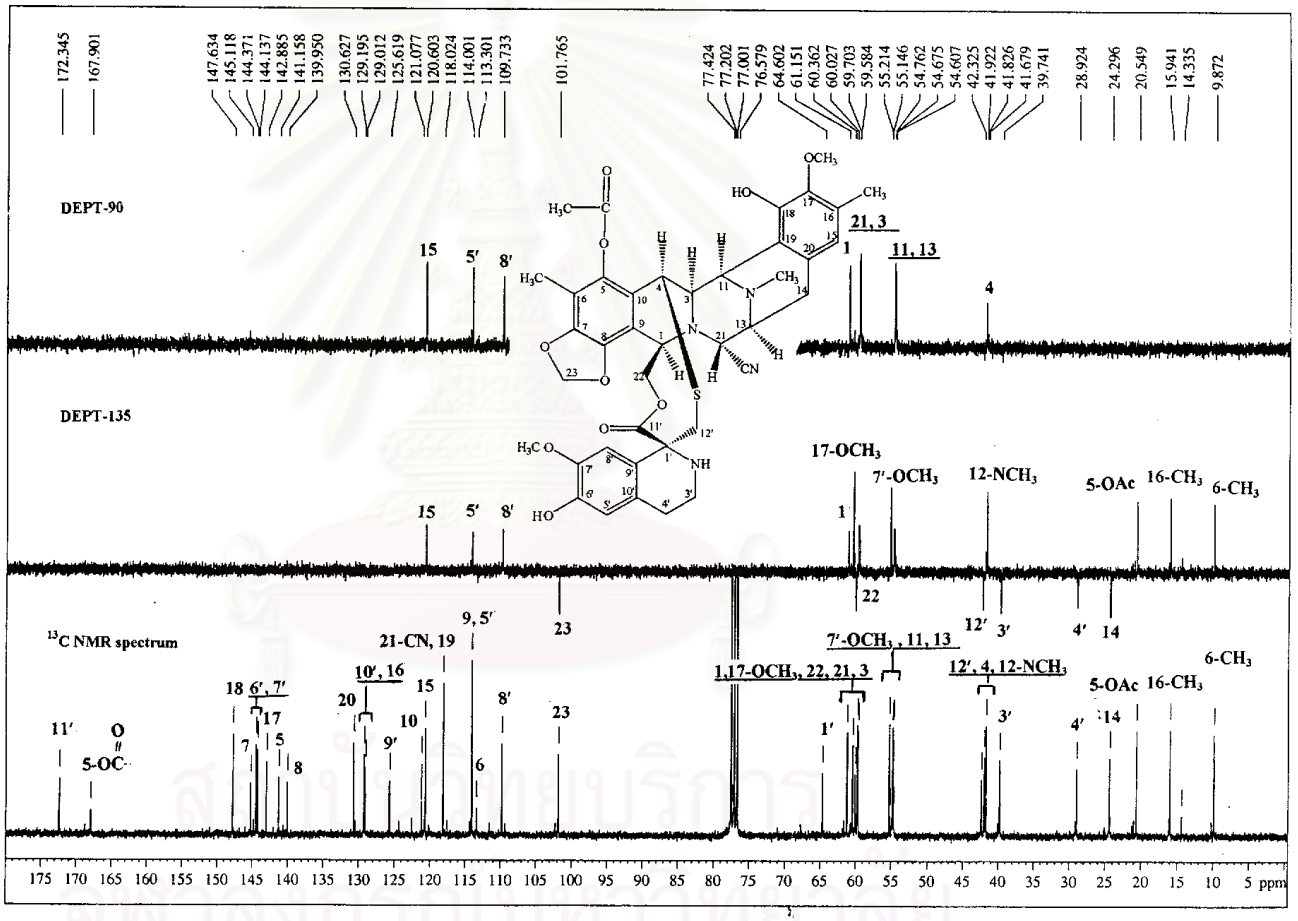

Figure 17 The 75 MHz ^{13}C NMR, DEPT-135,and DEPT-90 spectra (in $CDCl_3$) of ecteinascidin 770 (ET1K).

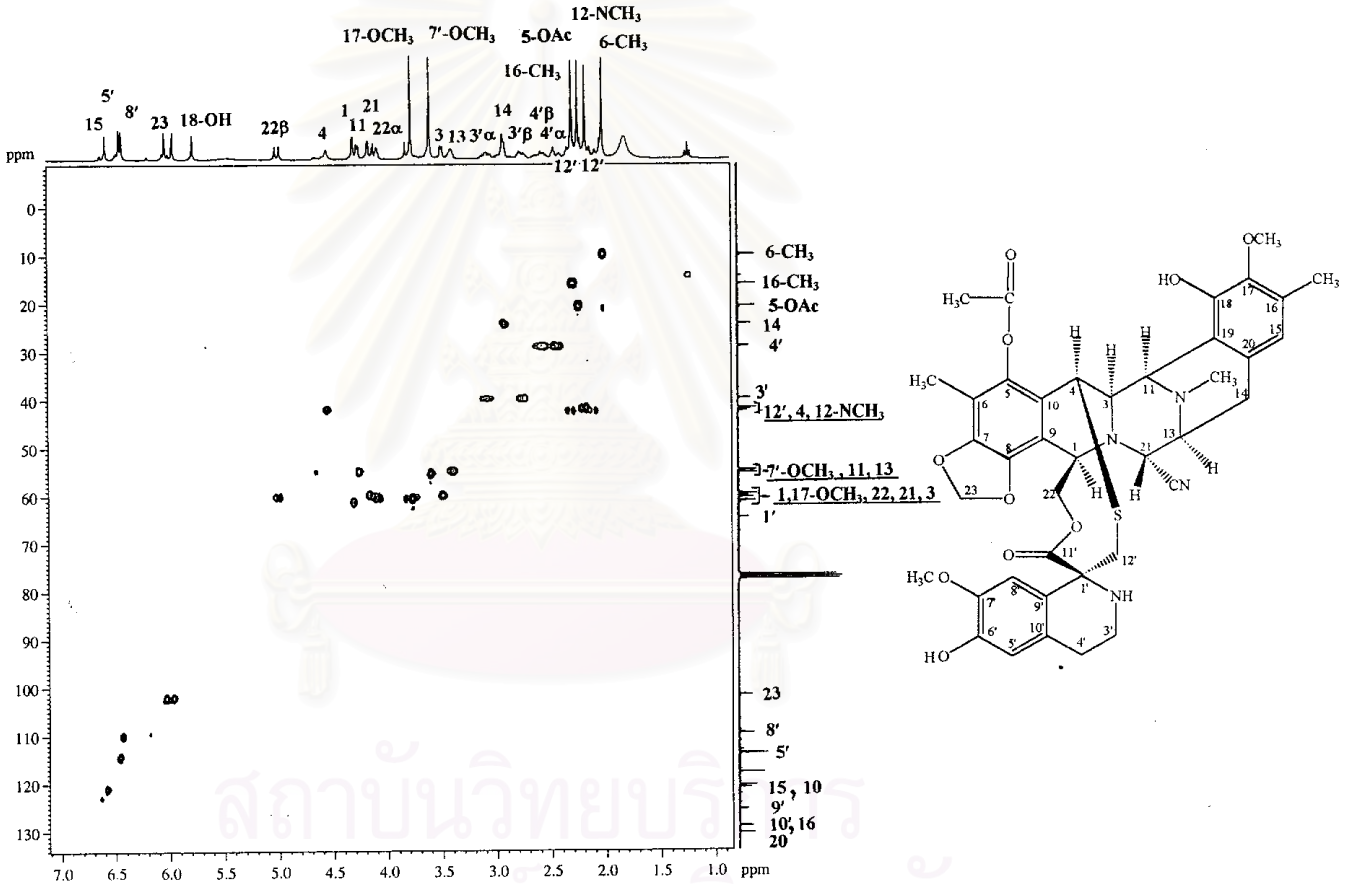

Figure 18 The 300 MHz HMQC spectrum (in $CDCl_3$) of ecteinascidin 770 (ET1K).

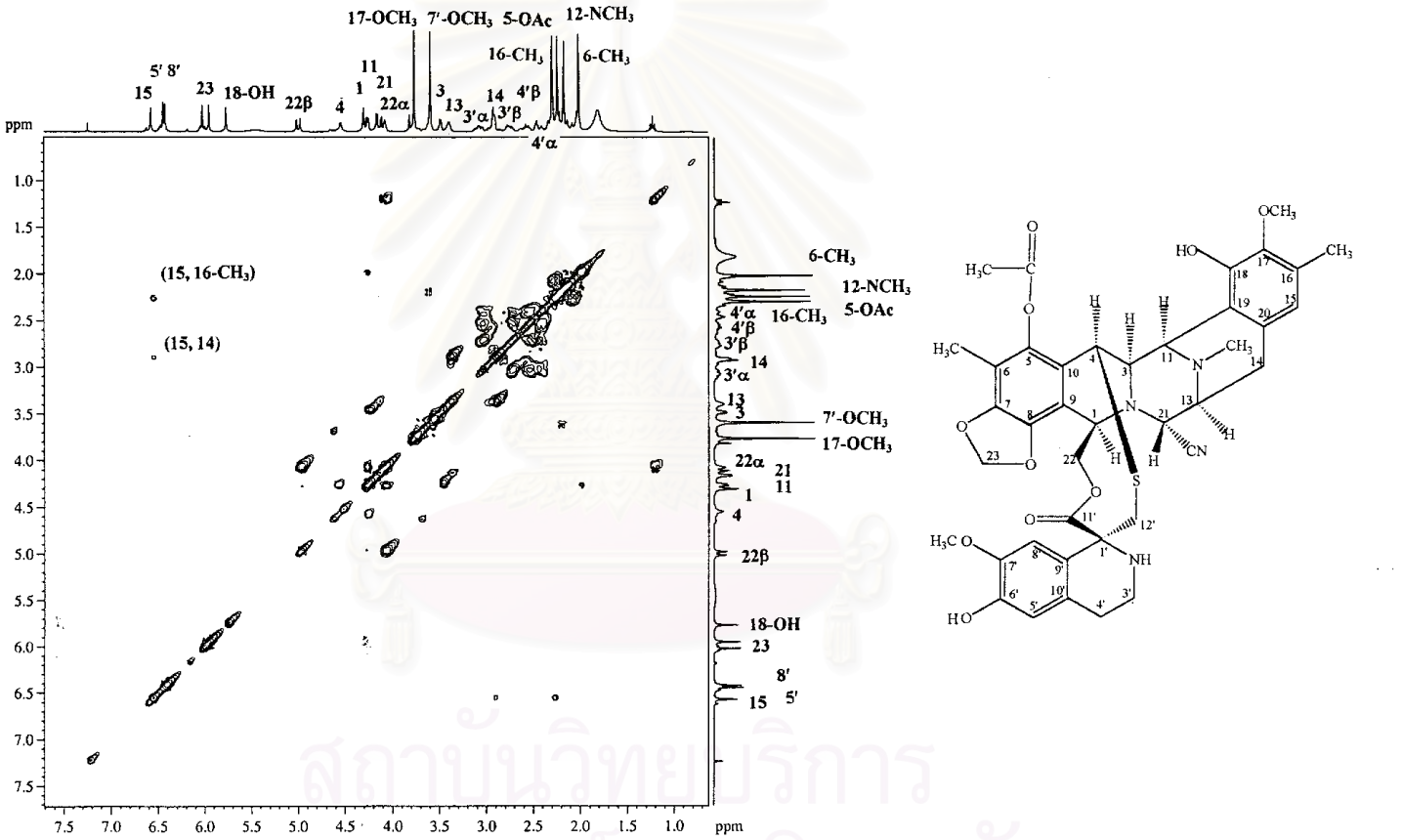

Figure 19 The 300 MHz ^{1}H-^{1}H COSY spectrum (in $CDCl_3$) of ecteinascidin 770 (ET1K).

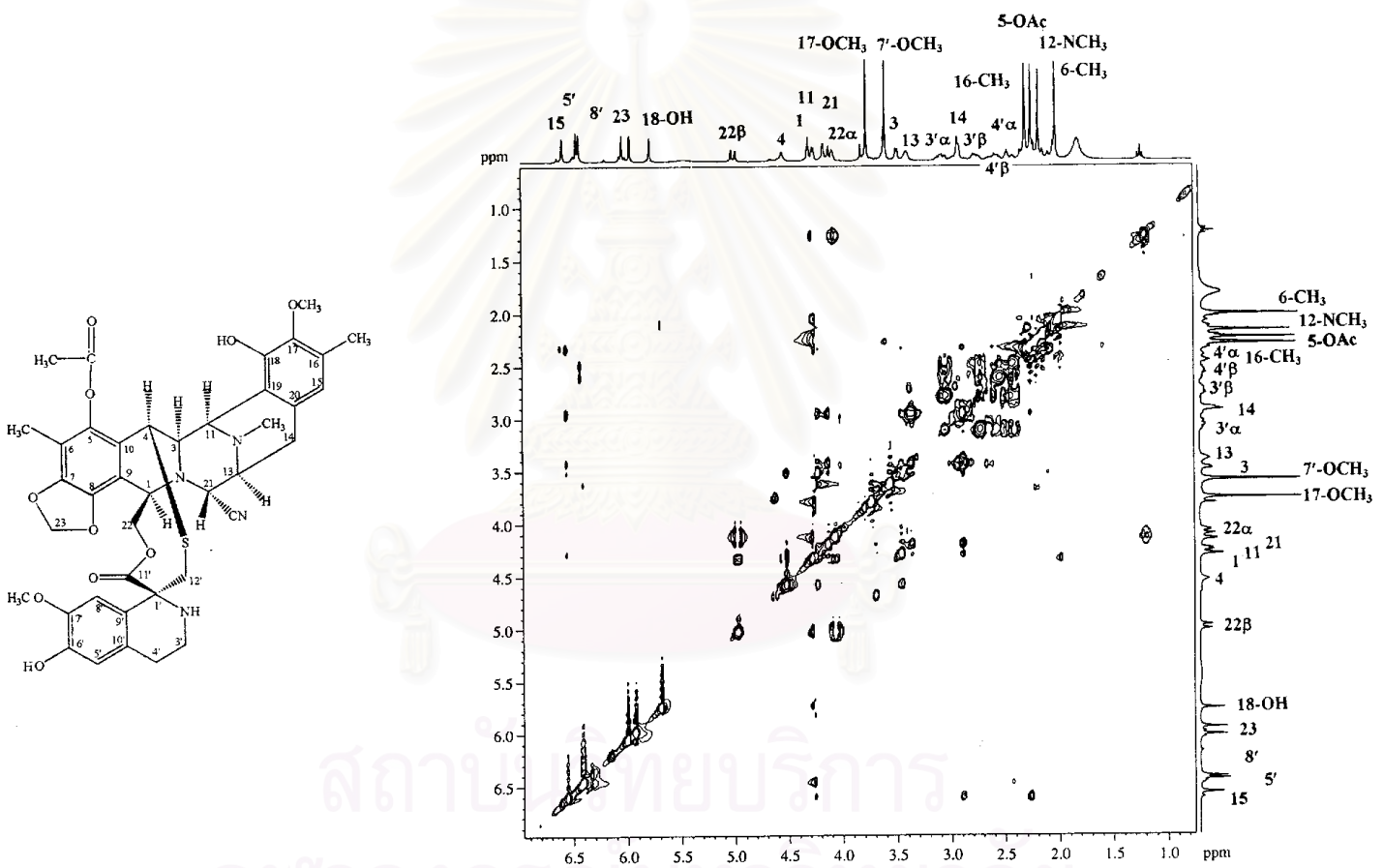

Figure 20 The 300 MHz TOCSY spectrum (in $CDCl_3$) of ecteinascidin 770 (ET1K).

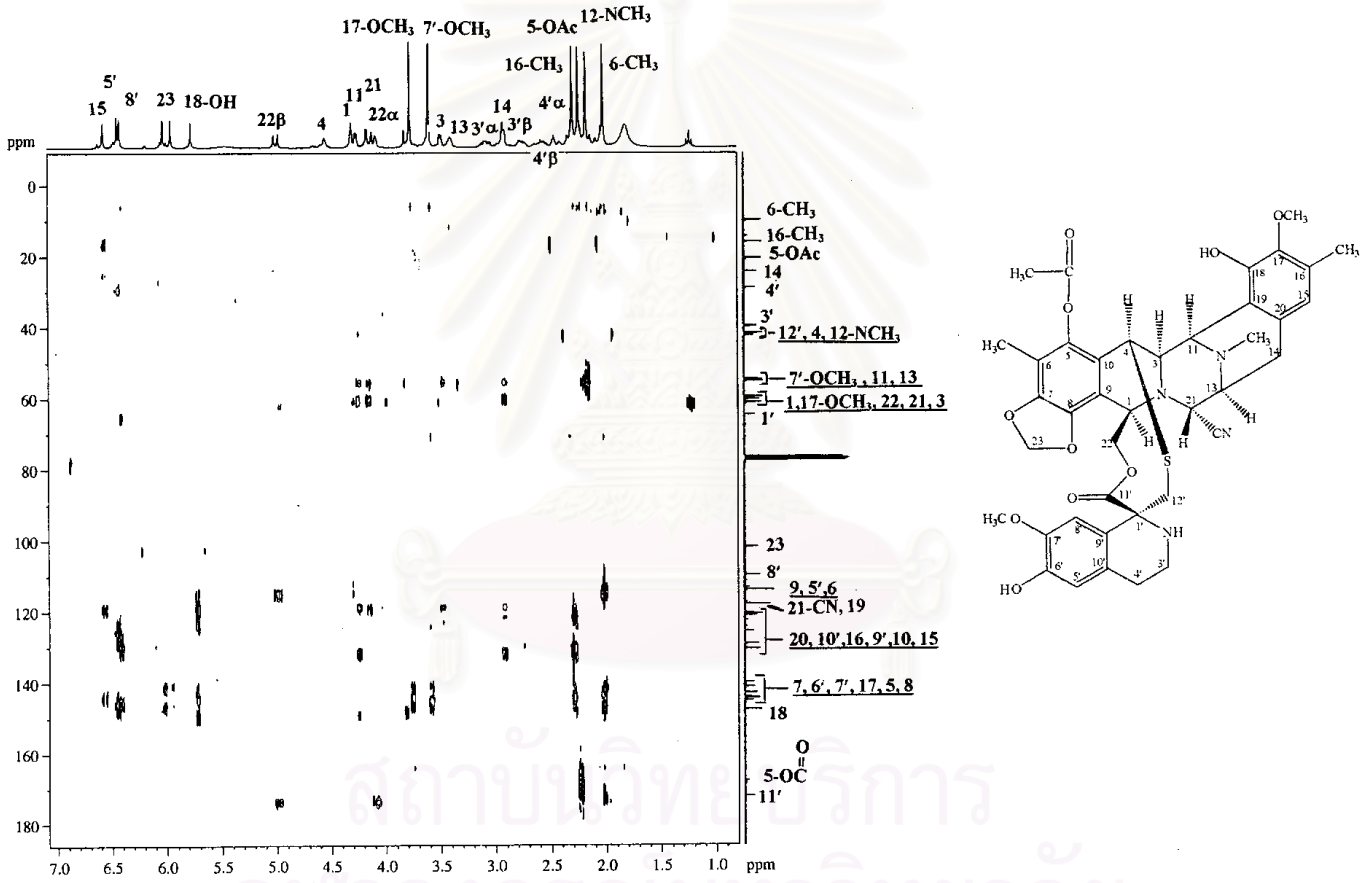

Figure 21 The 300 MHz HMBC spectrum ($^{n}J_{HC}$ = 8 Hz in $CDCl_3$) of ecteinascidin 770 (ET1K).

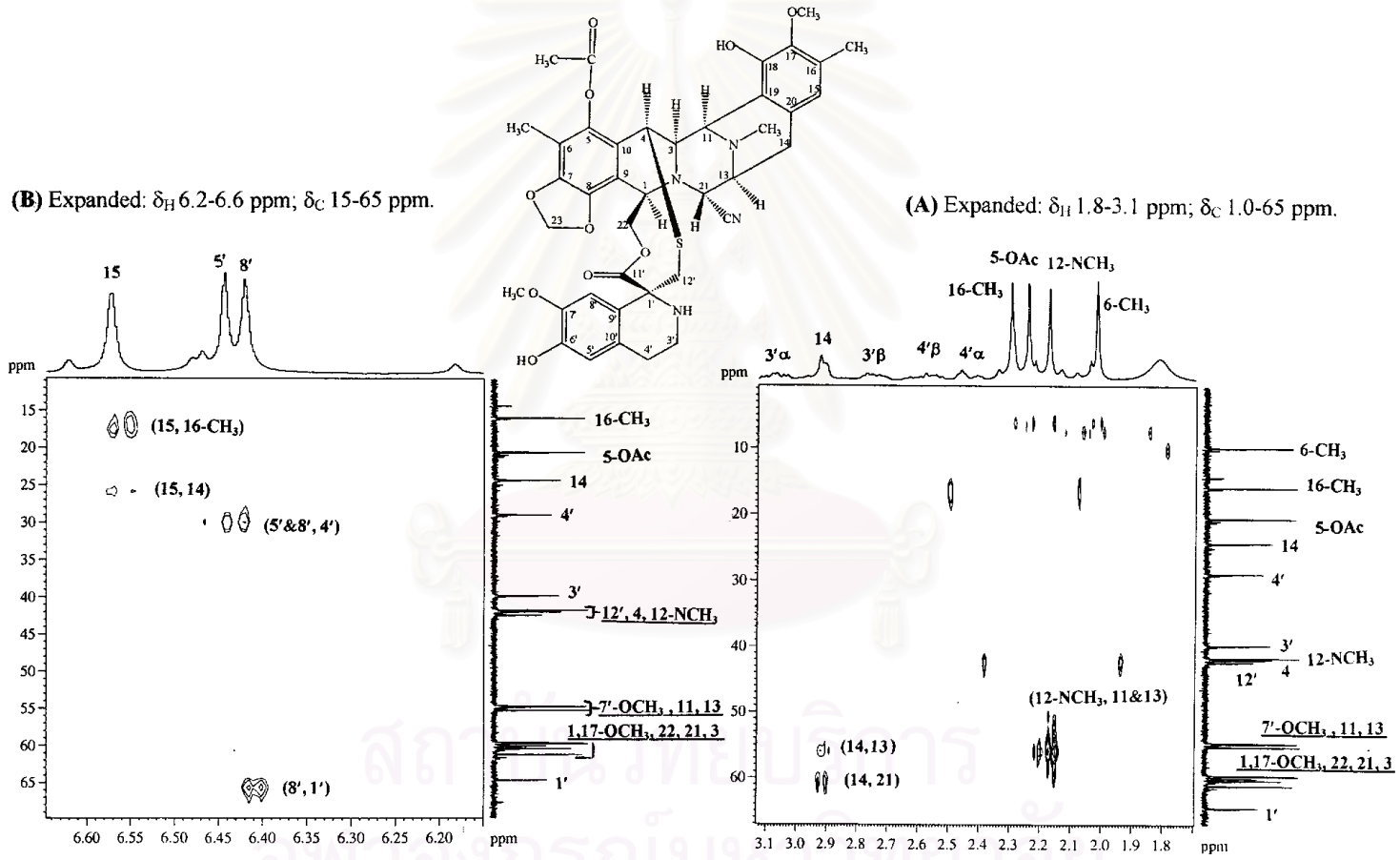

gure 22 The 300 MHz HMBC spectrum ($^{n}J_{HC}$ = 8 Hz in $CDCl_3$) of ecteinascidin 770 (ET1K) [expanded: δ_H 1.8-6.6 ppm; δ_C 1.0-65 ppm].

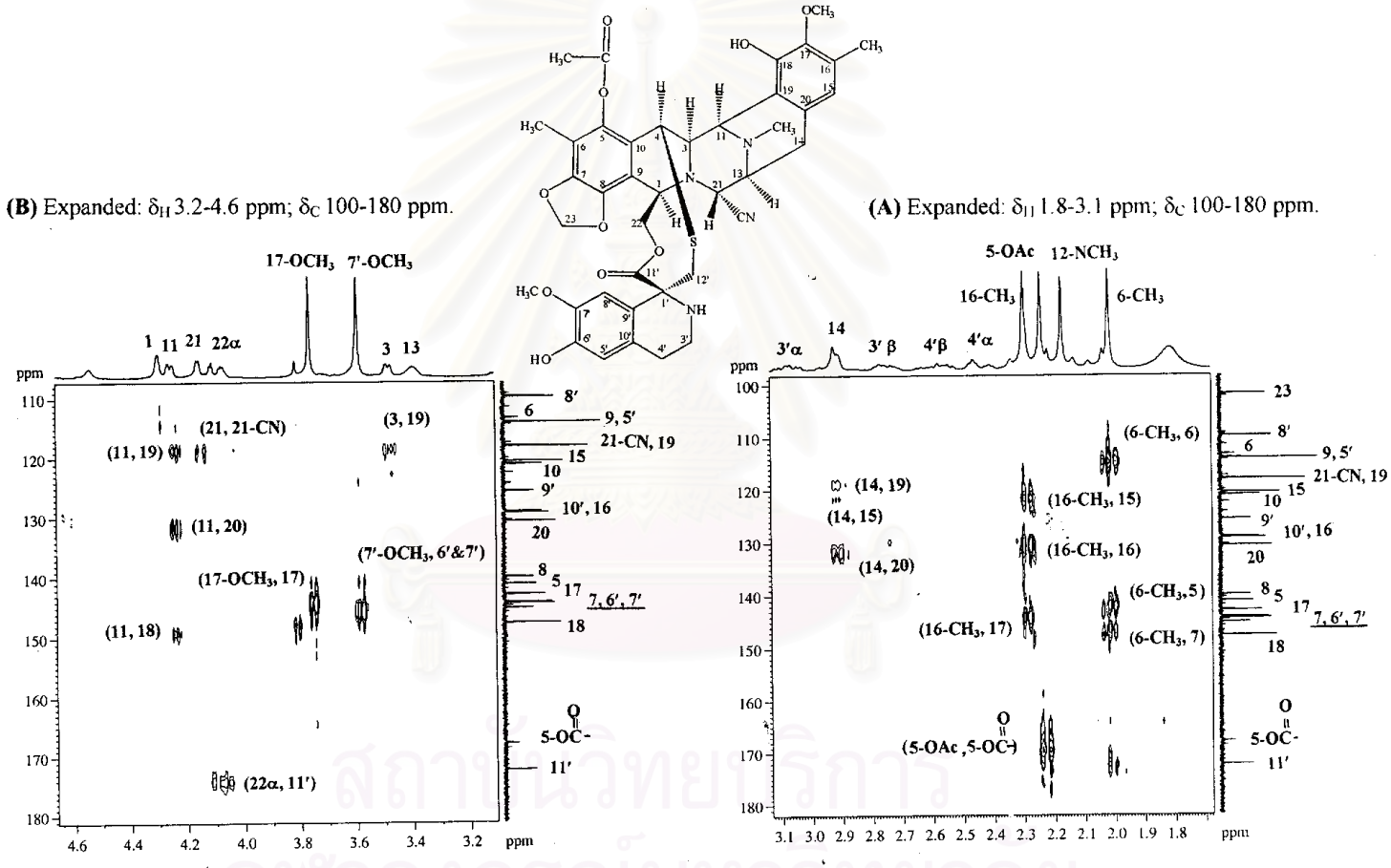

Figure 23 The 300 MHz HMBC spectrum ($^{n}J_{HC}$ = 8 Hz in $CDCl_3$) of ecteinascidin 770 (ET1K) [expanded: δ_H 1.8-4.6 ppm; δ_C 100-180ppm].

(B) Expanded: δ_H 5.5-6.8 ppm; δ_C 100-160 ppm.

(A) Expanded: δ_H 3.3-4.3 ppm; δ_C 40-70 ppm.

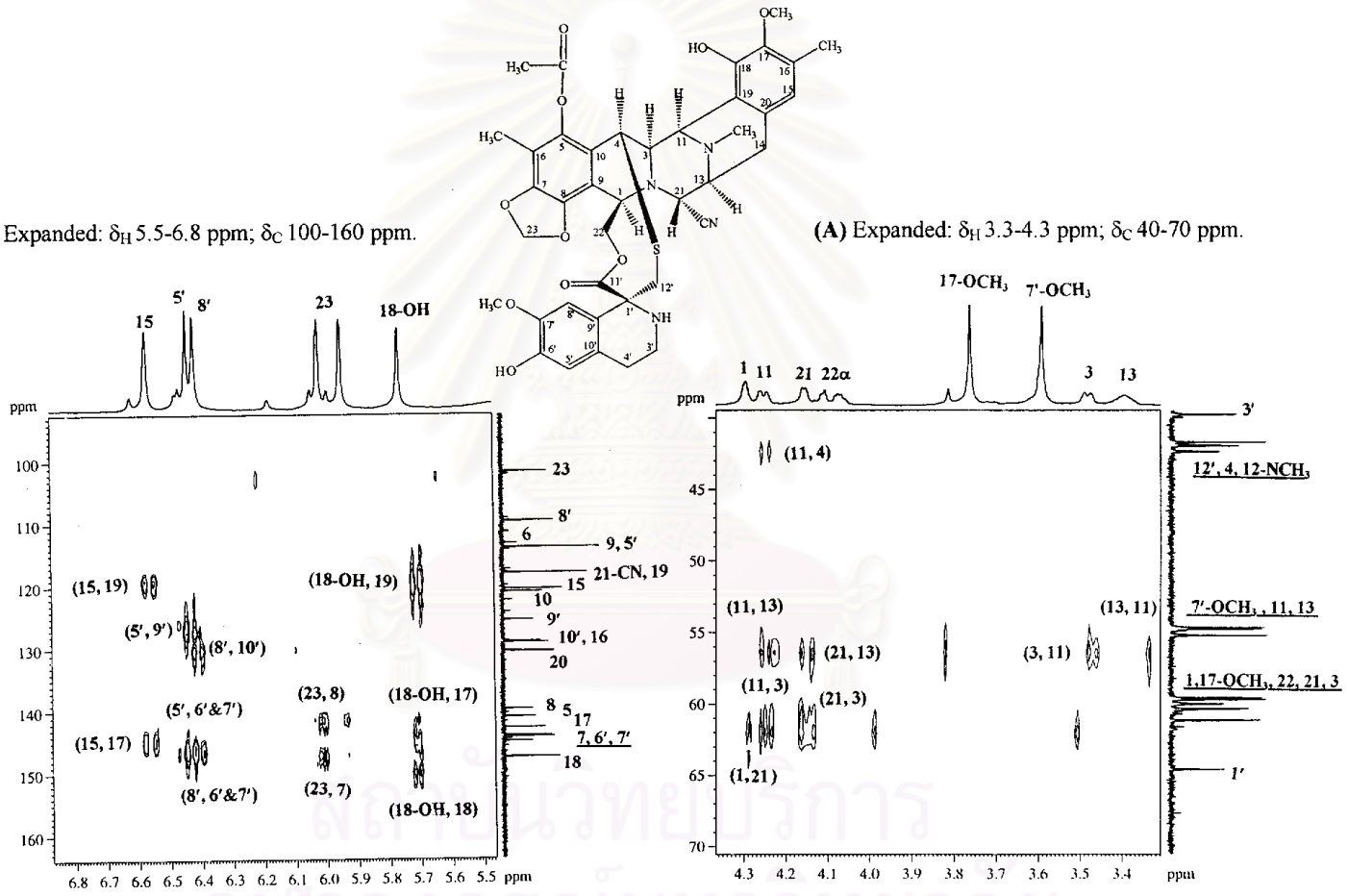

Figure 24 The 300 MHz HMBC spectrum ($^nJ_{HC}$ = 8 Hz in $CDCl_3$) of ecteinascidin 770 (ET1K) [expanded: δ_H 3.3-6.8 ppm; δ_C 40-160 ppm].

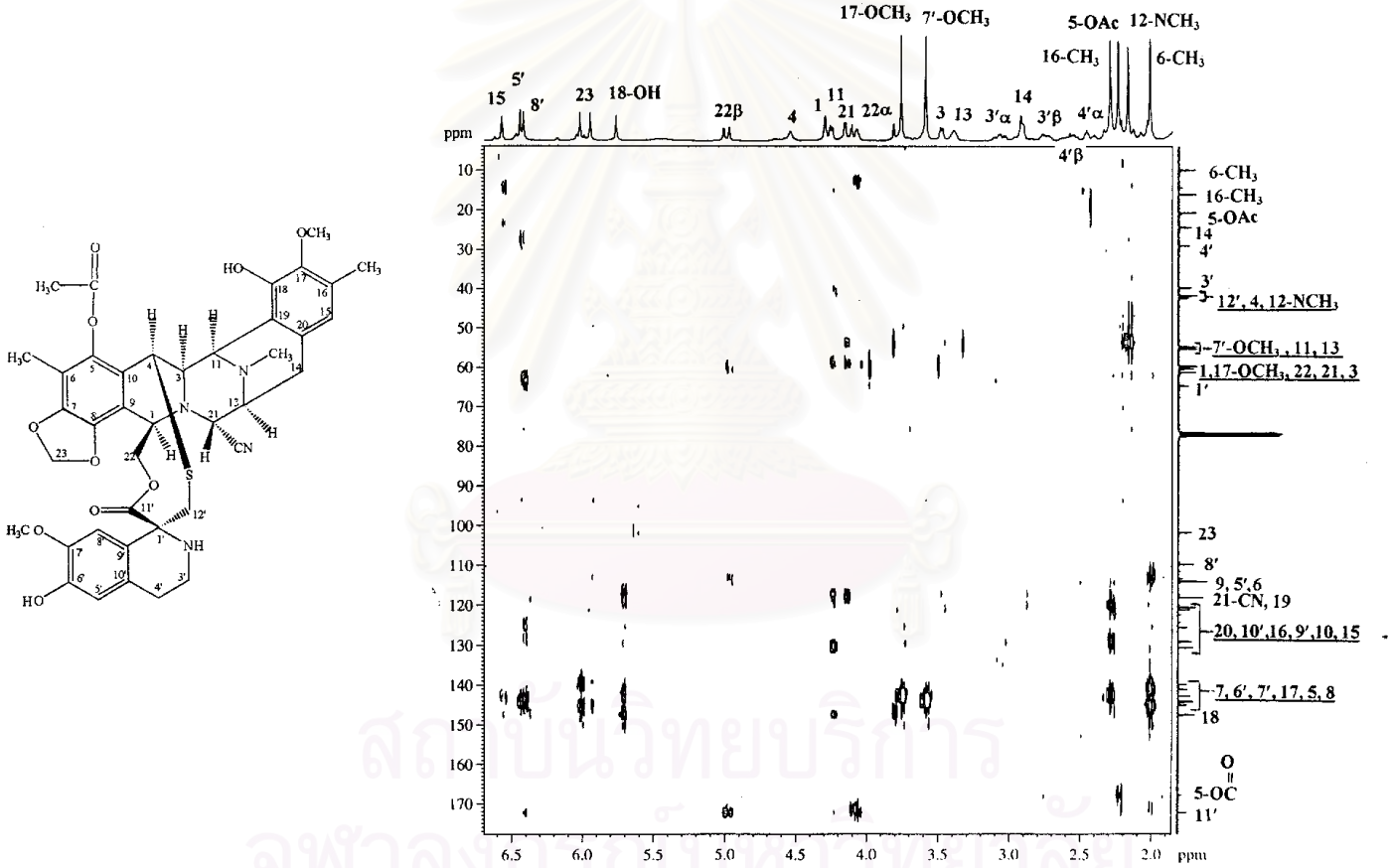

Figure 25 The 300 MHz HMBC spectrum ($^{n}J_{HC}$ = 4 Hz in $CDCl_3$) of ecteinascidin 770 (ET1K).

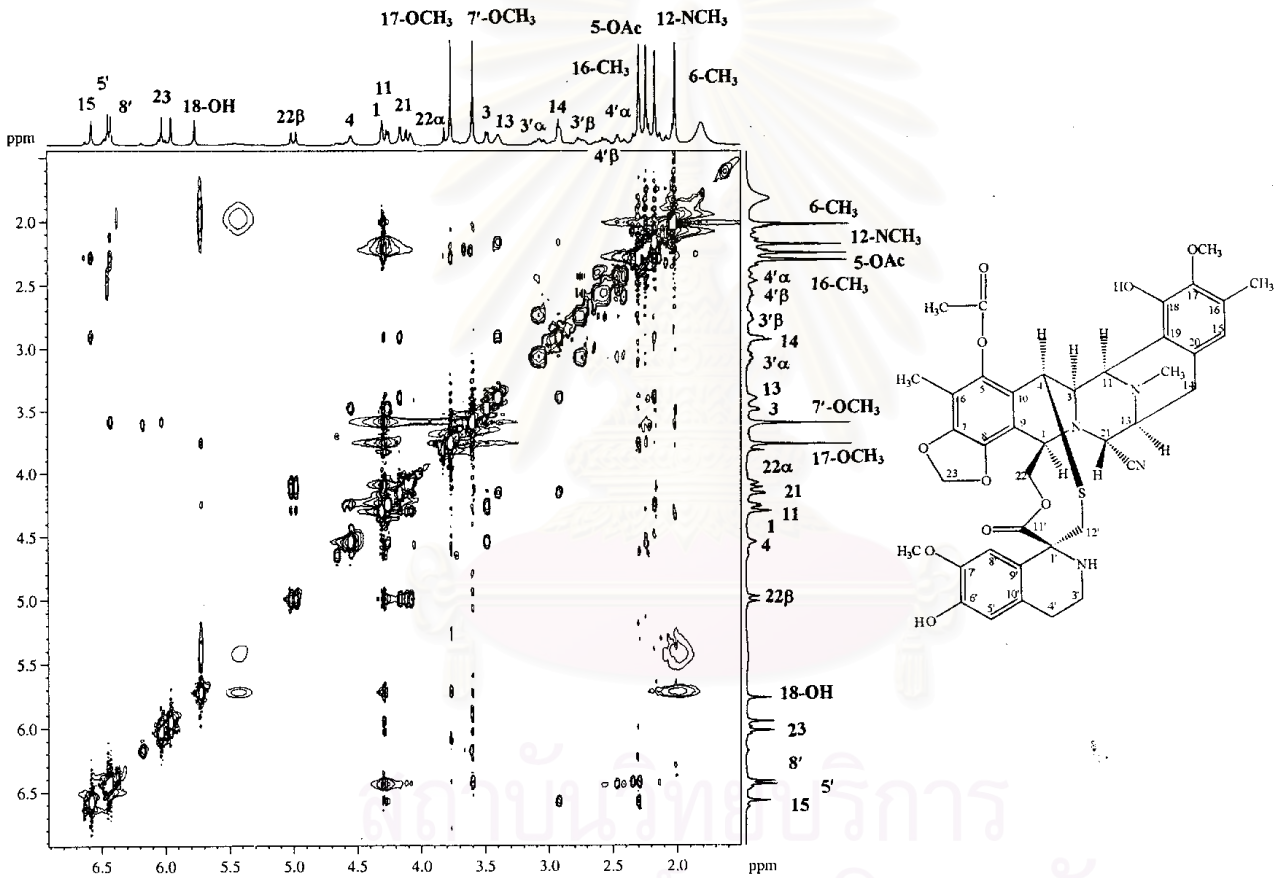

Figure 26 The 300 MHz NOESY spectrum (in $CDCl_3$) of ecteinascidin 770 (ET1K).

(B) expanded: δ_{Hx} 4.0-4.2 ppm; δ_{Hy} 4.3-5.1 ppm

(A) expanded: δ_{Hx} 2.8-3.6 ppm; δ_{Hy} 4.0-4.6 ppm

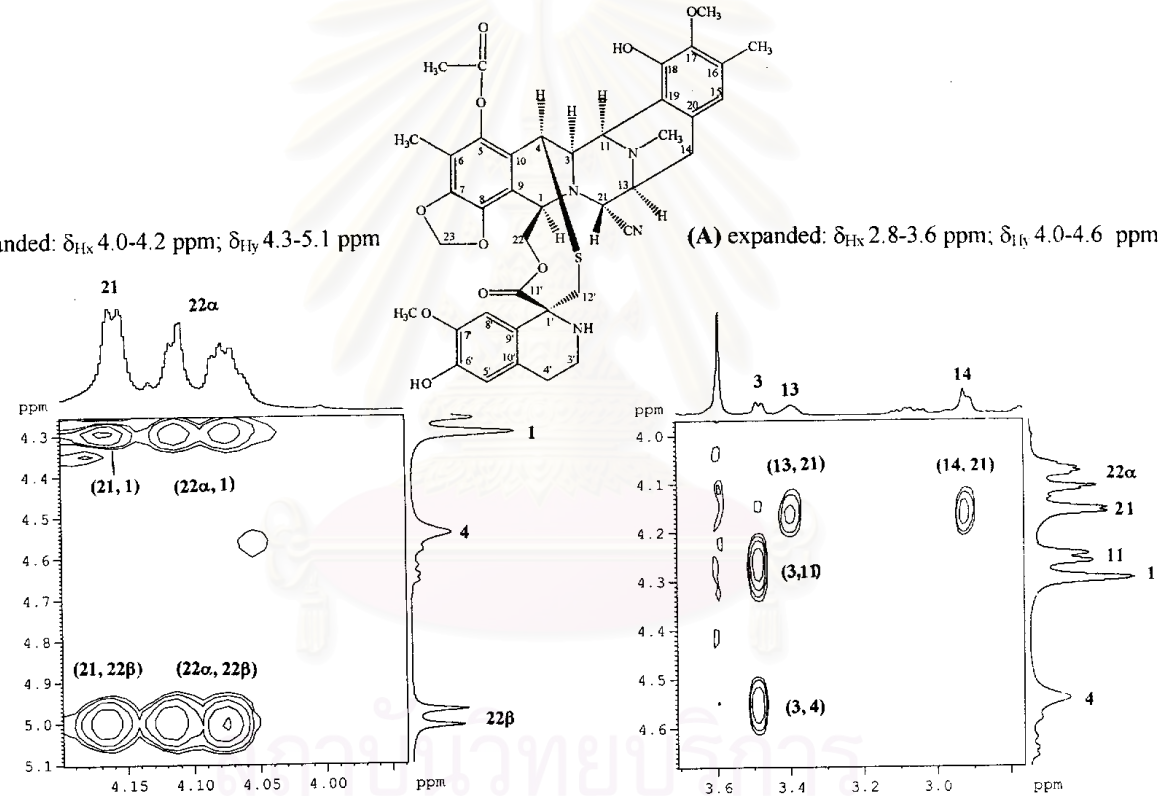

Figure 27 The 300 MHz NOESY spectrum (in $CDCl_3$) of ecteinascidin 770 (ET1K) [expanded: δ_{Hx} 2.8-4.2 ppm; δ_{Hy} 4.0-5.1 ppm].

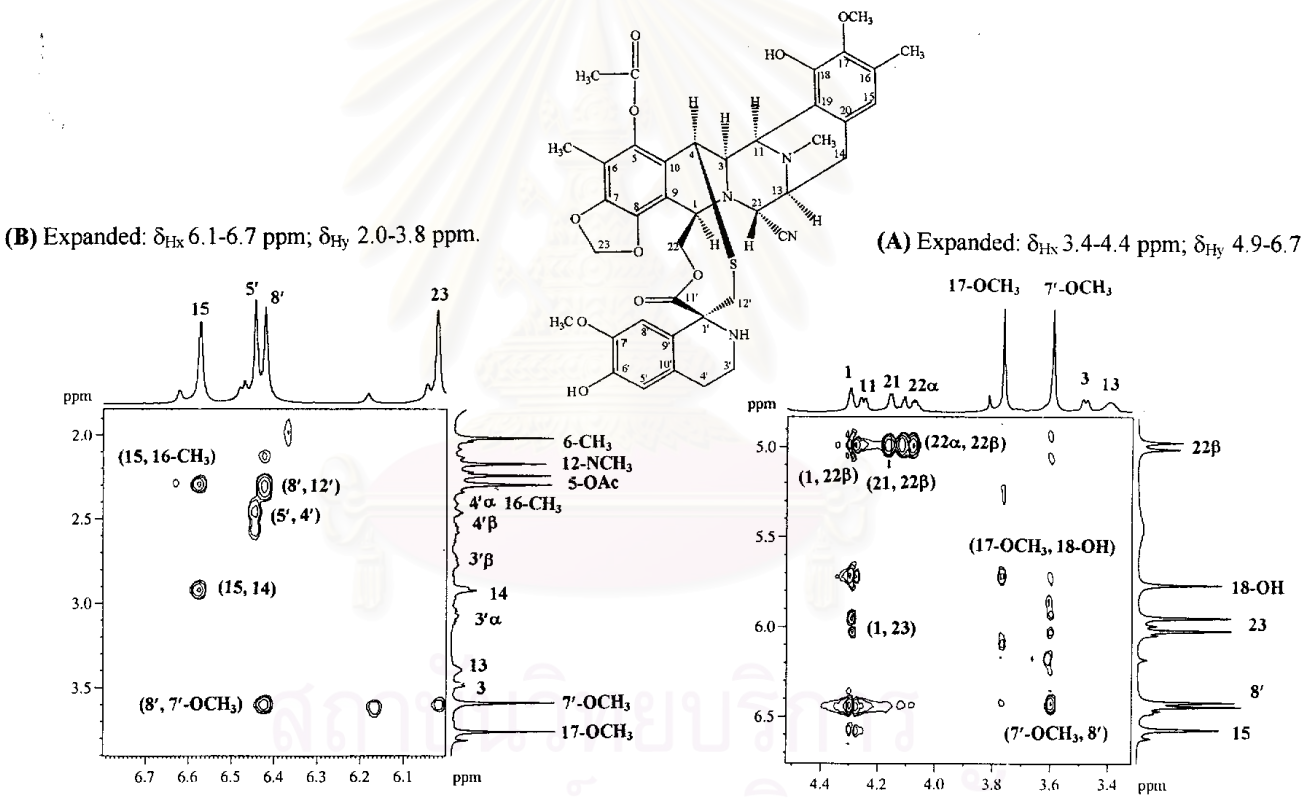

Figure 28 The 300 MHz NOESY spectrum (in $CDCl_3$) of ecteinascidin 770 (ET1K) [expanded: δ_{Hx} 3.4-6.7 ppm; δ_{Hy} 2.0-6.7 ppm].

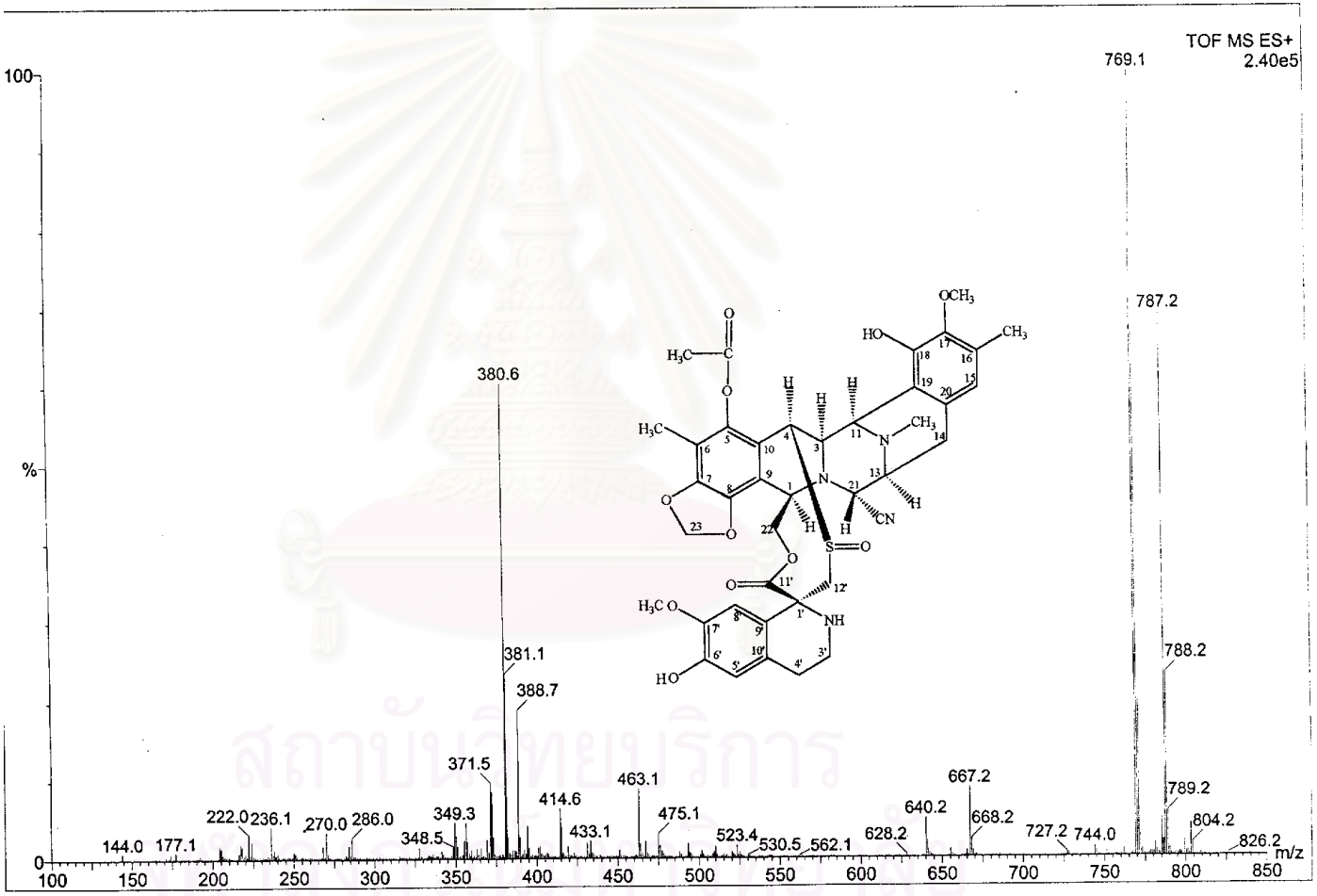

Figure 29 The ESI-TOF MS spectrum of ecteinascidin 786 (ET2K).

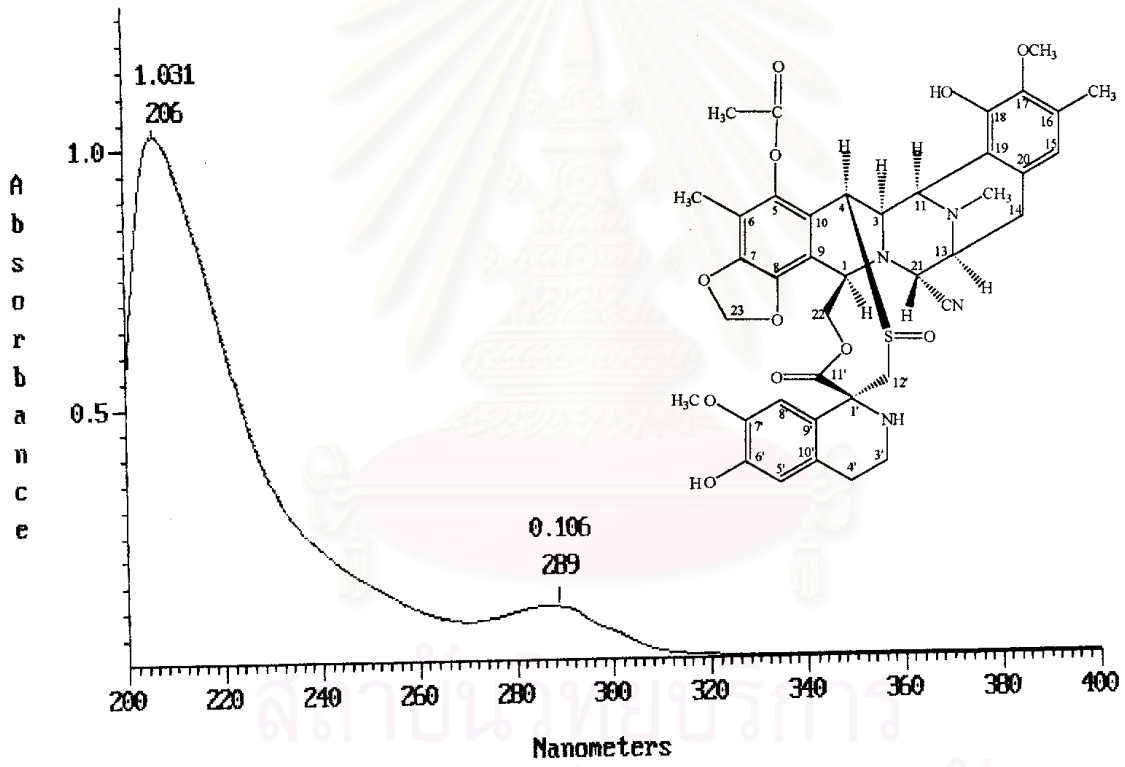

Figure 30 The UV spectrum (in MeOH) of ecteinascidin 786 (ET2K).

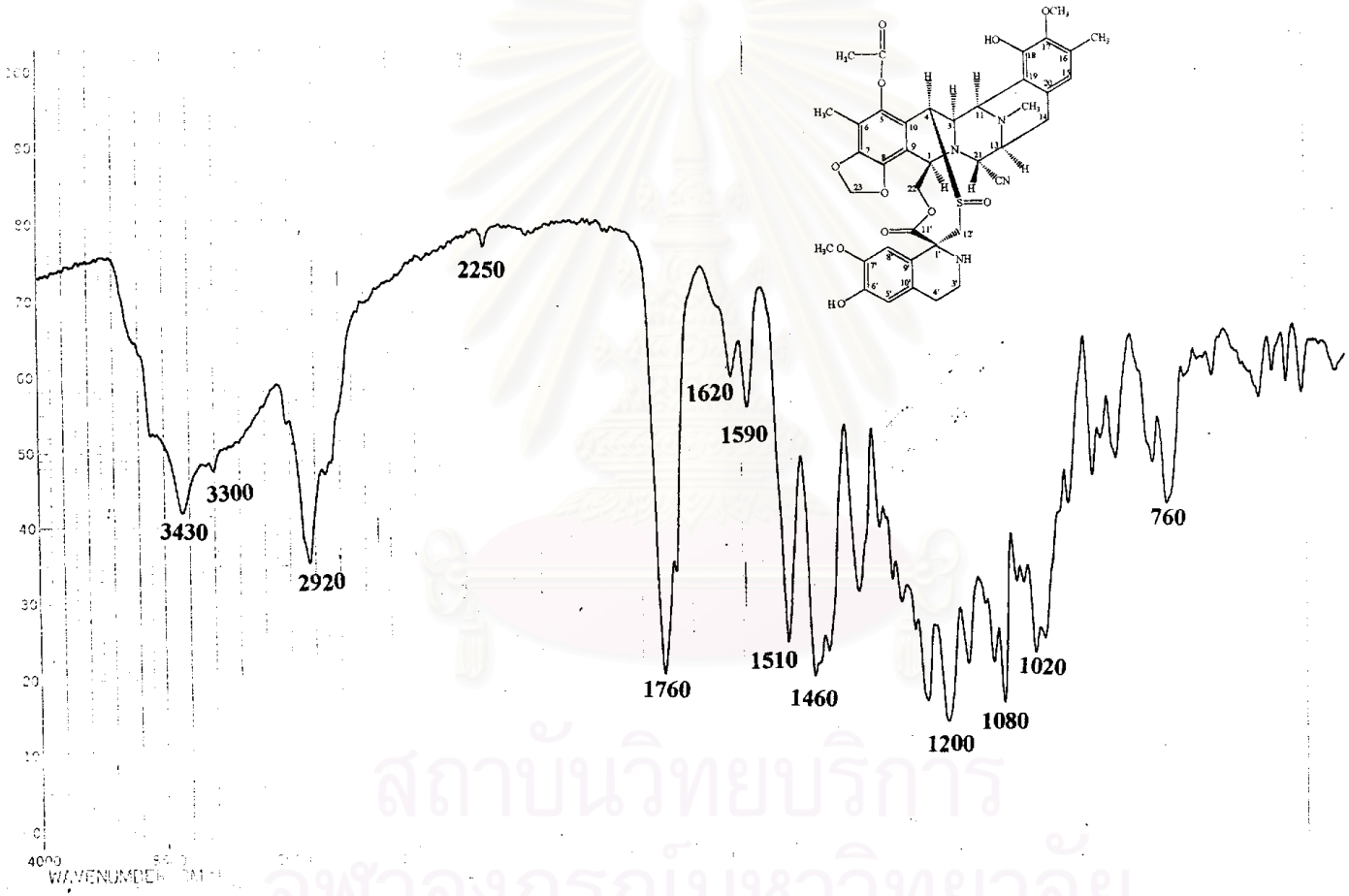

Figure 31 The IR spectrum (KBr disc) of ecteinascidin 786 (ET2K).

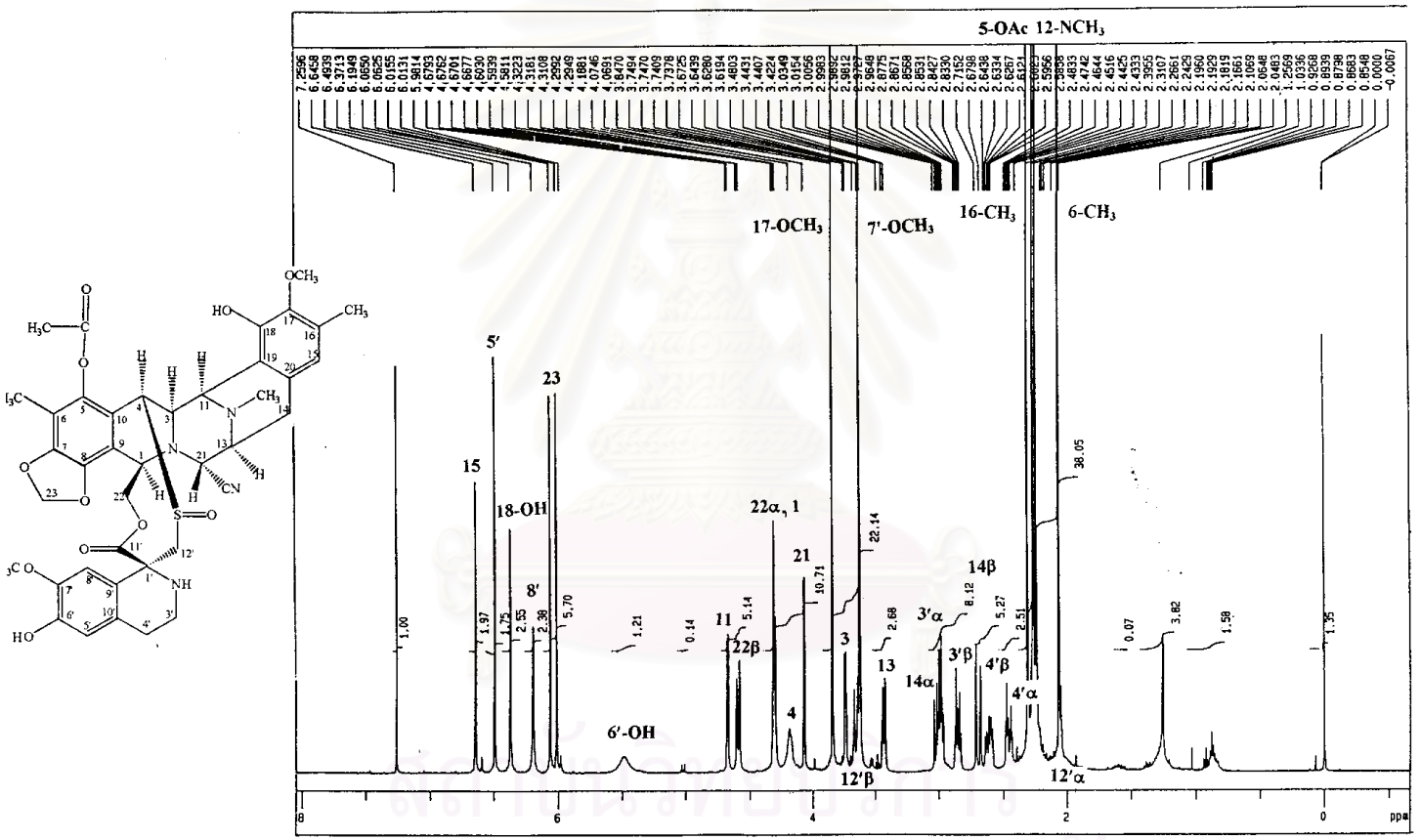

Figure 32 The 500 MHz ^{1}H NMR spectrum (in $CDCl_3$) of ecteinascidin 786 (ET2K).

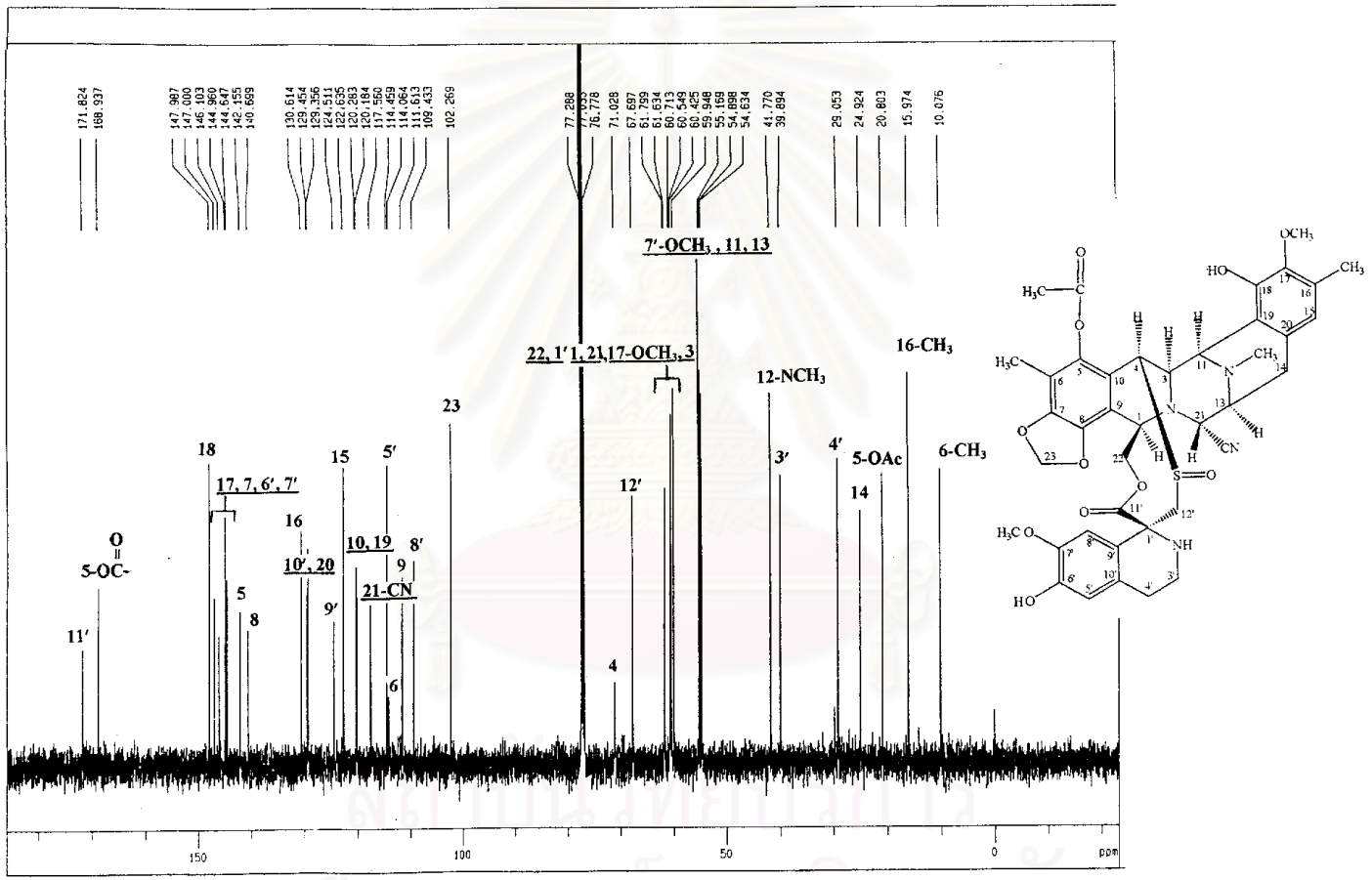

Figure 33 The 125 MHz ^{13}C NMR spectrum (in $CDCl_3$) of ecteinascidin 786 (ET2K).

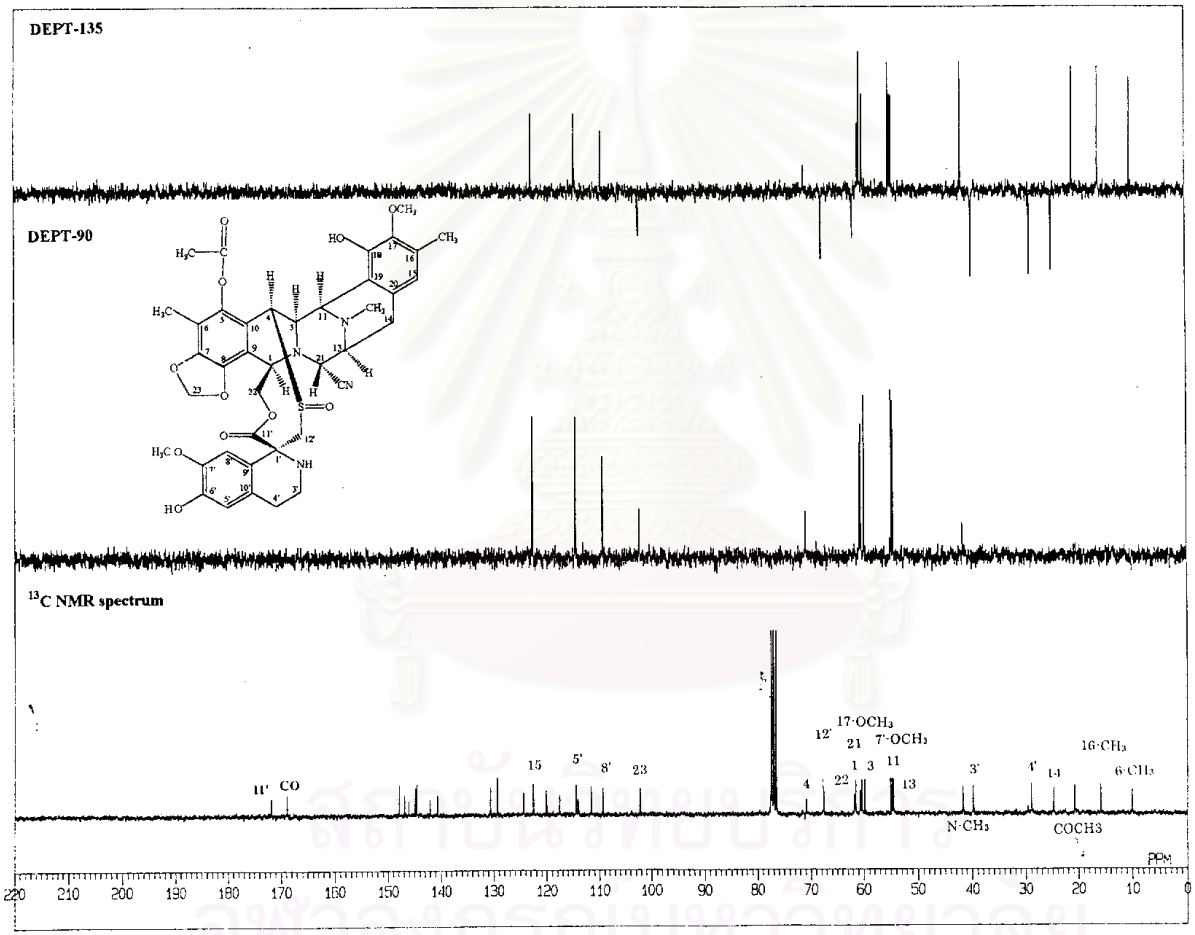

Figure 34 The 125 MHz ^{13}C NMR, DEPT-135,and DEPT-90 spectra (in $CDCl_3$) of ecteinascidin 786 (ET2K).

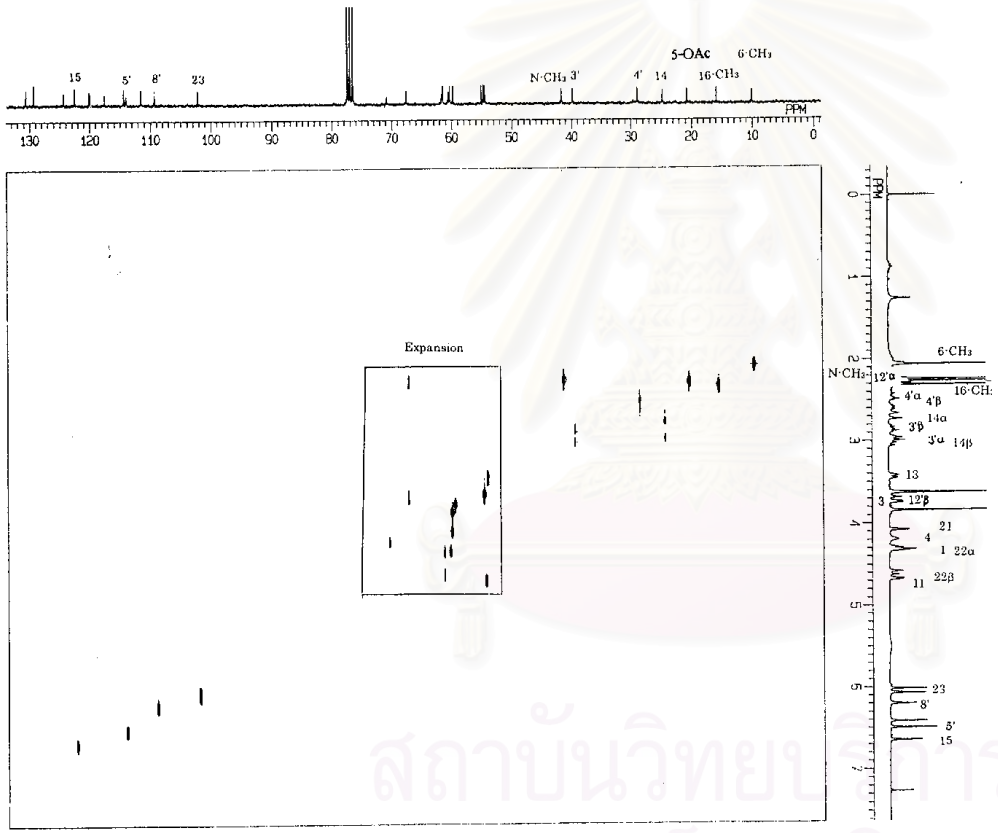

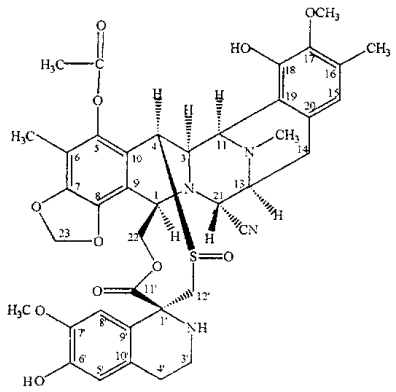

Figure 35 The 500 MHz HMQC spectrum (in $CDCl_3$) of ecteinascidin 786 (ET2K).

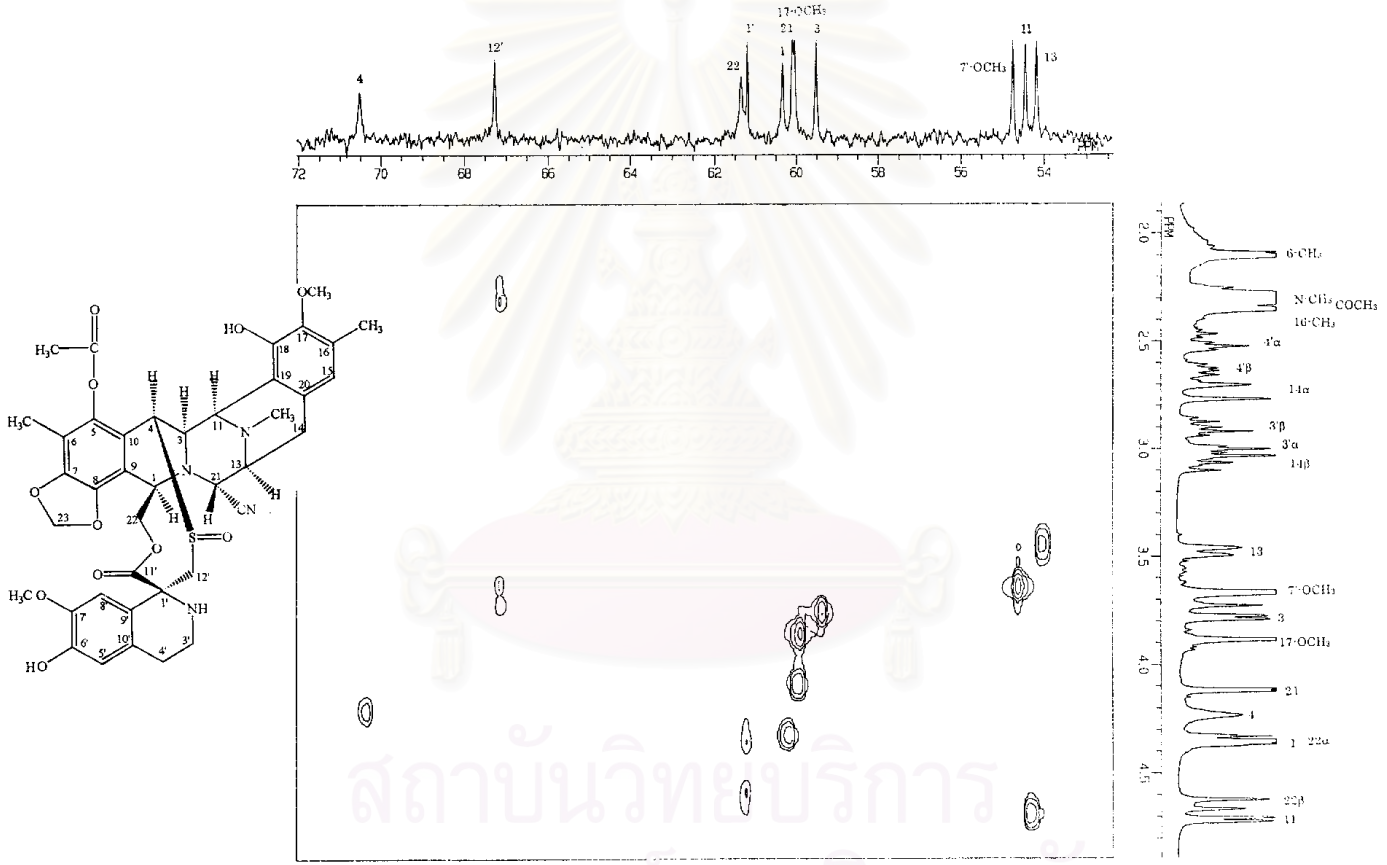

Figure 36 The 500 MHz HMQC spectrum (in $CDCl_3$) of ecteinascidin 786 (ET2K) [expanded: δ_H 2.0-4.8 ppm; δ_C 54-72 ppm].

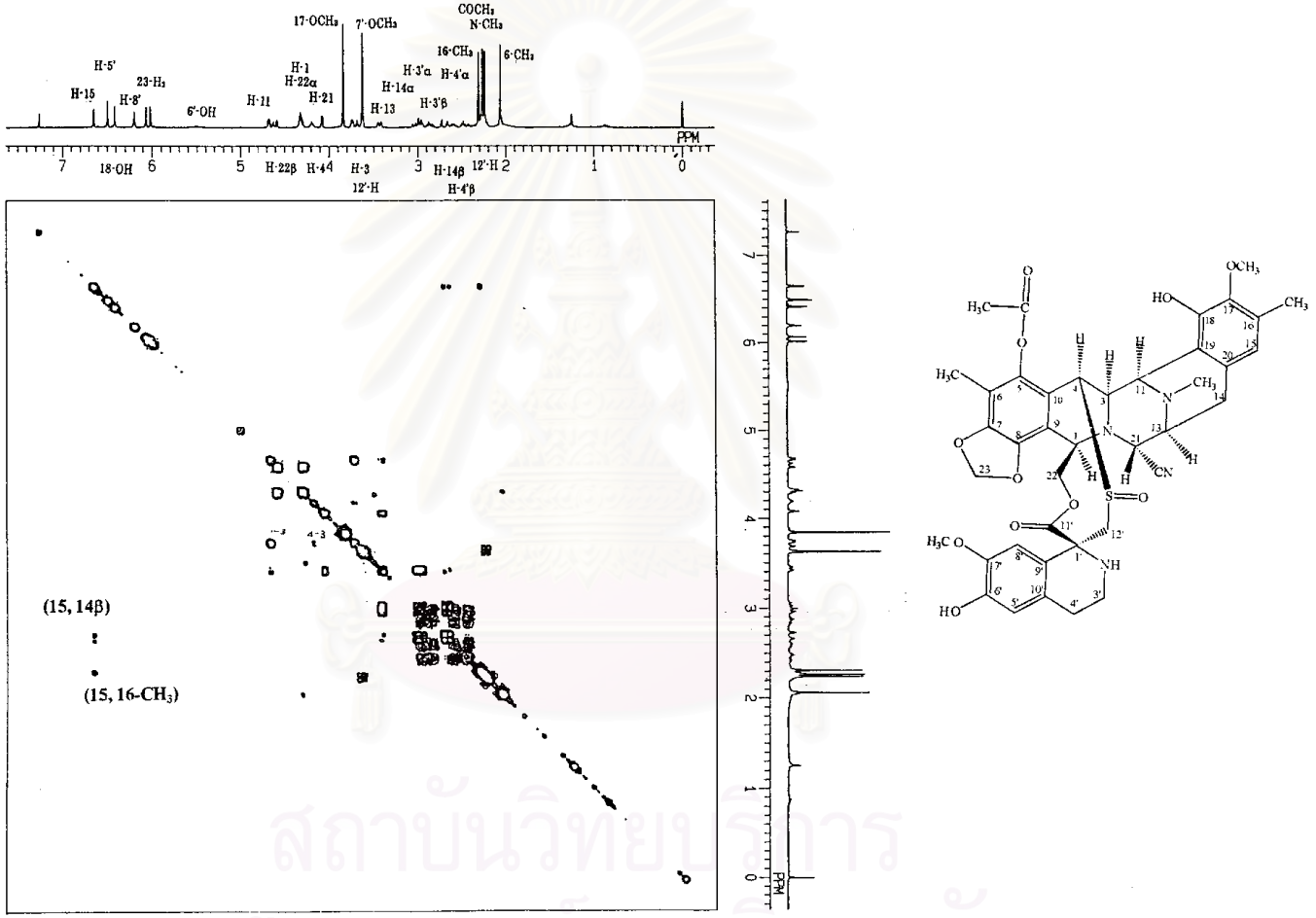

Figure 37 The 500 MHz ^{1}H-^{1}H COSY spectrum (in $CDCl_3$) of ecteinascidin 786 (ET2K).

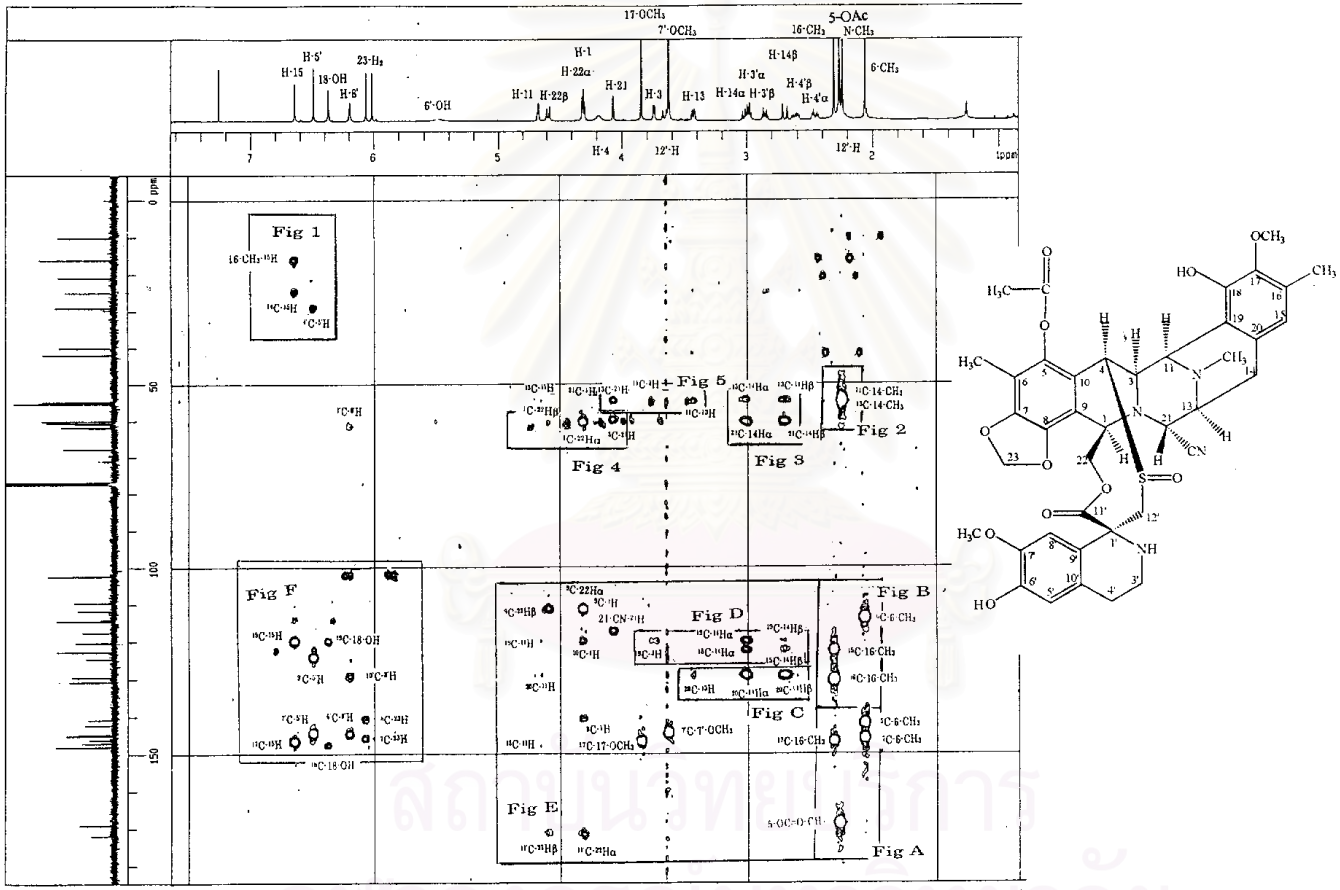

Figure 38 The 500 MHz HMBC spectrum ($^{n}J_{HC}$ = 8 Hz in $CDCl_3$) of ecteinascidin 786 (ET2K).

Fig E

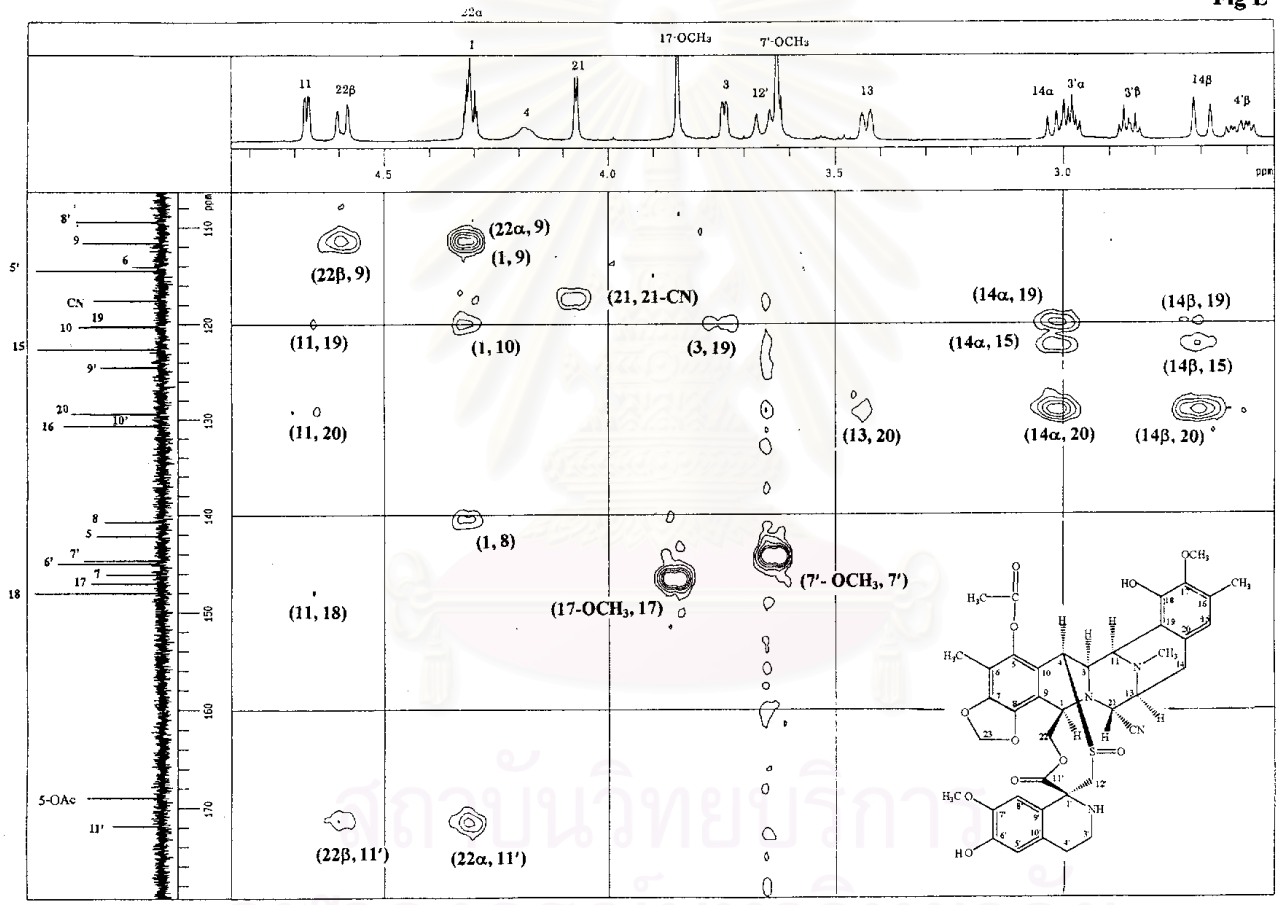

Figure 39 The 500 MHz HMBC spectrum ($^{n}J_{HC}$ = 8 Hz in $CDCl_3$) of ecteinascidin 786 (ET2K) [expanded: δ_H 2.6-4.8 ppm; δ_C 109-172 ppm].

Fig F

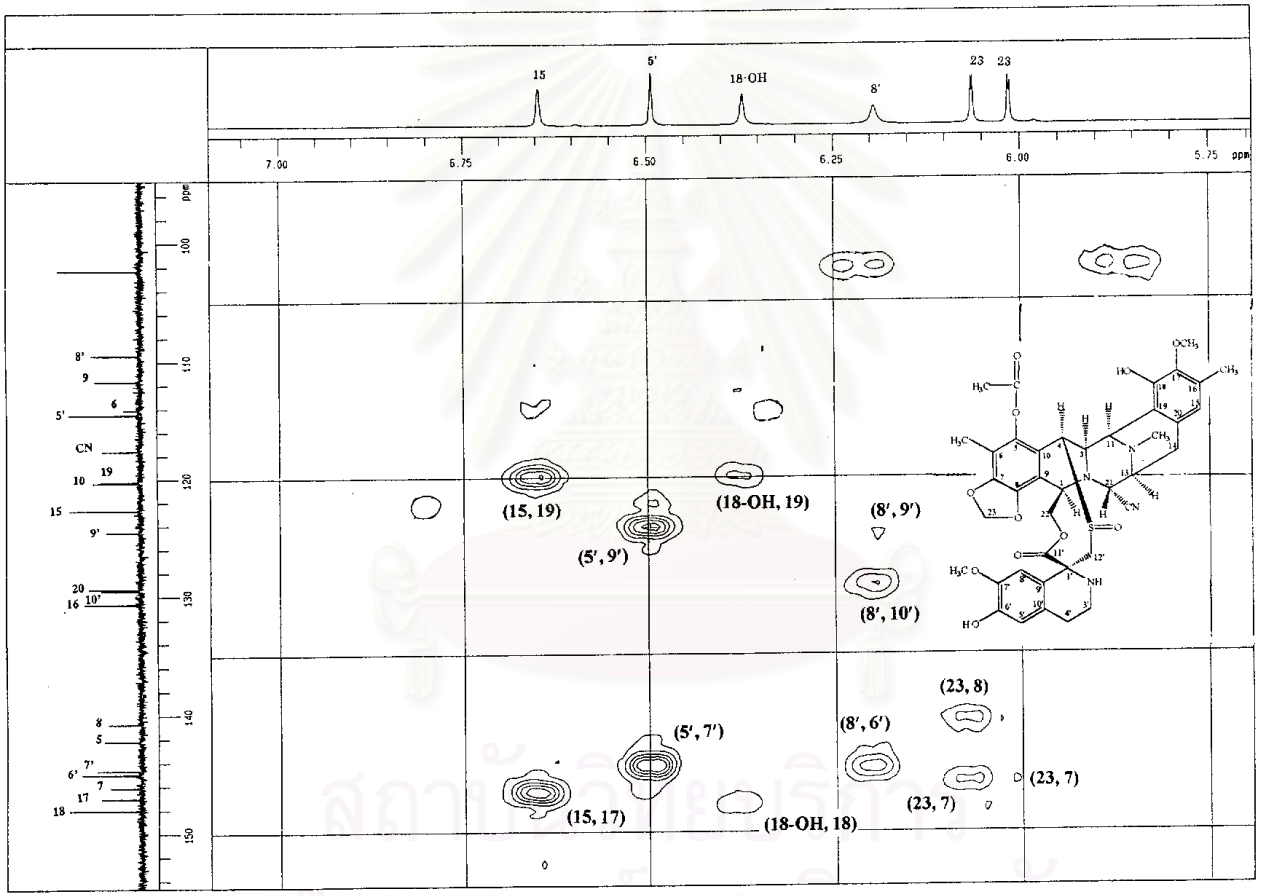

Figure 40 The 500 MHz HMBC spectrum ($^{n}J_{HC}$ = 8 Hz in $CDCl_3$) of ecteinascidin 786 (ET2K) [expanded: δ_H 5.7-7.0 ppm; δ_C 100-150 ppm].

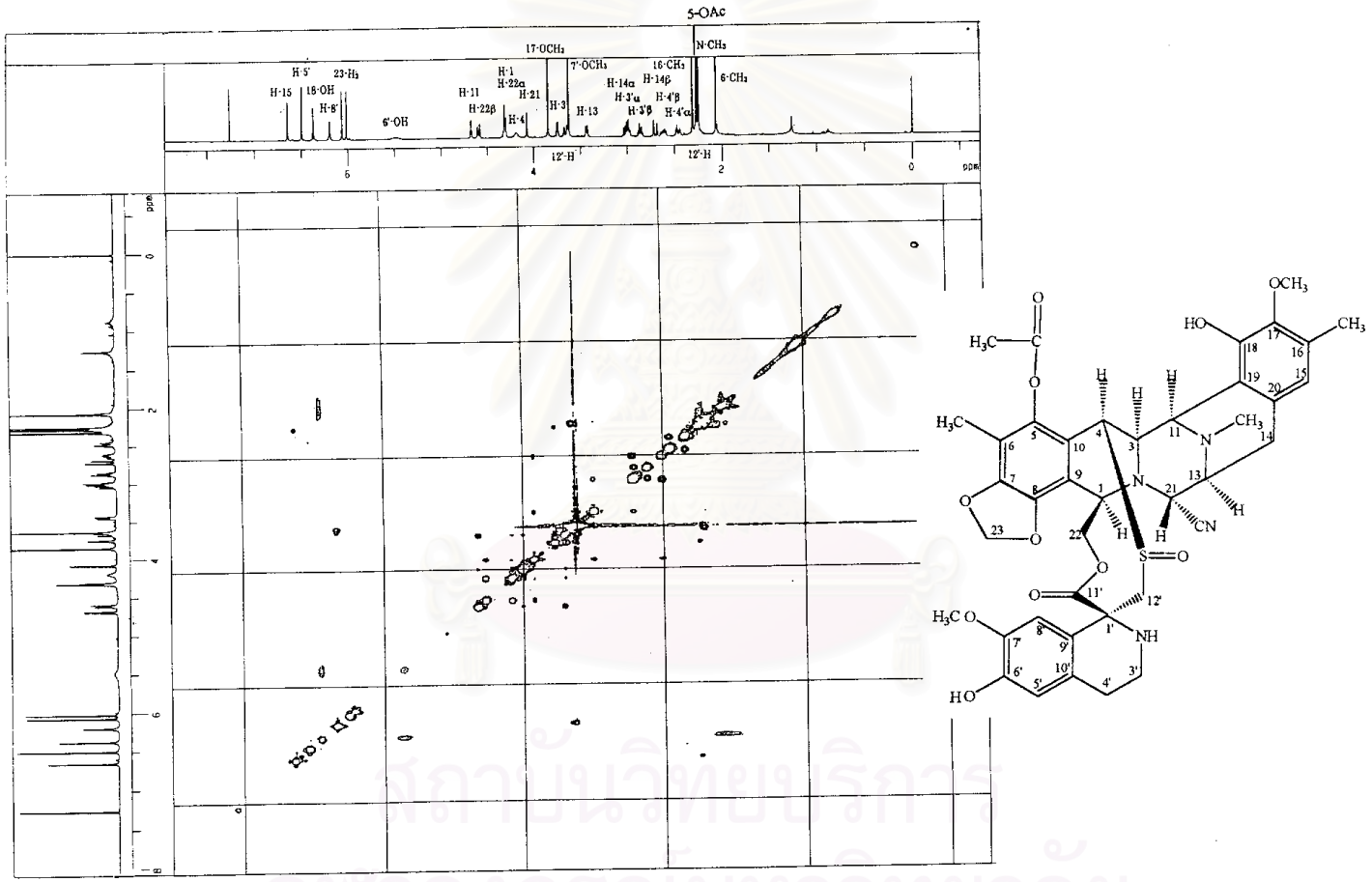

Figure 41 The 500 MHz NOESY spectrum (in $CDCl_3$) of ecteinascidin 786 (ET2K).

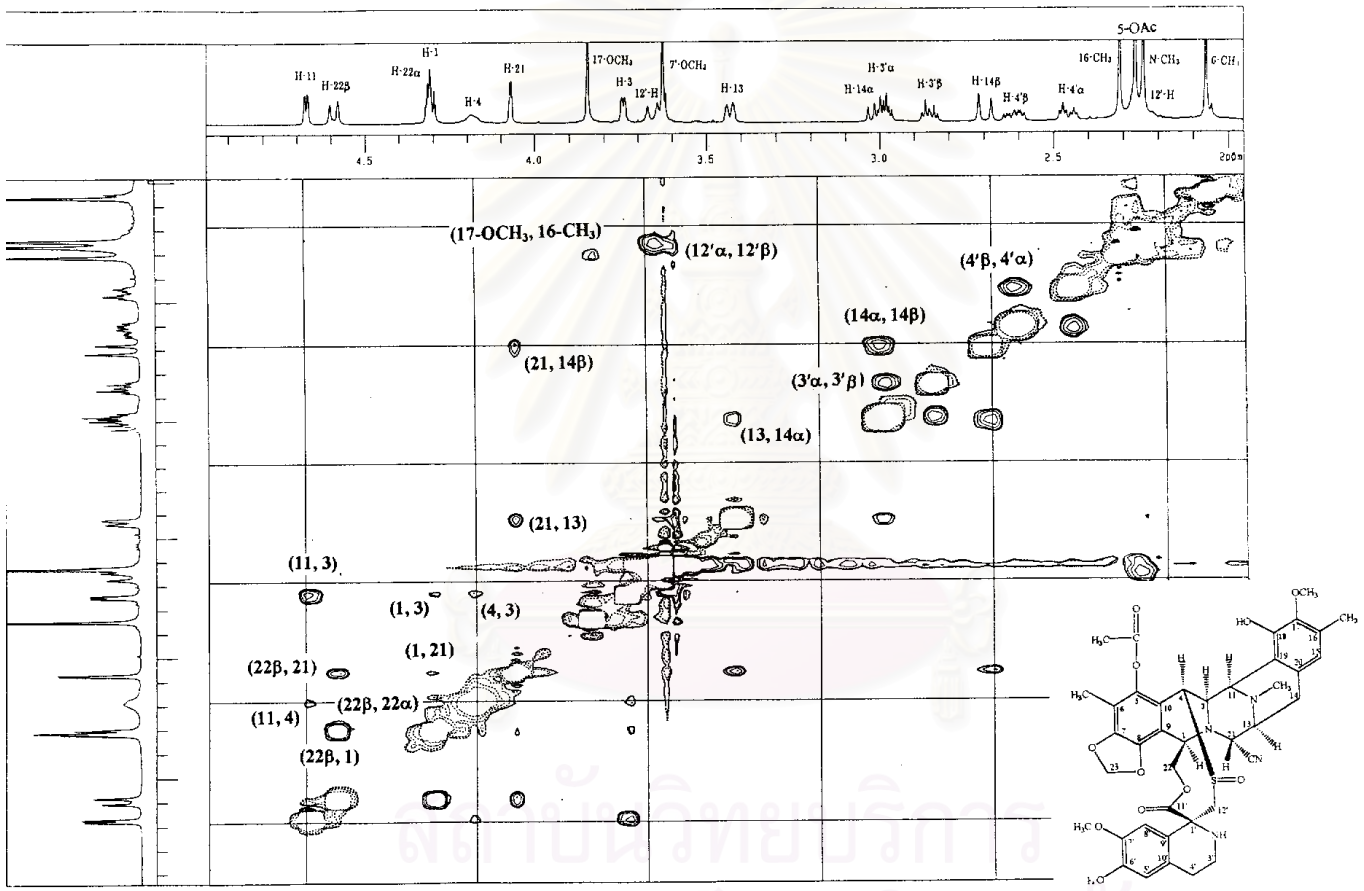

Figure 42 The 500 MHz NOESY spectrum (in $CDCl_3$) of ecteinascidin 786 (ET2K) [expanded: δ_{Hx} 2.0-4.8 ppm; δ_{Hy} 2.0-4.5 ppm].

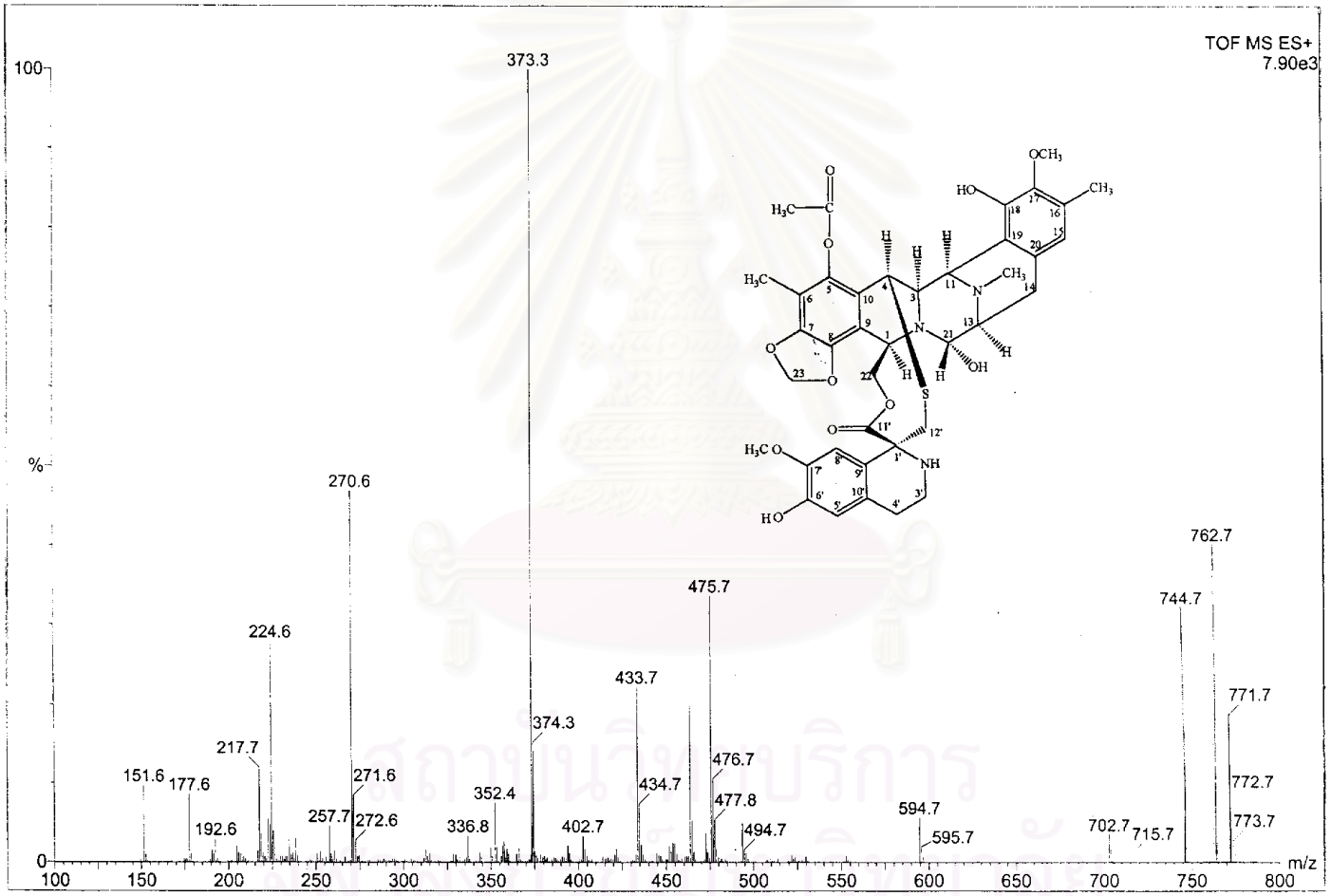

Figure 43 The ESI-TOF MS spectrum of ecteinascidin 743 (ET4K).

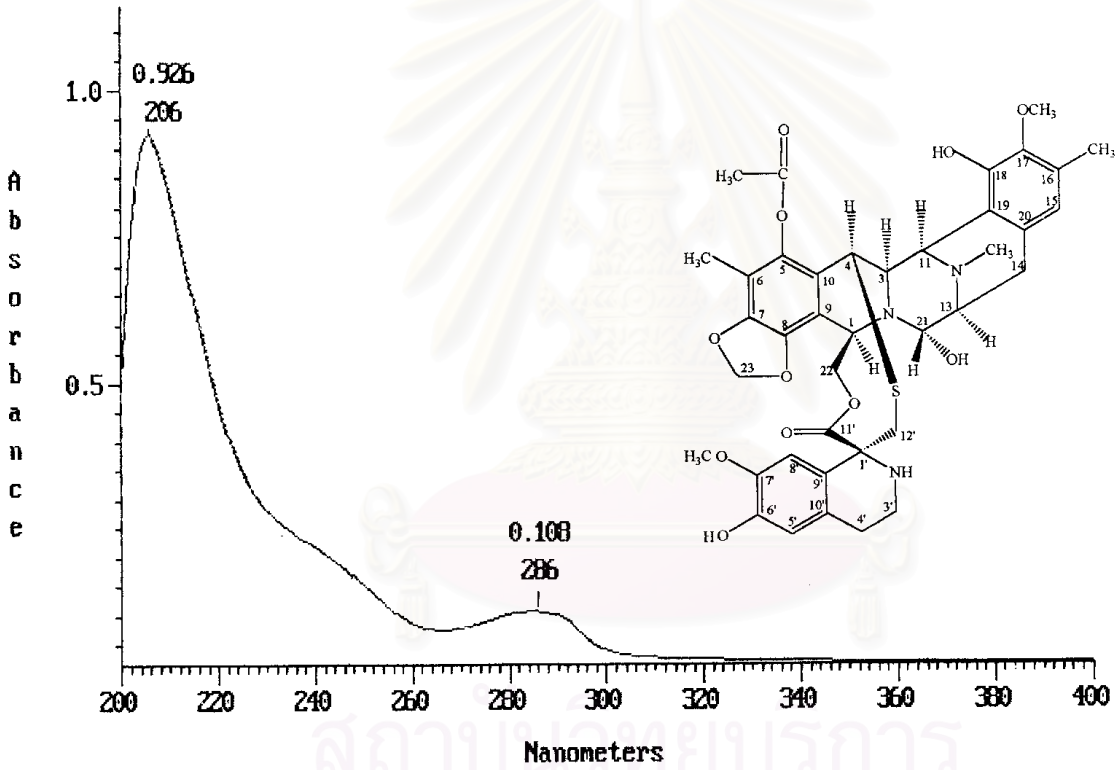

Figure 44 The UV spectrum (in MeOH) of ecteinascidin 743 (ET4K).

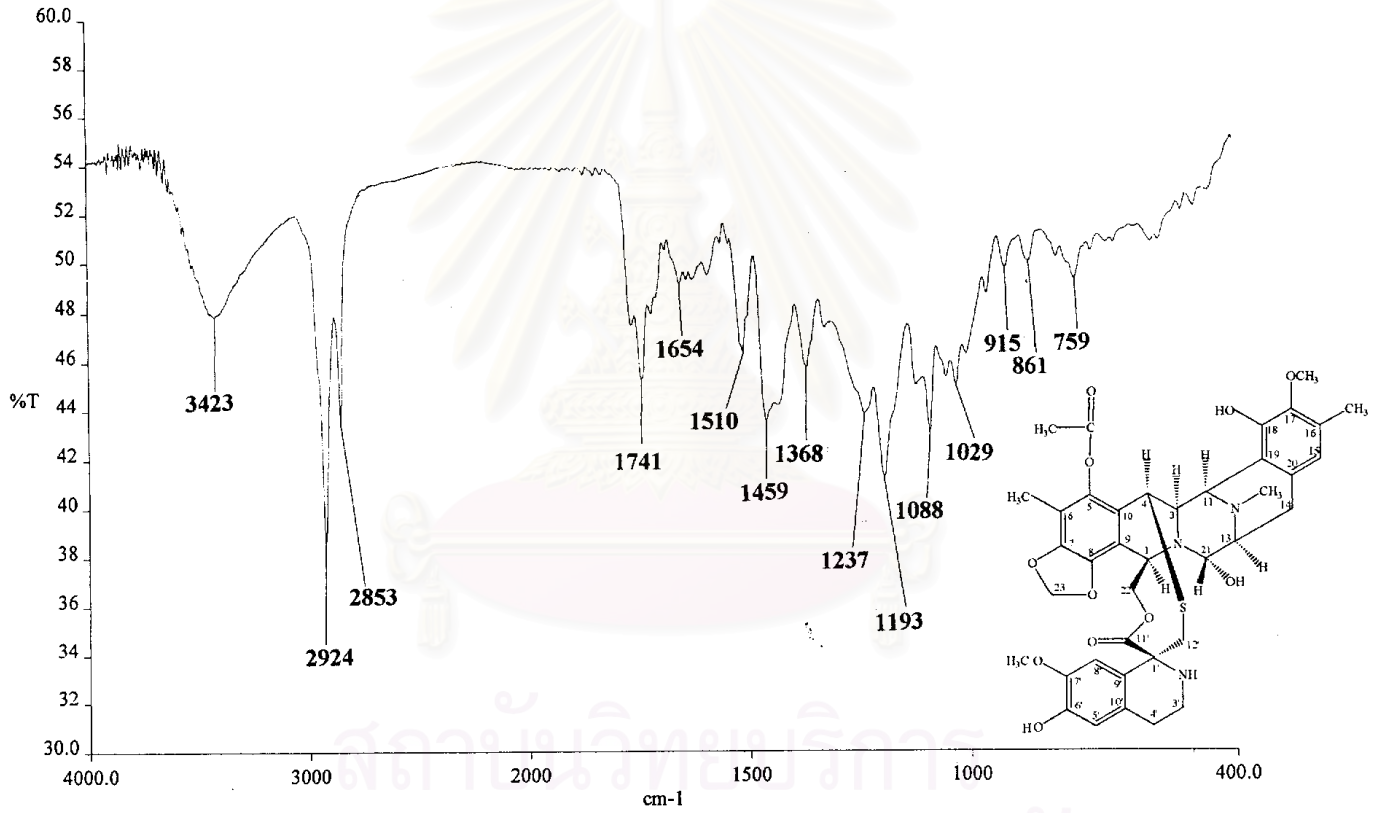

Figure 45 The IR spectrum (KBr disc) of ecteinascidin 743 (ET4K).

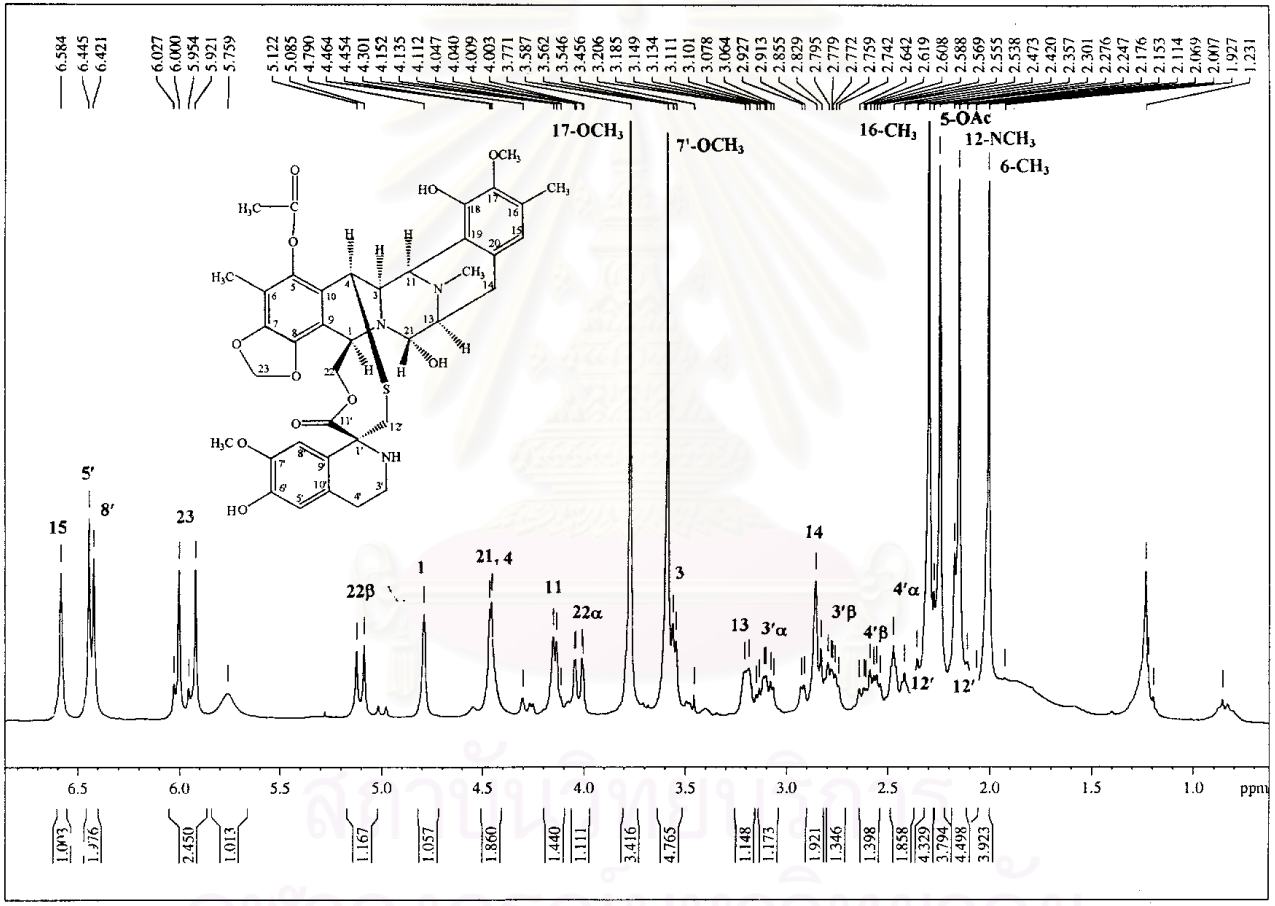

Figure 46 The 300 MHz ^{1}H NMR spectrum (in $CDCl_3$) of ecteinascidin 743 (ET4K).

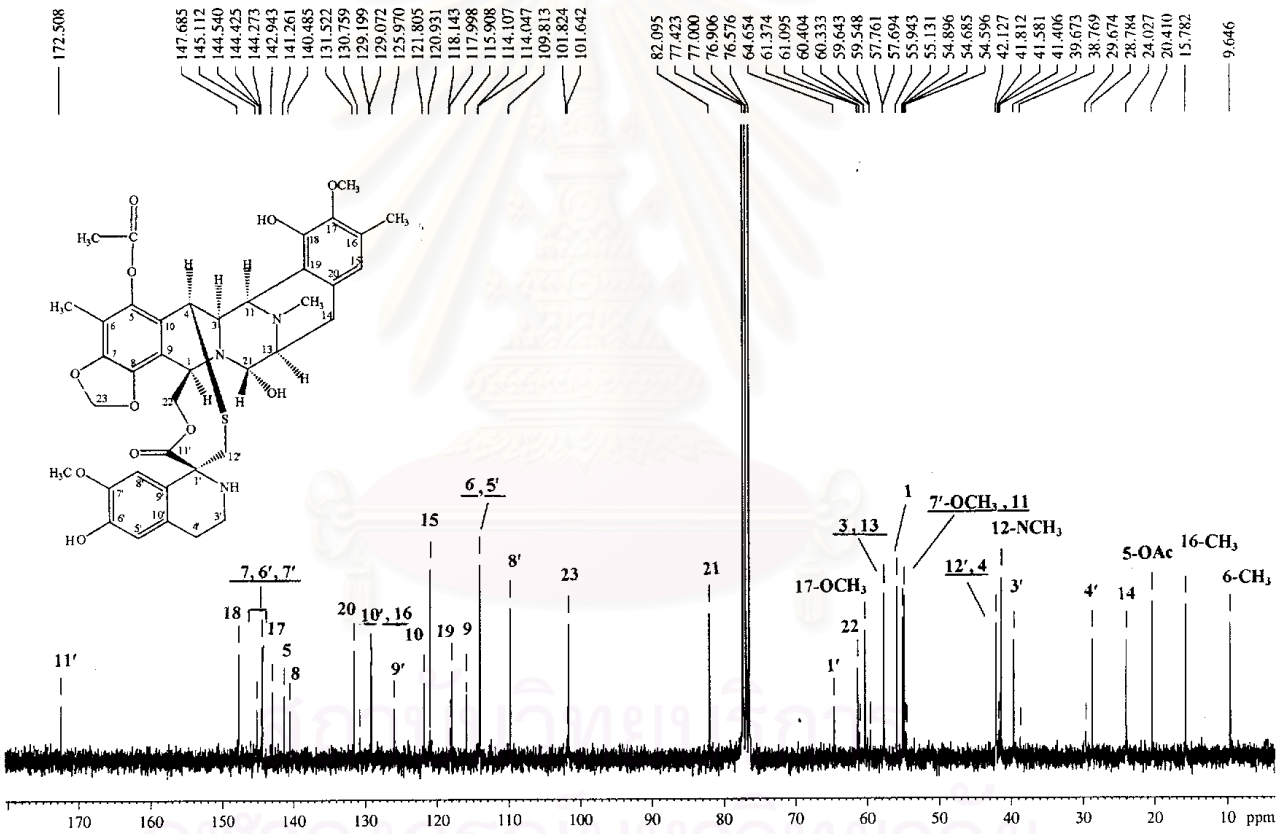

Figure 47 The 75 MHz ^{13}C NMR spectrum (in $CDCl_3$) of ecteinascidin 743 (ET4K).

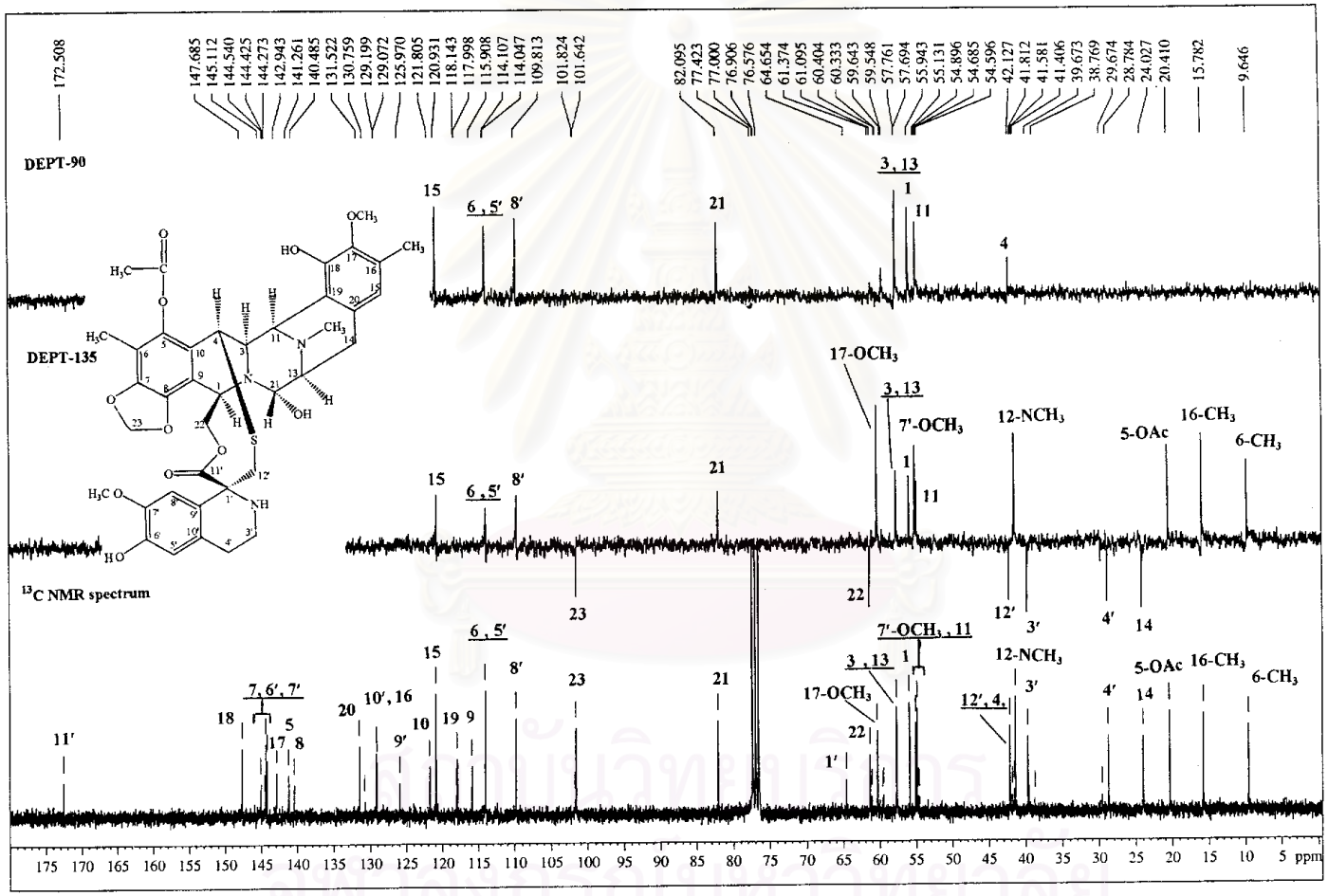

Figure 48 The 75 MHz ^{13}C NMR, DEPT-135,and DEPT-90 spectra (in $CDCl_3$) of ecteinascidin 743 (ET4K).

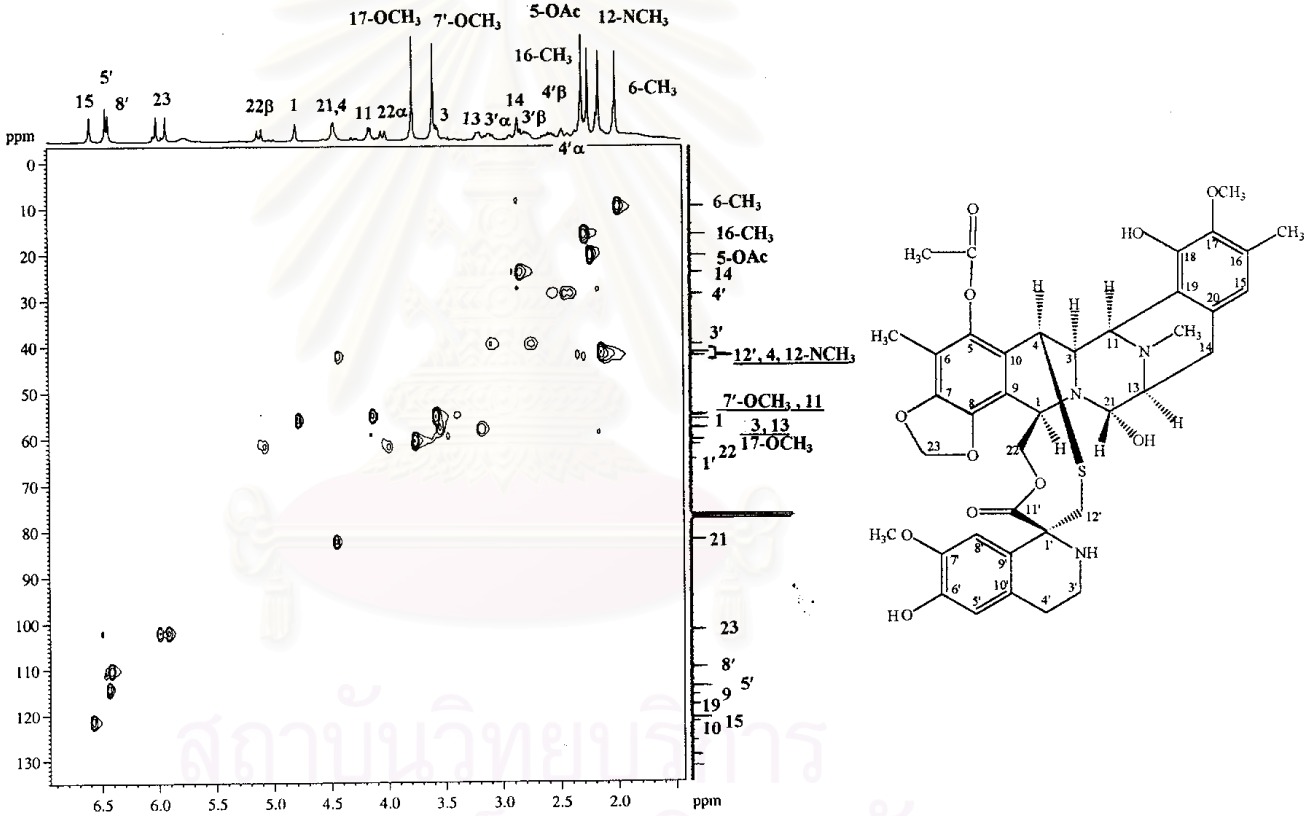

Figure 49 The 300 MHz HMQC spectrum (in $CDCl_3$) of ecteinascidin 743 (ET4K).

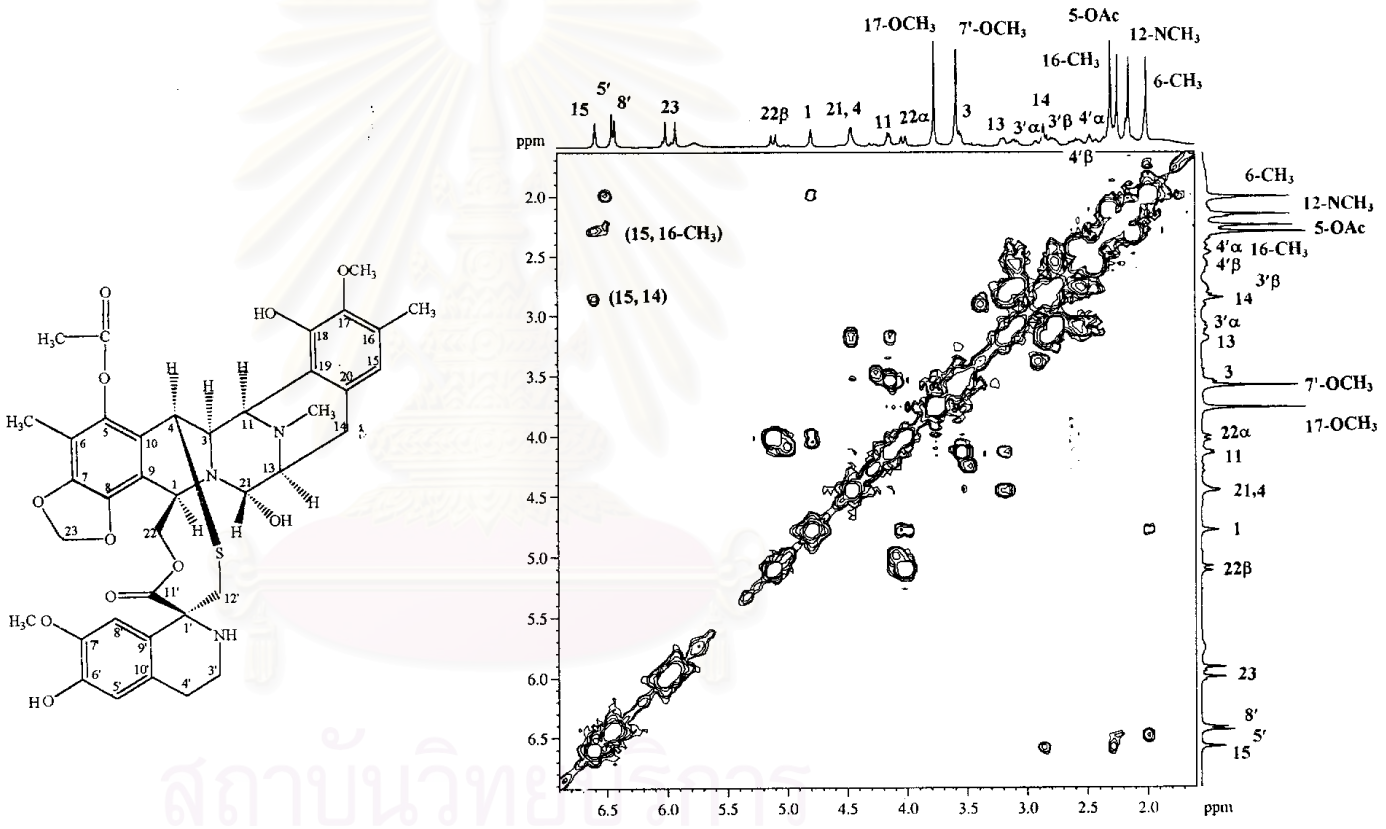

Figure 50 The 300 MHz ^{1}H-^{1}H COSY spectrum (in $CDCl_3$) of ecteinascidin 743 (ET4K).

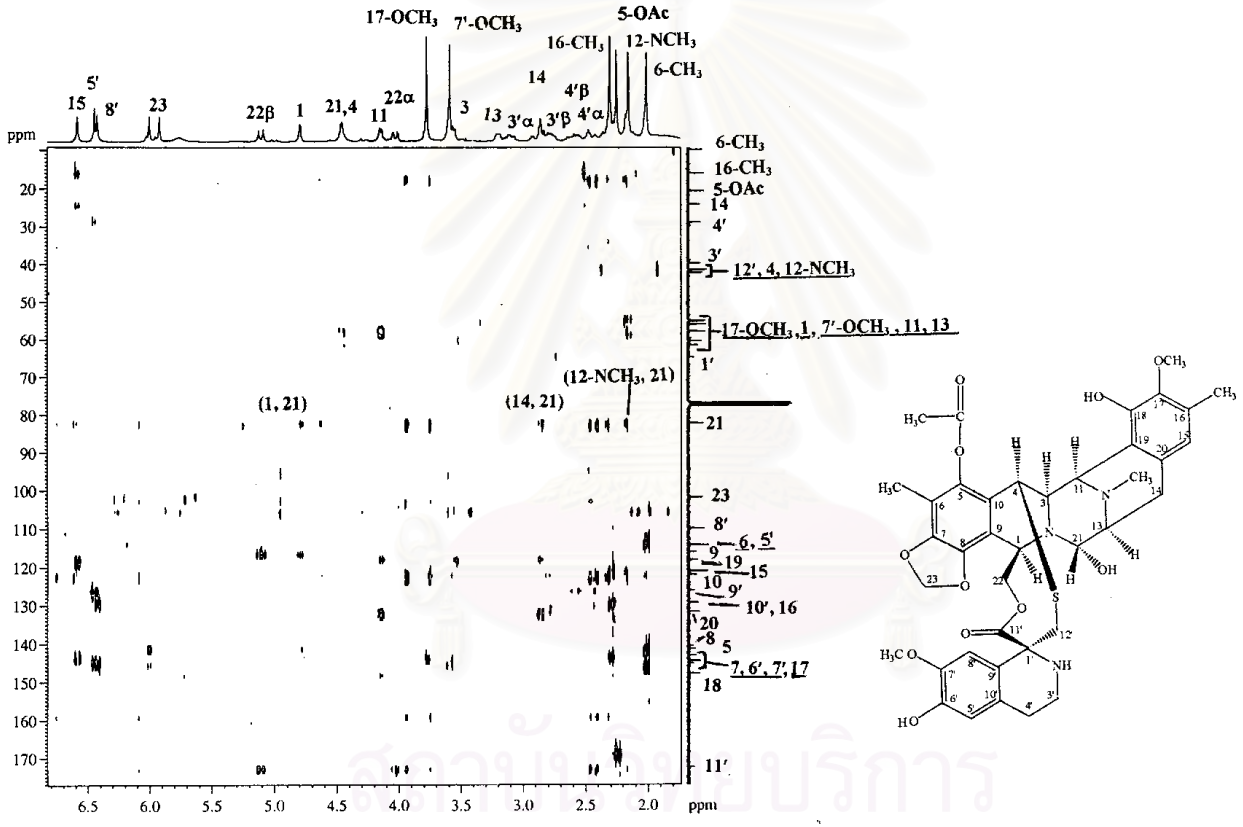

Figure 51 The 300 MHz HMBC spectrum ($^{n}J_{HC}$ = 8 Hz in $CDCl_3$) of ecteinascidin 743 (ET4K).

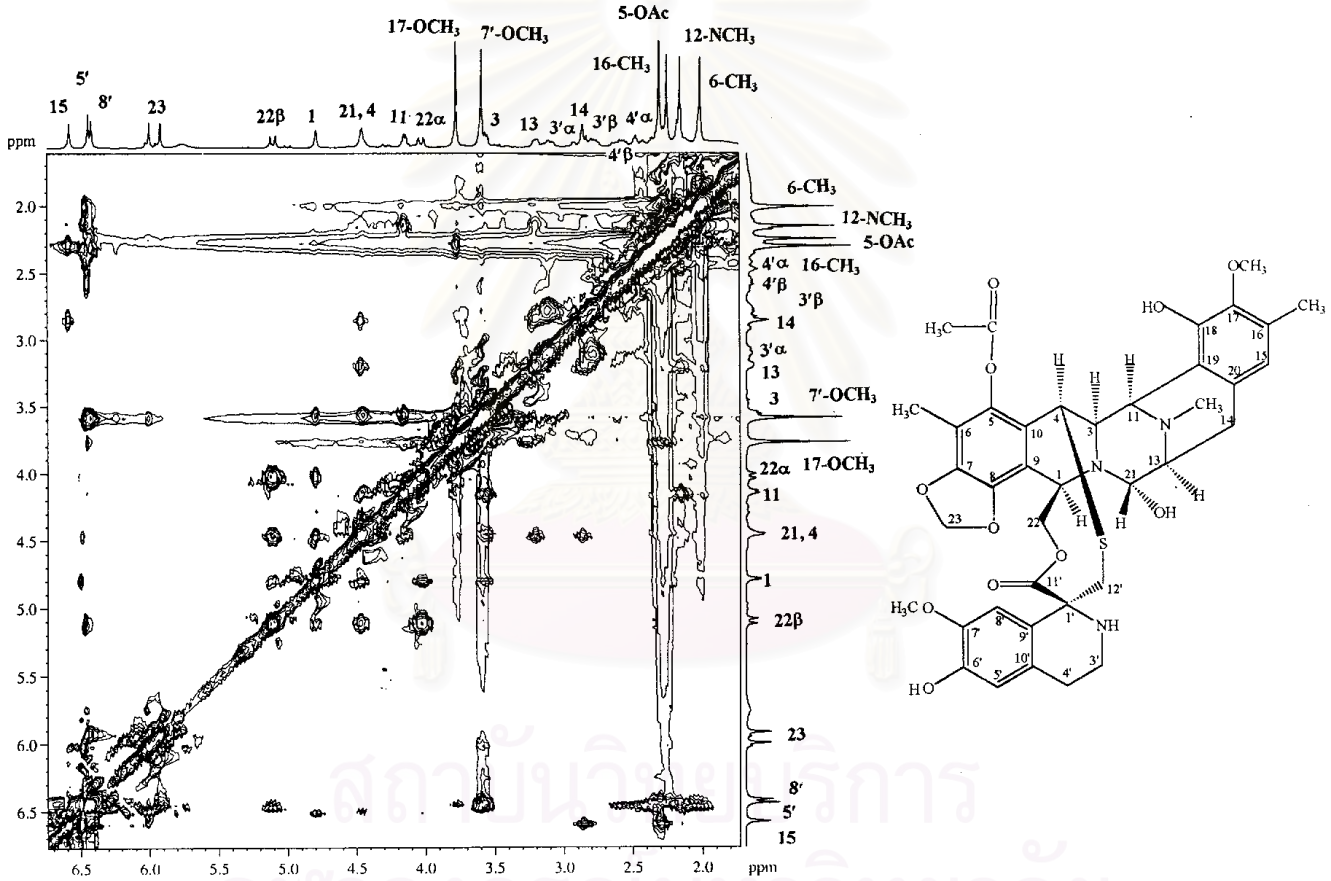

Figure 52 The 300 MHz NOESY spectrum (in $CDCl_3$) of ecteinascidin 743 (ET4K).

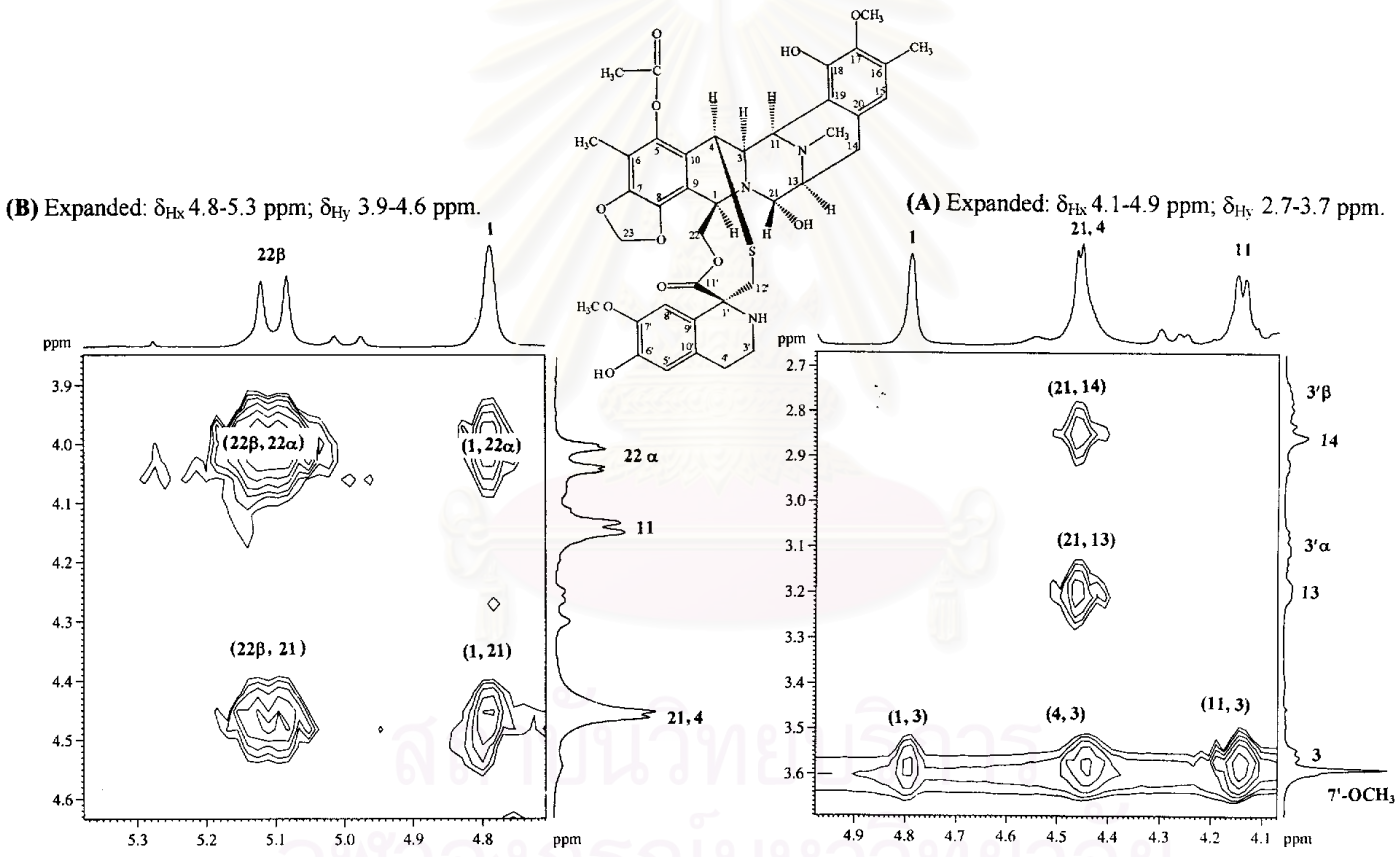

Figure 53 The 300 MHz NOESY spectrum (in $CDCl_3$) of ecteinascidin 743 (ET4K) [expanded: δ_{Hx} 4.1-5.3 ppm; δ_{Hy} 2.7-4.6 ppm].

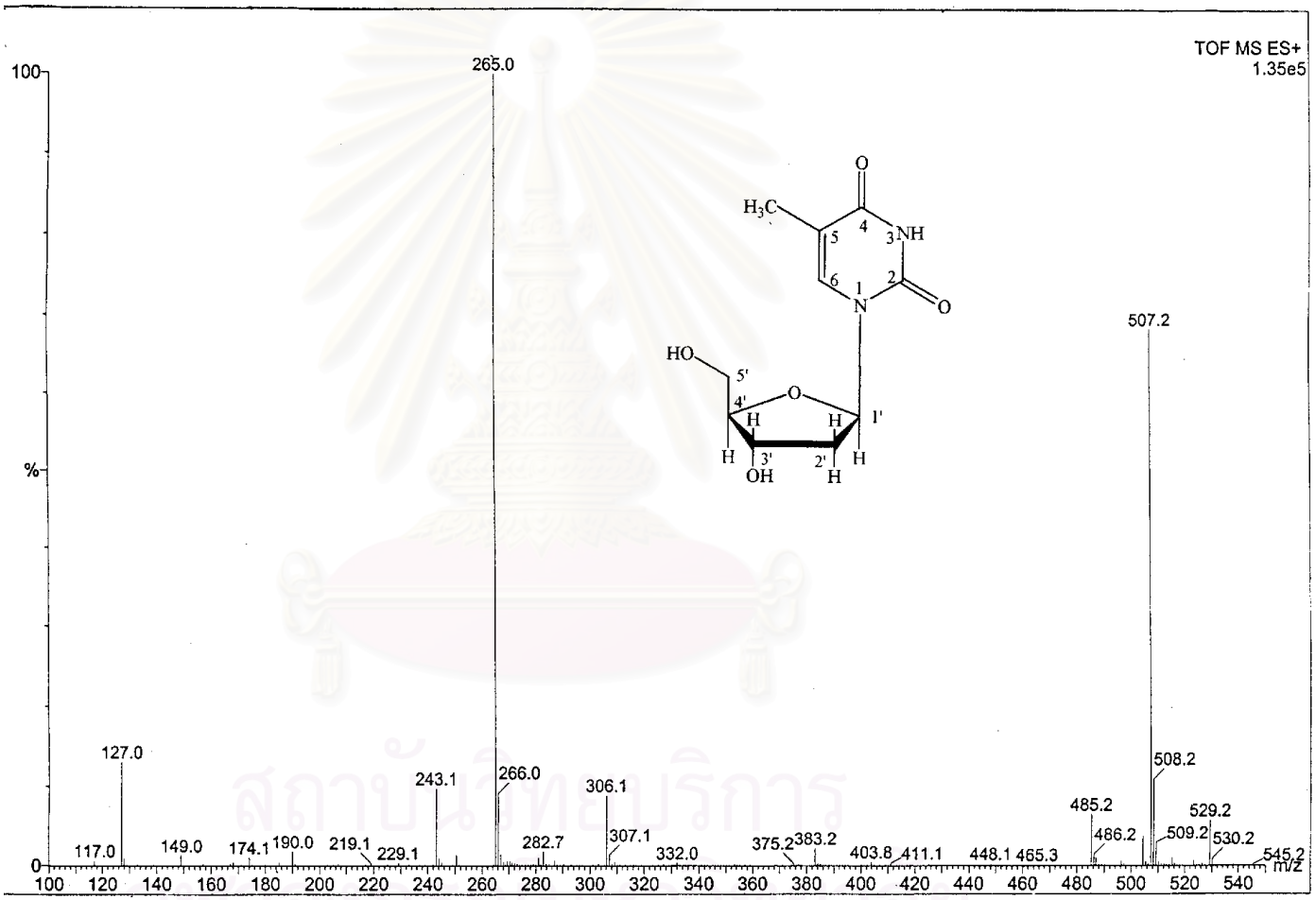

Figure 54 The ESI-TOF MS spectrum of thymidine (ET3K).

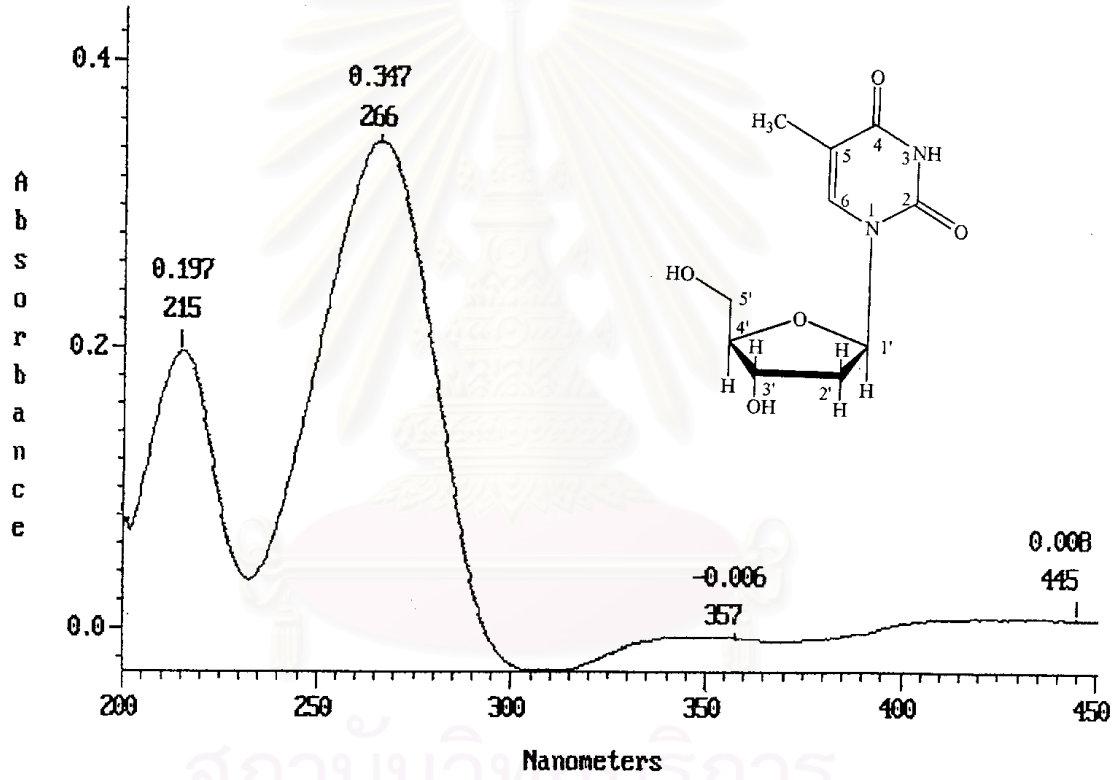

Figure 55 The UV spectrum (in MeOH) of thymidine (ET3K).

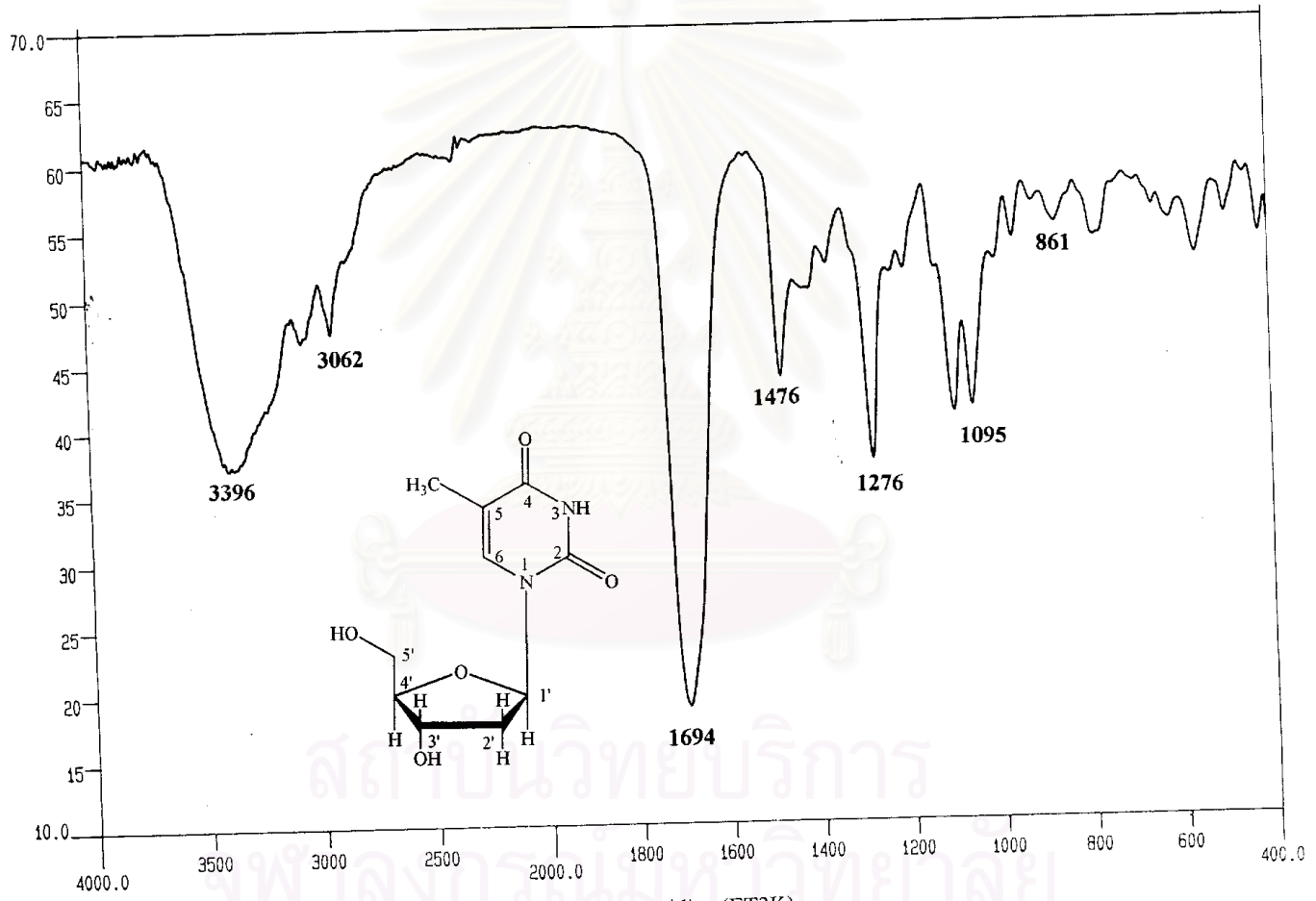

Figure 56 The IR spectrum (KBr disc) of thymidine (ET3K).

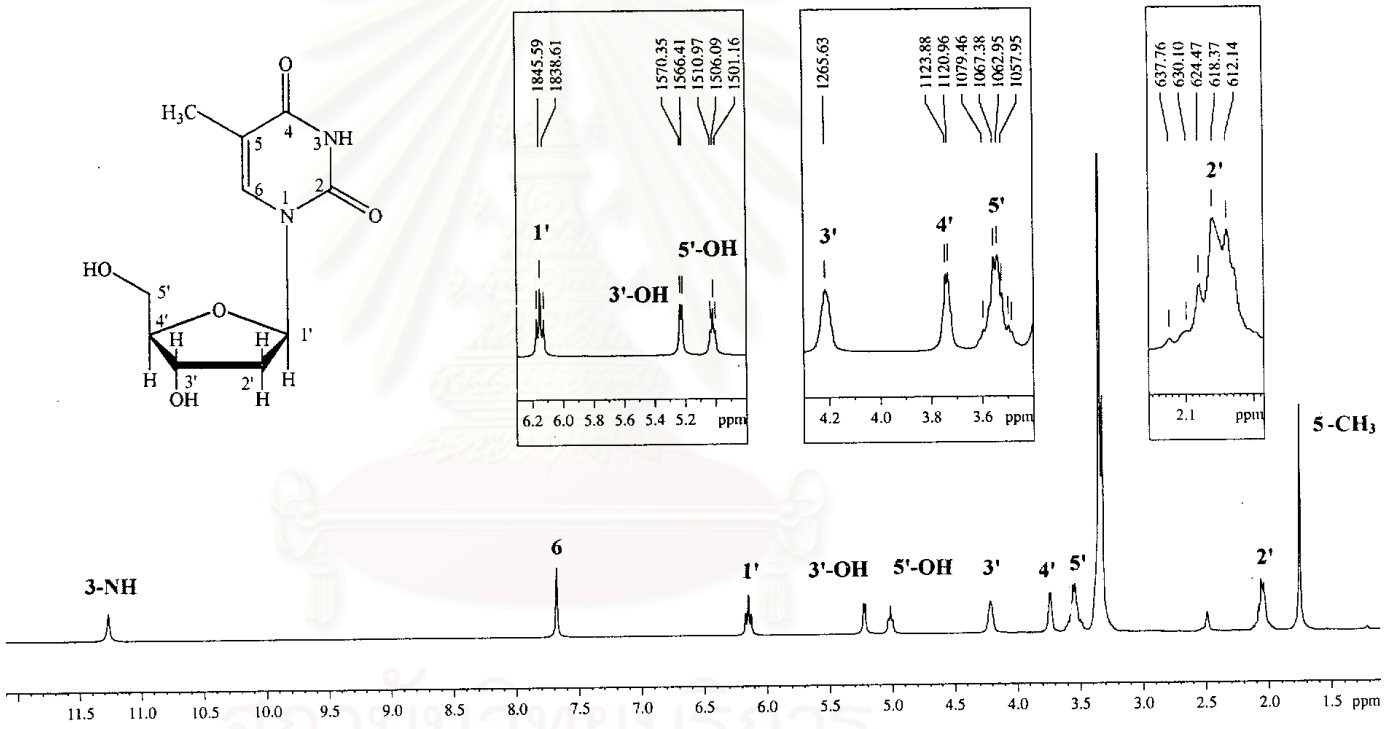

Figure 57 The 300 MHz ^{1}H NMR spectrum (in DMSO-d_6) of thymidine (ET3K) [expanded: δ_H 2.0-6.2 ppm].

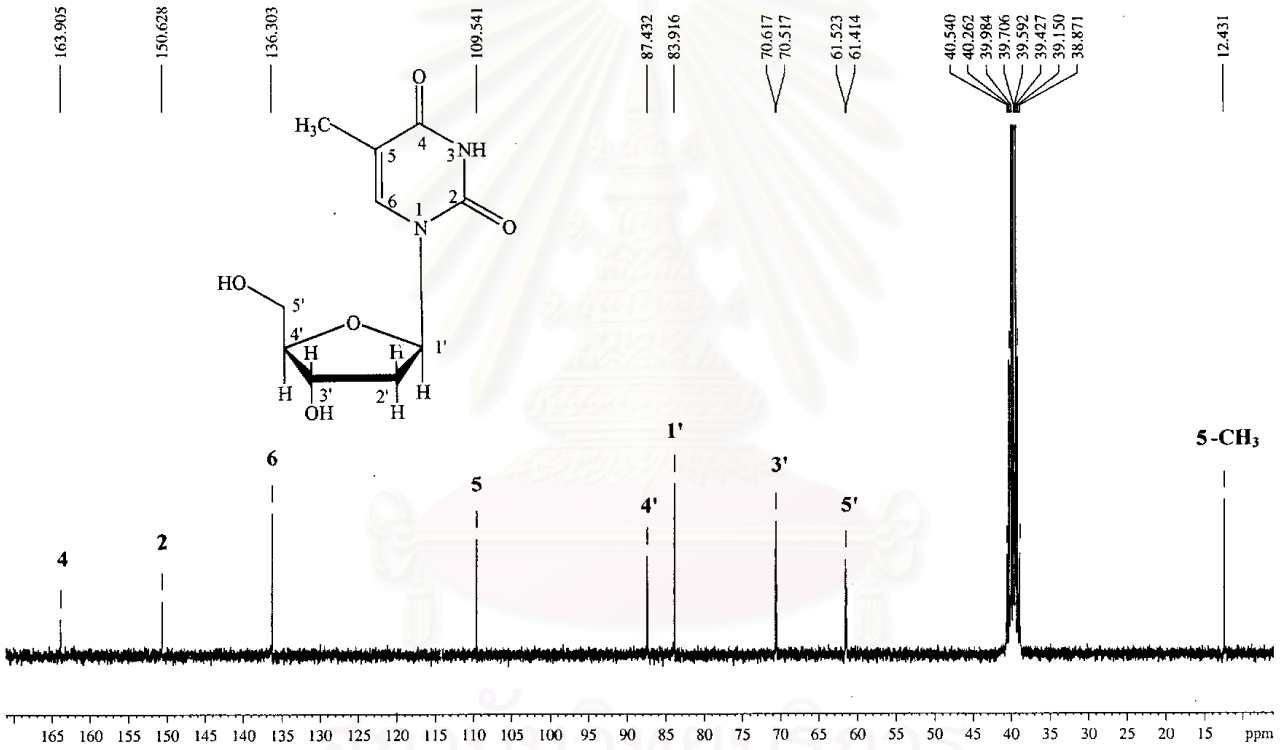

Figure 58 The 75 MHz ^{13}C NMR spectrum (in DMSO-d_6) of thymidine (ET3K).

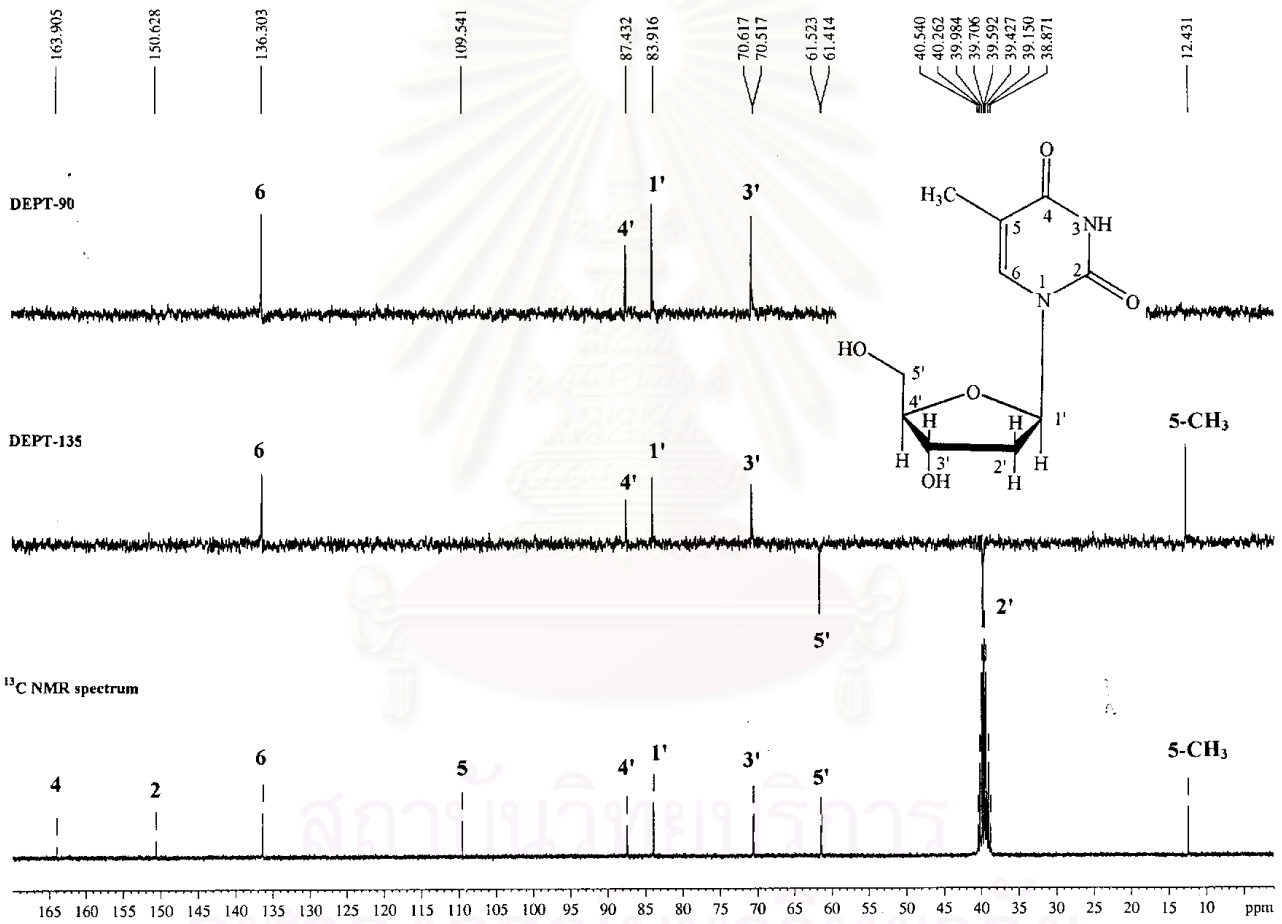

Figure 59 The 75 MHz ^{13}C NMR, DEPT-135 and DEPT-90 spectra (in DMSO-d_6) of thymidine (ET3K).

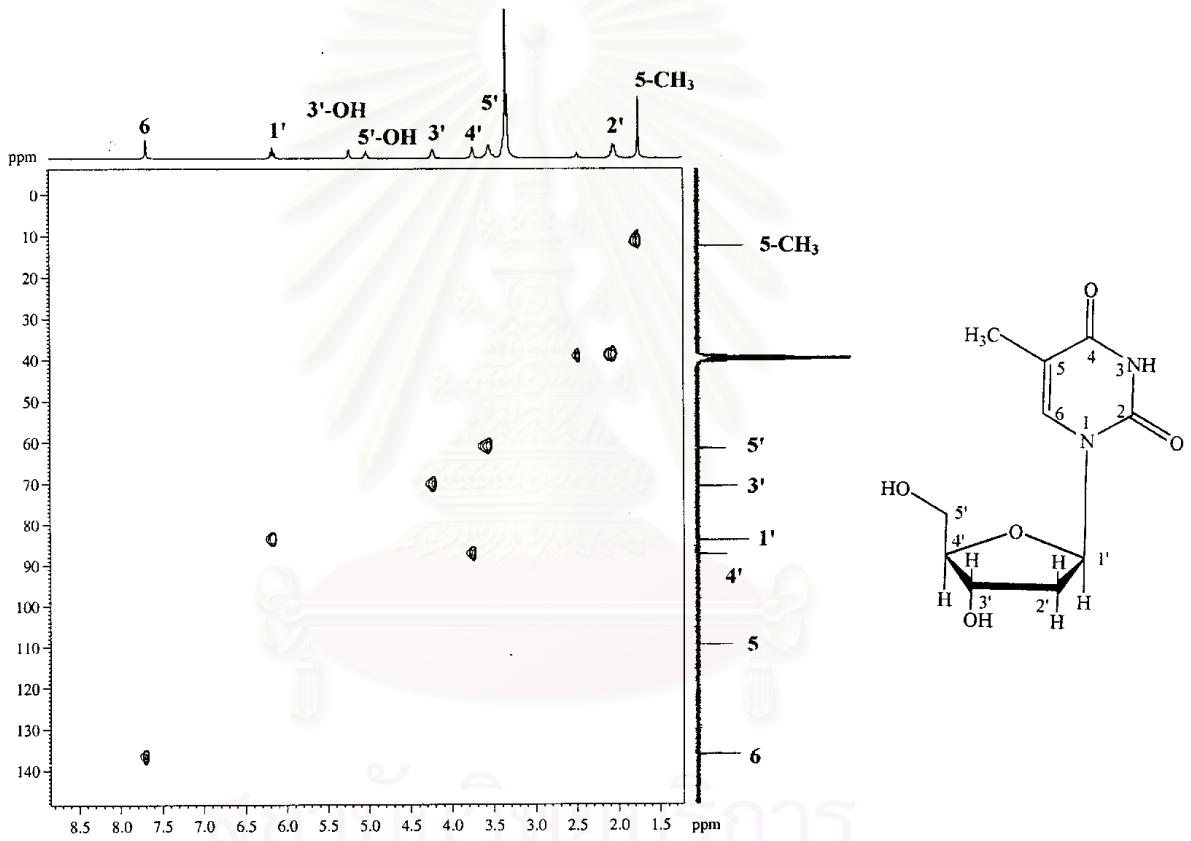

Figure 60 The 300 MHz HMQC spectrum (in DMSO-d_6) of thymidine (ET3K).

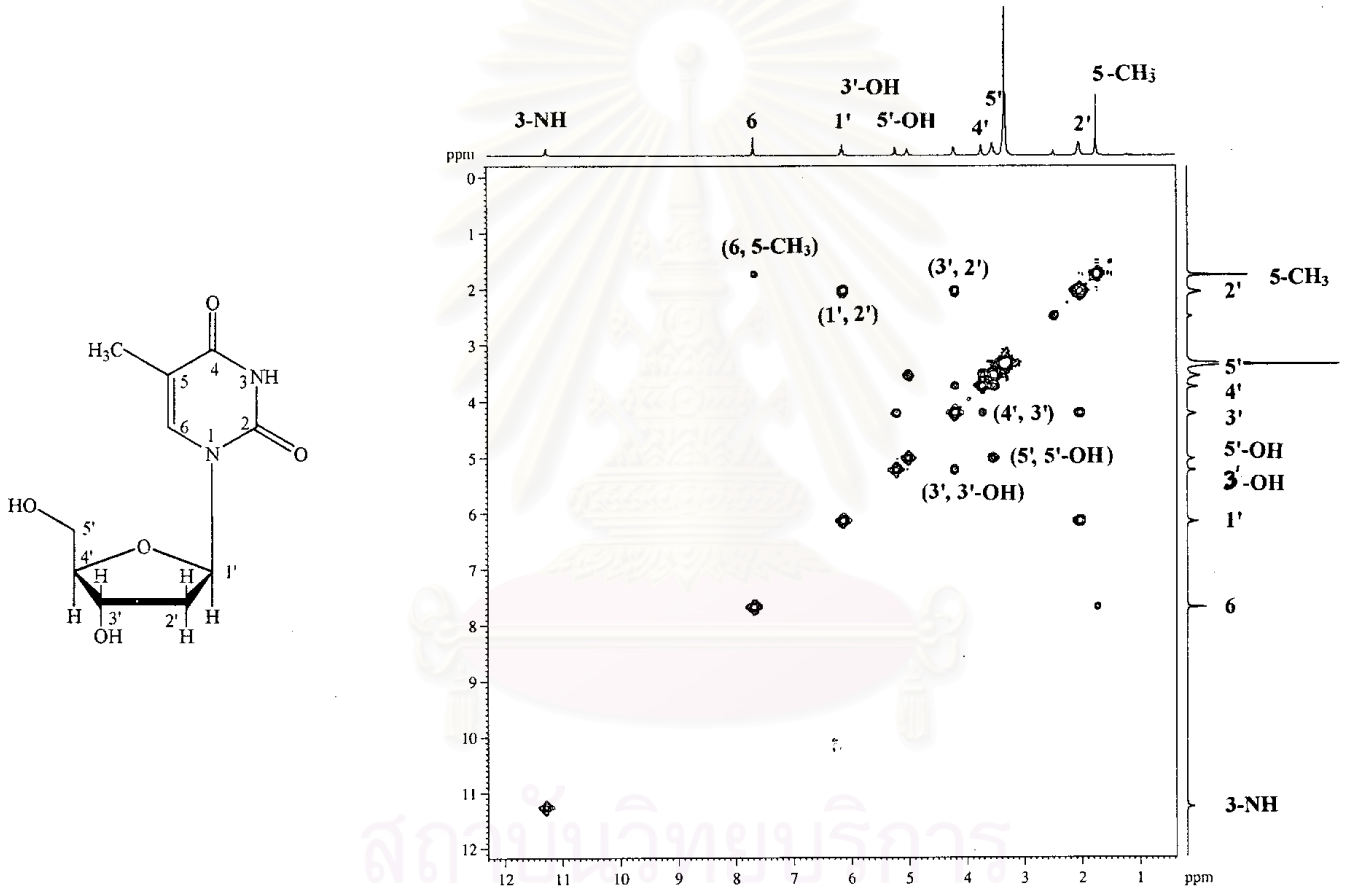

Figure 61 The 300 MHz ^{1}H-^{1}H COSY spectrum (in DMSO-d_6) of thymidine (ET3K).

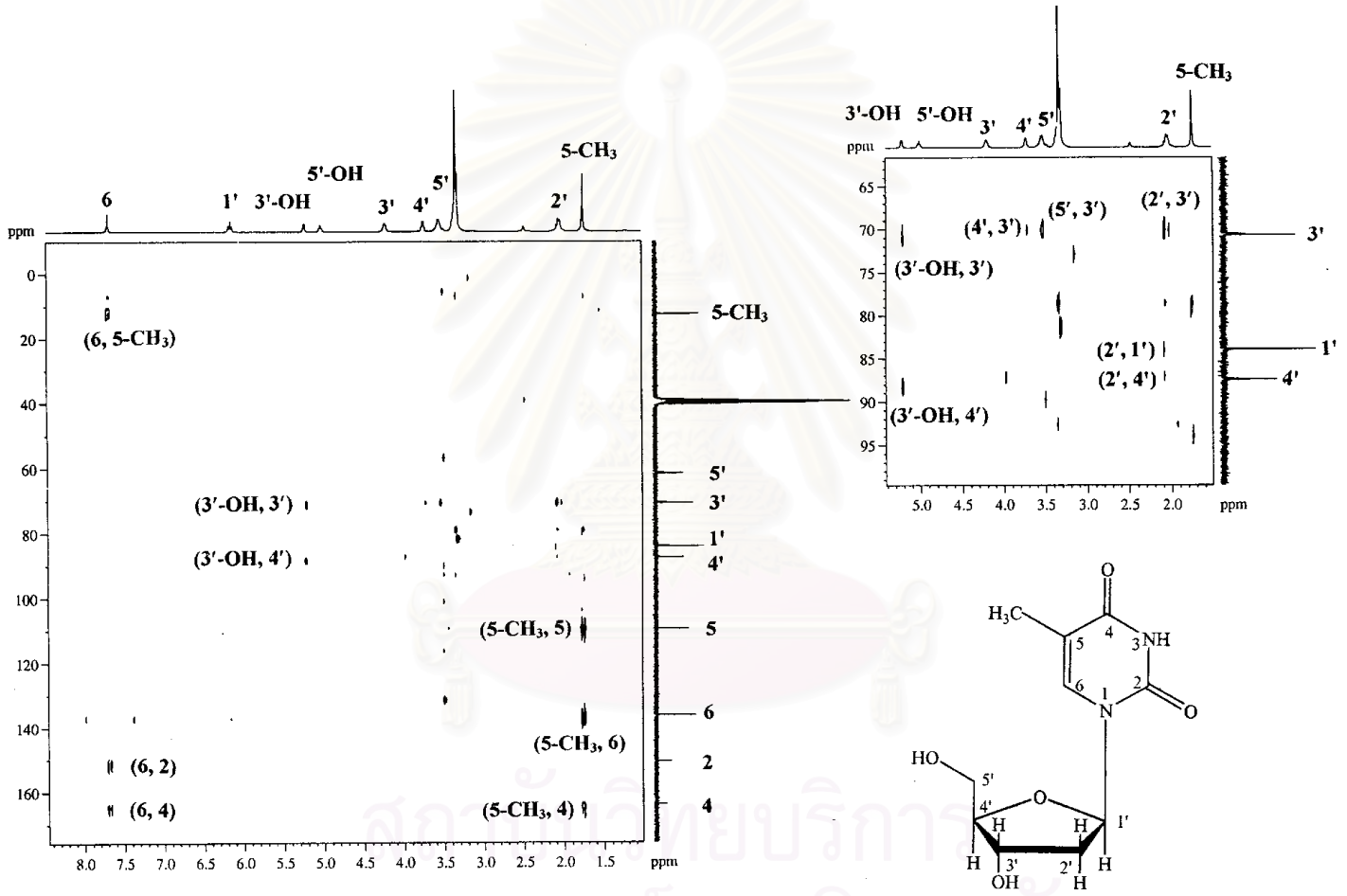

Figure 62 The 300 MHz HMBC spectrum ($^{n}J_{HC}$ = 8 Hz in DMSO-d_6) of thymidine (ET3K) [expanded: δ_H 1.5-5.4 ppm; δ_C 62-99 ppm].

VITA

Miss Kornvika Charupant was born on September 2, 1973 in Bangkok, Thailand. She received her Bachelor's Degree of Science in Pharmacy in 1997 from the Faculty of Pharmaceutical Sciences, Prince of Songkhla University, Thailand. Since her graduation, she has been working as a pharmacist at Division of Drug Analysis, Department of Medical Sciences, Ministry of Health.